EXPLORATION OF THERMODYNAMIC AND STRUCTURAL CHANGES RELEVANT TO THE ALLOSTERIC INHIBITION IN PHOSPHOFRUCTOKINASE FROM *BACILLUS STEAROTHERMOPHILUS*

A Dissertation

by

AMY MICHELLE WHITAKER

Submitted to the Office of Graduate and Professional Studies of
Texas A&M University
in partial fulfillment of the requirements for the degree of

DOCTOR OF PHILOSOPHY

Chair of Committee,	Gregory Reinhart
Committee Members,	Tadhg P. Begley
	J. Martin Scholtz
	Mary Bryk
Head of Department,	Gregory Reinhart

December 2015

Major Subject: Biochemistry

ABSTRACT

Phosphofructokinase from *Bacillus stearothermophilus* (BsPFK) and *Escherichia coli* (EcPFK) are allosterically inhibited by downstream glycolytic pathway intermediate phosphoenol-pyruvate (PEP). The coupling free energy, ΔG_{ay}, describes the interaction between substrate, Fru-6-P, and PEP. Positive for inhibition, ΔG_{ay} is the standard free energy for the following disproportionation equilibrium:

PEP:PFK + PFK:Fru-6-P ⟷ PFK + PEP:PFK:Fru-6-P

and quantitatively expresses the nature and magnitude of the allosteric effect. This reaction provides the key to understanding why ΔG_{ay} achieves its particular value. For EcPFK, the larger positive enthalpy term determines the positive sign for ΔG_{ay}. In BsPFK both components are negative, and the larger absolute value of the entropy term drives inhibition, suggesting fundamentally different mechanisms may transfer the allosteric signal between PEP and Fru-6-P binding sites. In this body of work, BsPFK and EcPFK structures are perturbed by both urea and engineered "holes", and the effect on the poise of the equilibrium in response is examined. Methyl-TROSY NMR was also used to obtain structural information on all four species of BsPFK that contribute to the equilibrium.

Both activity and ΔG_{ay} increase at low urea concentrations for BsPFK, but not for EcPFK. Van't Hoff analysis on BsPFK indicates that the absolute values for

both the entropy and enthalpy components of ΔG_{ay} change, and that the increase in allosteric coupling results from a larger change in entropy. Two of the three hole mutations had significant, but opposite, effects on the coupling. A 4-fold augmentation of coupling was seen for I153V-BsPFK, and the larger effect was determined to be on the enthalpy component. An analogous mutation in EcPFK, L154V, served as a control and had a minimal effect on the coupling. Methyl-TROSY NMR was used to probe structural changes throughout BsPFK related to allosteric coupling, and it was shown that there is not likely a discrete pathway involved in the propagation of the allosteric signal. Instead, residues throughout the enzyme are identified as contributors to the allosteric coupling. Together with the urea and hole mutant results we paint a picture of allosteric coupling in BsPFK that involves global changes in both the conformation entropy and structure.

DEDICATION

To my husband and family.

ACKNOWLEDGEMENTS

I would like to thank Dr. Reinhart, who has served not only as my boss and my committee chair, but also as a friend. I would also like to thank my committee members, Dr. Begley, Dr. Scholtz and Dr. Bryk for their guidance and support throughout the course of this research. In addition, I am grateful for all of the NMR help and expertise provided by Dr. Mandar Naik. Likewise, I thank Dr. Rockann Mosser and Dr. Tatyana Igumenova for doing the initial NMR experiments. Dr. Mauricio Lasagna deserves thanks for providing an abundance of technical help and scientific advice on fluorescence experiments.

I would like to thank all of the former and current members of the Reinhart lab who provided encouragement and scientific advice on a daily basis. Special thanks to David Holland for countless hours of scientific conversation. Thanks also go to my friends and colleagues and the entire Biochemistry and Biophysics faculty and staff for making my time at Texas A&M University a great experience.

TABLE OF CONTENTS

Page

LIST OF FIGURES

Page

LIST OF TABLES

Page

CHAPTER I

INTRODUCTION: A HISTORY OF ALLOSTERIC THEORY AND THE DYNAMICS OF ALLOSTERIC ENZYMES

Living cells do not synthesize or breakdown more material than what is required for their metabolism and growth. Functioning at this remarkable level of efficiency necessitates precise control mechanisms for the turning on and off of metabolic reactions. Enzyme catalysts play a major role in the regulation of metabolic processes by immensely accelerating the rates of specific biochemical reactions. The benefit of an enzymatic catalyst, in contrast to an inorganic catalyst, is that enzyme activity can be regulated.

Regulation of an enzyme can be accomplished by altering either its synthesis or catalytic activity. The magnitude of enzyme synthesis is modified by interfering with either the transcription that forms mRNA or the translation of the mRNA into protein. In prokaryotic cells transcription can be activated or inhibited when the function of RNA polymerase is altered due to the binding of a regulatory transcription factor and/or other protein to DNA. Bacteria often regulate translation by producing specific antisense RNA that is complementary to the mRNA that codes for synthesis of the enzyme. When the complementary antisense RNA binds to the mRNA it can no longer be translated into protein and the enzyme is not synthesized.

The regulation of enzyme activity can be achieved in a variety of ways including a change in pH, substrate availability, product inhibition, protein-protein interactions, covalent modification and allosteric effects. A change in pH, which can occur alongside some metabolic processes, may alter either the global conformation of the enzyme and/or the protonation state of a specific key amino acid side chain. These effects on the enzyme can result in a change in its activity. Substrate availability refers the cellular concentration of substrate available to the enzyme for turnover. If the concentration of substrate is much lower than the K_m the enzyme activity will be low. If the substrate concentration is much higher than K_m the active site will be saturated and the activity will be maximal. Sometimes a reaction product is structurally similar enough to the substrate that it can compete for binding at the enzyme's active site in a phenomenon termed product inhibition. Enzymes may be phosphorylated, acetylated, methylated, sulfated, glycosylated, amidated, hydroxylated, prenylated, myristoylated, or ubiquitinated. Many of these post-translational covalent modifications are reversible. Some of the ways that these modifications can affect enzyme activity are by inducing changes in the local or global shape of the enzyme and/or by activating or inhibiting binding interactions. Non-covalent interactions between an enzyme and another protein can also alter the activity of the enzyme. Allosteric regulation of enzyme activity, either activation or inhibition, is the result of the binding of an effector small molecule(s) or protein to a site distinct from the substrate binding site.

Enzymes poised at commitment steps in metabolic pathways are often subject to the most extensive allosteric regulation. One reason for this is that allosteric regulation is reversible. Another major advantage of allosteric regulation is that allosteric enzymes, unlike most enzymes, have ligand binding effectors that are not part of the pathways itself. The ability to adjust their rate in response to their physiological environment allows for the fine tuning of a pathway. Hence, the allosteric regulation of enzymes is particularly important in metabolic pathways such as glycolysis, Krebs cycle and other crucial and energetically expensive pathways. Given this central role that allosteric regulation plays in biochemical processes, the ability to decisively alter allosteric responses holds promise for drug design. In particular, because the binding of an allosteric effector can influence protein function, allosteric binding sites serve as potential drug targets. While the active sites of enzymes tend to be highly conserved, the evolutionary pressure on allosteric sites has been less severe[1], therefore it is reasonable to assume that species selectivity can be more easily obtained when targeting allosteric sites. For example, eukaryotic and bacterial homologs may catalyze the same reaction, but have different regulatory effectors. Unfortunately, the lack of specific knowledge on how enzymes are allosterically regulated at the molecular level hinders the potential of rational drug design.

Part 1: History and Theory of the Allosteric Effect

The study of allosteric regulation had its genesis when H. Edwin Umbarger recognized that the synthesis of L-isoleucine in *Escherichia coli* was regulated via a negative feedback mechanism. L-isoleucine, the end product of the biosynthetic pathway, inhibited selectively the activity of L-threonine deaminase, the first enzyme in the chain.[2] Umbarger's early observations of end-product inhibition in biochemical pathways were corroborated by Arthur Pardee's work with the enzyme aspartate transcarbamylase, the first enzyme in the pyrimidine biosynthesis pathway.[3,4] Jean-Pierre Changeux, then a junior doctoral student of Jacques Monod, confirmed Umbarger's observations and demonstrated that various chemical treatments of L-threonine deaminase lead to the loss of its sensitivity to inhibitor L-isoleucine. In addition, he took note that the kinetics suggested a bimolecular reaction, and it appeared that L-threonine and L-isoleucine were bound at unique sites.[5] At this time, it became clear that that the observed end-product inhibition could no longer be explained by a classical scheme where inhibitor and substrate molecules compete for the same binding site, instead a scheme involving distinct and non-overlapping sites was hypothesized. The word 'allosteric', allo- from the Greek meaning "other", was introduced by Monod in 1961 at the conclusion of the 26th Cold Spring Harbor Symposium on Cellular Regulation Mechanisms to emphasize the unique structure of the effector and necessary existence of separate binding sites to accommodate both substrates and allosteric

regulators.[6] This created a key distinction between allosteric inhibition and classic competitive inhibition, which is caused by steric hindrance from a structural analogue of the substrate. In an attempt to rationalize how the binding of an inhibitor to a site other than the active site could affect the catalytic activity of an enzyme, Monod originally applied the 'induced-fit' model, to describe the allosteric effect, proposed a few years earlier by Daniel Koshland[7] to explain ligand binding during catalysis. Specifically, he suggested that the binding of the regulatory ligand at the allosteric site may induce a conformational change of the protein that modifies the active site.

It has been more than 50 years since the first model attempting to describe the mechanism of allosteric regulation was invoked, and since several models with bases in both structure and thermodynamics have been employed. Before providing a detailed discussion of the various models used to elucidate the behavior of allosteric enzymes, a few features common to most of the models need to be described. The allosteric regulation of enzymes can occur either by altering the affinity of substrate binding to the enzyme or by altering the maximum velocity at which the enzyme can catalyze the reaction, termed K-type and V-type allosteric regulation, respectively. Since most allosteric enzymes are in K-type regulation systems, including phosphofructokinase, the focus from here on is on K-type regulation and the models used to account for these types of allosteric effects.

Allosteric communication occurs between distant ligand binding sites. When the ligands are different from each other the observed effect of one ligand binding

on the binding affinity of the other ligand is a heterotropic effect. When the ligands are the same as each other the analogous effect is termed homotropic. Cooperativity is a characteristic common to most oligomeric allosteric proteins, although is not required, and is limited to instances that produce non-hyperbolic binding curves. Positive cooperativity occurs when there is an increase in ligand binding affinity with increasing ligand concentration, while a decrease in ligand binding affinity with increasing ligand concentration is referred to as negative cooperativity. When no cooperativity is present the result is a hyperbolic binding profile that can be described by Michaelis-Menton kinetics in the case of an enzyme. When negative cooperativity is observed the subsequent decrease in binding affinity is characterized by a shallow slope in the binding profile. Positive cooperativity occurs when the binding of the first ligand enhances the binding affinity of the subsequent ligand, and results in a sigmoidal binding profile. The resulting non-hyperbolic ligand binding curve cannot be adequately fit by the Michaelis-Menten equation. Archibald Hill formulated what we have now come to know as a Hill plot to describe the cooperative behavior of oxygen binding to hemoglobin.[8] The Hill equation is used to fit the sigmoidal binding profiles of various enzymes with cooperative binding. In the absence of a unique second ligand only the homotropic coupling contributes to the non-hyperbolic binding curve that defines cooperativity.

According to our formalism, when a unique second ligand alters the cooperativity it is termed a heterotropic effect. Heterotropic cooperativity exists in

two forms: (1) heterotropically induced homotropic cooperativity and (2) subsaturating heterotropic cooperativity.[9] The first class refers to an effect on the magnitude of the homotropic coupling in the presence of the second ligand. At a saturating concentration of second ligand, the cooperativity can be either increased or decreased relative to the amount of cooperativity in the absence of the second ligand. The second class of heterotropic cooperativity arises when the allosteric ligand is present at intermediate concentrations and is positive regardless of the nature of the heterotropic interaction.[9-11]

The Classical MWC and KNF Models

The phenomenon of allosteric regulation was formally described by Jacques Monod and François Jacob for the first time in 1961[6] and the first protein crystal structures of myoglobin and hemoglobin were reported only a few years earlier.[12,13] In fact, the 1962 Nobel Prize in chemistry was awarded to Max Ferdinand Perutz and Sir John Cowdery Kendrew for solving the X-ray crystallography structure of hemoglobin. The dramatic appearance of protein X-ray crystallography structures greatly influenced scientific thinking about the molecular basis of biological function. It is no surprise that as the fields of protein allostery and structural biology matured in parallel that developments in one field influenced the other.[14] The binding events associated with enzymatic catalysis had been traditionally described using a lock and key model of molecular recognition[15], and with a new appreciation of the structural changes that can occur upon binding

came its revision and the proposal of the induced fit[16] and fluctuation fit[17] models. At about the same time two complementary models describing allostery were proposed, namely the concerted[18] and the sequential models[19] (Figure 1-1).

In 1965 "A Plausible Model" on the nature of allosteric transitions was proposed by the trio of Jacques Monod, Jeffries Wyman Jr., and Jean-Pierre Changeux after analyzing more than a dozen allosteric enzyme systems. This model, which was inspired by the observation of two conformational states of deoxy- and oxyhemoglobin, became known as the concerted or MWC model.[18] The MWC model

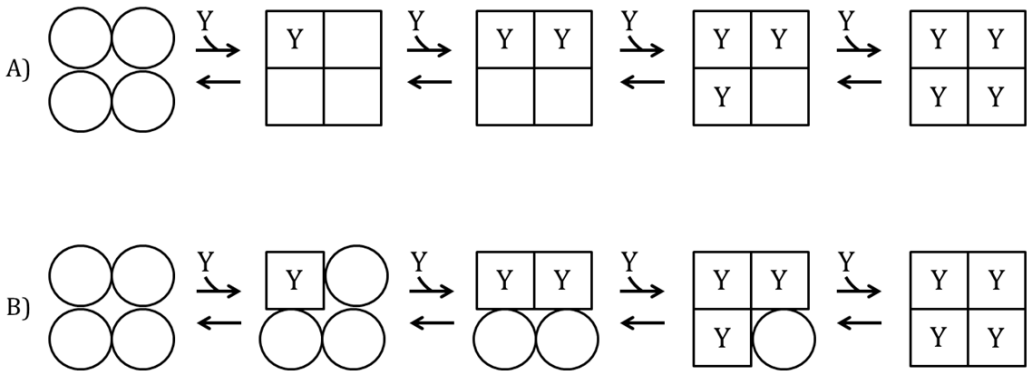

Figure 1-1: Schematic diagrams of the A) concerted (MWC) and B) sequential (KNF) models of allosteric regulation of a homotetramer. For the concerted model, only one equivalent of inhibitor (Y) is required to bind for the enzyme to undergo the allosteric transition from the "R" state (circles) to the "T" state (squares). The sequential model, on the other hand, requires four equivalents of inhibitor to bind for the enzyme to be converted from the R state to the T state.

suggests that allosteric proteins are symmetric oligomers with identical subunits. Each subunit exists in two possible conformational states, tense or "T" and relaxed or "R", which have different affinities for ligands.[18] According to the model, oligomers cannot exist in a hybrid form composed of subunits in both the T state and the R state. The basic assumption of the model is that there is a pre-existing equilibrium between these two conformational states, and when the substrate binds to the free enzyme it shifts the equilibrium to the R state in a concerted transition. This diverges from the Koshland inspired induced-fit based hypothesis Monod spoke of earlier to describe the allosteric effect, in which a conformational change induced by the interaction with the ligand leads to a structurally different state. It is because all of the subunits shift to the R state when the first ligand binds that positive cooperativity is observed as the first substrate binding event facilitates the binding of the subsequent substrates. Activators also bind to the R state, and shift the equilibrium towards the R state. In the presence of an activator, the enzyme is already in the R state, so the substrate binding profile lacks cooperativity. On the other hand, when an inhibitor binds to the enzyme, the equilibrium is shifted towards the T state in a concerted transition reducing the number of R sites available to bind substrate. Thus, when performing a substrate saturation profile at any given inhibitor concentration, positive cooperativity will be observed since the number of the competent substrate binding sites are increased as the equilibrium is shifted back towards the R state. A major shortcoming of the concerted model is its inability to explain negative

cooperativity, a deficit which served as part of the motivation for the development of the sequential model.

It was only a few years after the MWC model was published that D. E. Koshland Jr., G. Nemethy, and D. Filmer challenged the concerted model with a sequential hypothesis. The model they proposed became known as the KNF or sequential model.[19] Akin to the MWC model, the KNF model is composed of two distinct enzyme conformations, termed the "R" or relaxed state and "T" or tense state, where substrates and activators bind to the R state and inhibitors bind to the T state through an induced fit mechanism. The sequential model differs from the concerted model in that the subunits change conformation one at a time without affecting their neighboring subunits. Thus, a hybrid form of the enzyme composed of subunits in both the T state and the R state can exist in the sequential model. The KNF model also differs in that it does not invoke a pre-existing equilibrium between the two states, but rather a conformational change occurs within the enzyme to each subunit as a result of the binding of a ligand. This conformational change can affect the conformation of the other neighboring subunit, which can alter their binding affinities. Consequentially, the KNF model allows negative cooperativity in addition to positive cooperativity to be explained, something not addressed by the MWC model. The subsequent subunits change conformation sequentially with the binding of each ligand equivalent. As a result, the complete conversion from one state to another is only achieved when all sites are bound with ligand.[19]

The models are similar in that both employ only two conformational states of the allosteric protein, a low-affinity form and a high-affinity form. Another similarity is that an allosteric conformational change is favored when a ligand binds. A key difference between the models is that in the concerted model the bound conformations preexist at equilibrium, even in the absence of ligand. The sequential model postulates induced fit[16], meaning that the bound conformations are only adopted once in the presence of ligand. Notably, the concerted model is considered more restrictive in that symmetric oligomers are required and negative cooperativity cannot be treated.

More than 50 years since their inception, the MWC and KNF models are still able to explain allosteric phenomena in a multitude of molecular systems. However, in spite of the ability of these models to capture the qualitative relationship between the affinities of ligands at distinct sites, neither model provides insight into exactly how allostery works at the molecular level. An additional major shortcoming of the two-state models is that they limit themselves to the existence of the binary complexes, enzyme-substrate and enzyme-effector, and do not consider the ternary complex in the case of inhibition. The ternary complex has both substrate and effector bound at the same time, making it intuitively the most important complex to consider when modeling the allosteric effect. In addition, when one considers that allostery is a comparison of how a ligand binds in the absence and presence of a second ligand it follows that you have to consider two binding events, each involving two protein complexes. Such a comparison,

involving four species as opposed to two, is required to distinguish allosteric from non-allosteric protein changes. Because of the limitations of the two-state models, it is clear that a more complete model for allosterism is needed.

The Ensemble Allosteric Model (EAM)

Allosteric coupling can be understood in terms of the conformational 'energy landscape' of the protein in a way analogous to protein folding. After Cyrus Levinthal demonstrated that the rapid process of protein folding could not be explained by a random search for the most stable thermodynamic state, the hypothesis that there was a folding pathway was adopted.[20] Experimental observations did not fit such a simplistic model and it became clear that there were multiple parallel pathways for protein folding. In the late 1990s a new vision of protein folding progressively emerged as the displacement in an energy landscape of multiple partially folded conformations. This landscape is represented as an imperfect, irregular funnel.

This way of modeling protein folding also had an impact on the description of catalysis, challenging explanations based on induced-fit mechanisms. Some difficulty in mimicking induced-fit processes with artificial enzymes[21] pointed toward the more general problem of reproducing the dynamics of protein behavior. People began employing a protein folding like model to describe catalysis that would account for changes in dynamics in addition to structural changes.[22] According to this model, the transition from one catalytic step to the next one

corresponds more to a re-equilibration between an ensemble of dynamic and structural states than to the formation of new states. What represented a minor species at one step becomes the major species at the next step, and it all happens as if the ensemble of conformational states anticipated the progression of the reaction. The same statistical description could easily be adapted to model allosteric transitions.[23] In this case native states are ensembles of pre-existing populations; thus, the binding of an allosteric effector causes an equilibrium shift of pre-existing conformational states.

This theory is experimentally applied using a statistical thermodynamic formalism where the high resolution structure of the unligated state is used as a template to generate a large ensemble representing as many conformational states as possible. Then, a computer algorithm considers single amino acid substitutions to each residue in a protein and examines the effects of those perturbations on the distribution of conformational states with the goal of mapping a network of associated interactions within the protein. All of the predicted conformations of the protein are sampled according to their energies, with lower energy states sampled more often than those of higher energy. The binding of any ligand to a particular state increases how often that state is sampled, so according to the EAM allosteric ligands effectively remodel the energy landscape of allosteric proteins. Stabilities and coupling energies in allosteric enzymes are generally quite modest, which according to the EAM suggests that no single state, or set of allosteric states, will necessarily dominate the ensemble. In other words, the EAM suggests that

allosteric mechanisms may be more statistical, and less deterministic, than classical models suggest. A prominent feature of the EAM is that the energy landscape can be smooth with numerous accessible conformational states in its ensemble, discrete with few states, or anything in between, with each scenario providing its own unique conformational, dynamic and biologically functional effects.[24]

This view is far less limiting than the concerted and sequential models proposed in the late 1960s. The MWC and KNF models are limited to oligomeric proteins and to the existence of only two different conformational states, either of which represents the ternary complex. In addition, the classical structure based allosteric models do not distinguish between changes in the protein due to the allosteric transition and the modifications in protein structure that take place during catalysis. The EAM provides one way to describe allosteric behavior that results from a change in the dynamics of the system, without any additional conformational changes.[25] However, like the MWC model, the EAM is still limited to pre-existing states –just more of them. Potential unique structural and dynamic effects on the conformation of the enzyme due to the binding energy of the ligand are not accounted for.

Allosteric Linkage

Allosteric linkage is a model free thermodynamic approach that quantifies the nature and magnitude of the allosteric response by comparing the difference in the substrate binding affinity for the enzyme in effector-free and effector-saturated

forms. The central concepts of thermodynamic linkage were first presented by Jefferies Wyman Jr. in a series of papers published between 1948 and 1965 in which he proclaimed that through the study of linkage between multiple reactions within a complex molecule one could describe the function of that molecule.[26-28] Shortly after collaborating with Jacques Monod and Jean-Pierre Changeux on the MWC model, Wyman published a paper describing allosteric linkage in which he related the allosteric nature of a protein to thermodynamics for the first time.[29] He introduced the allosteric binding potential, which can be used to quantify the allosteric response of a protein. This binding potential quantified the allosteric response of a protein. Wyman used chemical potentials to demonstrate the principle of reciprocity, which is the fact that the binding of the effector has the same influence on the binding of the substrate as the binding of the substrate has on the binding of the effector.

Gregorio Weber modified and expanded Jefferies Wyman Jr.'s linkage theory in several papers published during the 1970s. Most importantly, Weber established that allosteric linkage can be written in thermodynamic terms of free energy, and introduced the concept of coupling free energy.[10,11] The advantage of examining protein-ligand interactions in terms of free energy is that the relationship between binding energies and the actual molecular forces which cause them are more evident. Gregory D. Reinhart simplified Weber's free energy description of protein-ligand and ligand-ligand interactions by applying both the kinetic notations introduced by W. Wallace Cleland[30] and the single substrate-single modifier scheme

devised by C. Frieden[31] enabling the description of the pertinent thermodynamic relationships in allosteric enzymes[9,32,33].

The power of the allosteric linkage approach to studying allostery is in its ability to describe ligand binding in free energy terms without assuming the nature of structural changes caused by ligand. The basic principle of thermodynamic linkage is reciprocity, which is to say that the effect that substrate A has on the binding of effector Y to the enzyme E must equal that of Y on the binding of A to E. The simplest allosteric kinetic mechanism can be described by the scheme shown in Figure 1-2.

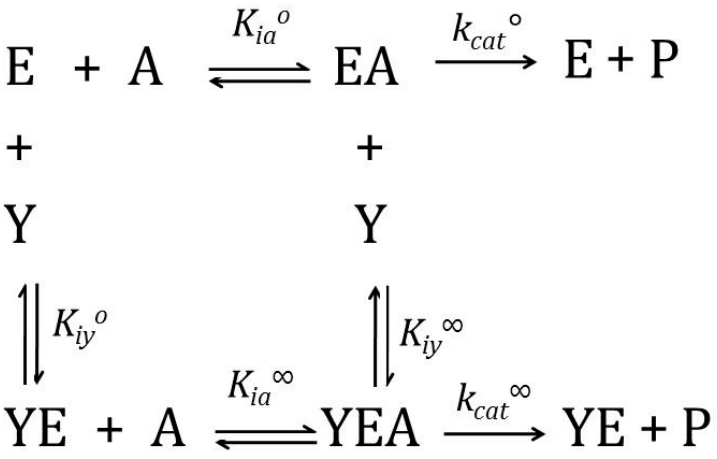

Figure 1-2: Schematic diagram of the simplest allosteric mechanism with a single substrate (A) and a single allosteric modifier (Y). E and P stand for enzyme and product, respectively. Ks represent dissociation constants and are defined in the text.

The dissociation constant for each equilibrium in the thermodynamic box is described as follows:

$$K_{ia}^{o} = \frac{[E][A]}{[EA]} \tag{1-1}$$

$$K_{ia}^{\infty} = \frac{[EY][A]}{[YEA]} \tag{1-2}$$

$$K_{iy}^{o} = \frac{[E][Y]}{[EY]} \tag{1-3}$$

$$K_{iy}^{\infty} = \frac{[EA][Y]}{[YEA]} \tag{1-4}$$

where K_{ia}^{o} and K_{ia}^{∞} represent the dissociation constants for A in the absence of Y and in the saturating presence of Y, respectively. K_{iy}^{o} and K_{iy}^{∞} represent the dissociation constants for Y in the absence of A and in the saturating presence of A, respectively. The relationship between A and Y can be described by the coupling constant, Q_{ay}, which gives the nature and magnitude of the allosteric effect.

$$Q_{ay} = \frac{K_{ia}^{o}}{K_{ia}^{\infty}} = \frac{K_{iy}^{o}}{K_{iy}^{\infty}} \tag{1-5}$$

$$Q_{ay} = \frac{[YEA][E]}{[EA][YE]} \tag{1-6}$$

The value of Q_{ay} describes the nature of the effect caused by Y. When $Q_{ay} > 1$, Y is an activator and when $Q_{ay} < 1$, Y is an inhibitor. When $Q_{ay} = 1$, Y has no effect on the binding of A to E. Q_{ay} also represents the thermodynamic disproportionation equilibrium constant for the following reaction:

$$[YE] + [EA] \overset{Q_{ay}}{\longleftrightarrow} [E] + [YEA] \tag{1-7}$$

Understanding the basis for the allosteric effect requires one to understand why the disproportion equilibrium achieves its particular value. Since Q_{ay} is a thermodynamic parameter, the equilibrium constant is related to the coupling free energy by the following equation:

$$\Delta G_{ay} = -RTln(Q_{ay}) \tag{1-8}$$

Correspondingly, inhibition has a positive coupling free energy ($\Delta G_{ay} > 0$), activation has a negative coupling free energy ($\Delta G_{ay} < 0$), and a ΔG_{ay} equal to zero means there is no allosteric effect. ΔG_{ay} represents a standard free energy, although the superscript "0" is dropped from the designation to avoid confusion with the use of that superscript for other purposes in notation.[32]

The rate equation for the mechanism shown in Figure 1-2 can be written as shown below as long as the substrate is assumed to achieve rapid equilibrium during the steady-state[32,34]:

$$\frac{v}{[E]_t} = \frac{V^o K_{iy}^o [A] + Q_{ay} W_{ay} [A][Y]}{K_{ia}^o [Y] + K_{iy}^o [A] + K_{iy}^o [Y] + Q_{ay} [A][Y]} \tag{1-9}$$

where v is the initial velocity, and V^o is the maximal activity in the absence of Y. K_{ia}^o is the dissociation constant for substrate A in the absence of effector Y, and K_{iy}^o is the dissociation constant for effector Y in the absence of substrate A. W_{ay} is the ratio of V^∞/V^o, where V^∞ is the maximal activity in the presence of a saturating concentration of effector Y. When the maximal activity is affected by the allosteric ligand W_{ay} will not be equal to 1.

Experimentally the coupling constant, Q_{ay}, can be obtained by determining the apparent dissociation constants for the substrate A as a function of effector concentration and can be graphically depicted for Y being either an inhibitor (Figure 1-3) or an activator.[35] Q_{ay} is represented as the ratio between the two

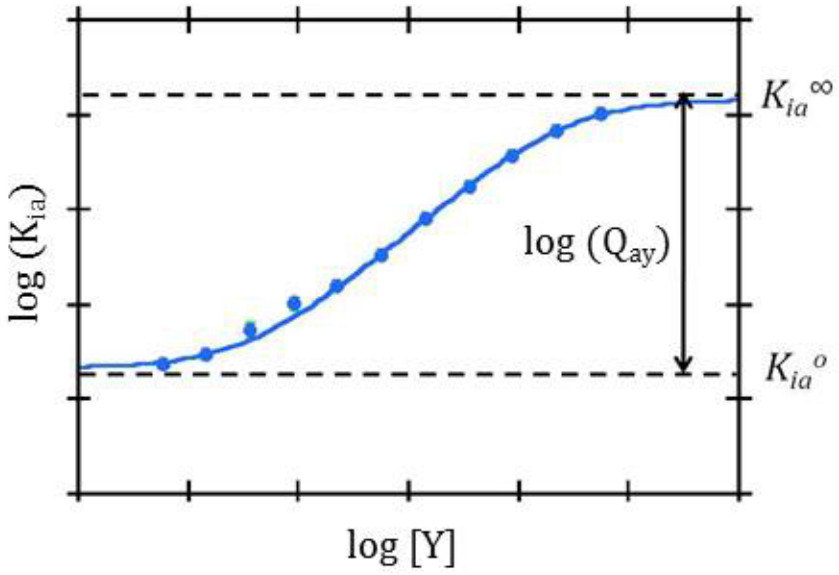

Figure 1-3: Graphical representation of the allosteric coupling, Q_{ay}, between substrate (A) and inhibitor (Y).

plateaus, K_{ia}^{∞} and K_{ia}^{o}. The dependence of the apparent dissociation constant of substrate, K_a , on the effector concentration can be determined by the following equation:

$$K_a = K_{ia}^{o}\left[\frac{K_{iy}^{o} + [Y]}{K_{iy}^{o} + Q_{ay}[Y]}\right] \tag{1-10}$$

Although no cooperativity is predicted by eq 1-9 and Figure 1-2, eq 1-10 can still be applied to an oligomeric protein, like EcPFK.[32] The Hill equation can be utilized to describe the degree of saturation for an oligomeric protein as a function of ligand concentration. The apparent dissociation constant for substrate, K_a, is the concentration at which the velocity is at half maximum and is described by the Hill equation[8]:

$$\frac{v}{[E]_t} = \frac{k_{cat}[A]^{n_H}}{K_a^{n_H} + [A]^{n_H}} \tag{1-11}$$

where v is the rate of the reaction, $[E]_t$ is total concentration of enzyme active sites, k_{cat} is the turnover number and n_H is the Hill number that depicts cooperativity in substrate binding. Since the assumption of infinite cooperativity is physically impossible, n_H must be considered not as a number of subunits per protein, but rather as a measurement of the degree of cooperativity among interacting ligand-binding sites. When n_H = 1, there is no cooperativity and the binding curve should fit according to Michaelis-Menten kinetics. However, when n_H > 1, positive cooperativity is observed and when n_H < 1 negative cooperativity is obtained.

The Hill number can be related to the allosteric coupling constant between substrate binding events in a dimer using the following equation[9]:

$$n_H = \frac{2(Q_{aa})^{1/2}}{1 + (Q_{aa})^{1/2}} \tag{1-12}$$

where Q_{aa} is the coupling between the binding of the two substrate molecules in a dimer. Upon inspection of this equation one can determine that the Hill coefficient

resulting from ligand-ligand couplings in a dimer has an upper limit of 2 and a lower limit of 0. These limits are only achieved as the coupling constants approach infinity and 0, respectively.

A unifying aspect of the allosteric linkage and EAM is that an explicit structural basis for the allosteric coupling is not required: only the magnitude and sign of the coupling free energy matter. Cooper and Dryden theoretically described in a classic paper almost 30 years ago the possibility of allostery being manifested without structural change.[36] The practical implication is that an understanding of the determinants of allostery does not rely upon an inspection of the bonds that are made and lost in the average structure. Indeed, since that pioneering work, numerous examples have emerged that clearly demonstrate the need for allosteric descriptions that are independent of structural change. For example, direct confirmation of allostery without a conformational change[37], allostery in the absence of a structural pathway[38-40], negative cooperativity[41], entropy driven allosteric coupling[35,42-44], allosteric changes from surface mutations that do not affect structure[45,46], and allosteric communication facilitated by intrinsically disordered proteins[41] are all examples of allosteric phenomena that are difficult, if not impossible, to rationalize in the context of static structural changes alone. Another puzzling example is when an allosteric ligand elicits agonistic effects under some conditions and antagonistic effects under others while binding to the same site.

Never the less, the EAM is based on the same selective origins as the classical MWC model. Specifically, the ligands do not induce the formation of new conformational states, but select one state among the ensemble of pre-existing ones and ignores the energy input to the system by ligand binding. This limitation of pre-existing conformations does not exist in allosteric linkage, which describes the allosteric regulation in terms of the energetics. Therefore, potential unique structural and dynamic effects on the conformation of the enzyme due to the binding energy of the ligand are accounted for only by allosteric linkage.

Part 2: The Study of Dynamic Allosteric Systems and Large Allosteric Systems

A fundamental unanswered question in field of allostery is how perturbation due to ligand binding at one site is transmitted through the protein to remote sites to effect ligand binding or enzymatic activity regulation. The early crystallographic work on allosteric systems helped to advance and establish a purely mechanical view of allosteric regulation. In recent years our understanding of allostery has shifted from a solely structural view to the current one calling for both structural and dynamic changes to be considered as potential routes for the propagation of the allosteric signal. Allostery is fundamentally thermodynamic in nature, and transmission of the allosteric signal through the protein can be mediated not only by changes in the mean conformation but also by changes in the internal motions about the mean conformation. In other words, there can be an enthalpic

contribution, an entropic contribution or a combination of both effects to the allosteric coupling free energy. In their 1984 classic paper "Allostery without conformation change", Cooper and Dryden demonstrated for the first time how long range interactions between ligand binding sites on a macromolecule could be produced by purely dynamic processes even in the absence of any conformational change.[36] They propose that the effect arises out of the possible changes in frequencies and amplitudes of macromolecular thermal fluctuations in response to ligand binding, and can involve all forms of dynamic behavior, ranging from highly correlated, low frequency vibrations to random local anharmonic motions of individual or groups of atoms or groups. Cooper and Dryden used the simplest case, that of an interaction between two identical sites, to estimate that allosteric coupling free energies of several kJ/mol can exist due to dynamics alone. Sure enough, their theoretical observations were followed by a growing list of examples, from which I have selected a few to describe below, to illustrate the link between dynamics over a wide range of time scales and allosteric regulation.

Two scientific advances of very different natures have proven to be vital for the continued advancement of allosteric theory, and to generate a multitude of examples in the literature of dynamic allostery. First is the establishment of more sophisticated descriptions of allosteric behavior. Namely, the structural based Ensemble Allosteric Model (EAM) and the energetic based allosteric linkage, which allow for a quantitative description of both the nature and magnitude of allosteric effects even in the absence of a structural change. The second major driving force

towards a more dynamic view of allostery has been offered by recent technological advances, predominately in nuclear magnetic resonance (NMR) spectroscopy. NMR, in addition to providing the structural information of a biological system in solution, is unique in providing information about the amplitude of motions taking place on a wide range of time scales[47,48], accessing lowly populated conformational states[49] and providing a residue specific information of conformational entropy[50]. In addition, technical advances in molecular dynamics have expanded its limitations from information on just the local, fast conformational changes[51] exhibited to include information on the slowest, global conformational changes of proteins. Combined with NMR, these technological developments have been used to demonstrate the existence of multiple enzyme conformational states and have provided access to the dynamics of interconversion between these different states.[52] In addition, methodological advances in labeling strategies and specifically designed pulse sequences have recently enabled the application of NMR approaches to characterizing the allosteric properties of more challenging and larger protein systems.

Indeed, over recent years the important role of protein motions in mediating allosteric interactions has been demonstrated by numerous examples in the literature from which I have selected a few to review below.

Dynamic Allostery

An unusual observation on the binding of cyclic AMP (cAMP) by the catabolite activator protein (CAP)[37] provided the first experimental evidence that an allosteric signal can be propagated through a protein in the absence of structural changes, as it was theoretically predicted almost three decades earlier by Cooper and Dryden[36]. CAP is a homodimeric transcription regulator protein, and each subunit consists of both a cAMP-binding domain and a DNA-binding domain. Two cAMP molecules bind the CAP dimer with negative cooperativity and function as allosteric effectors by increasing CAP's affinity for its DNA substrate. The strong negative cooperativity has been taken advantage of by researchers to figuratively "freeze" binding conformations at intermediate stages. The conformation of the unbound state is referred to as the inactive state, and the conformation with 2 cAMP molecules bound is referred to as the active state. Using chemical shift and relaxation NMR analyses it was exposed that although the binding of the first cAMP molecule to CAP has a minimal effect on the fast dynamics of CAP, the binding of the second cAMP molecule substantially reduces the fast dynamics thereby incurring a large conformational entropy penalty. Isothermal calorimetry (ITC) studies established that the negative cooperativity was purely entropy driven indicating that allosteric interactions may be mediated by changes in dynamics.[37,53] Surprisingly, a CAP mutant, CAP-S62F, failed to form the active conformation upon the binding of cAMP. NMR and ITC analyses of the mutant showed that despite the fact that CAP-S62F-cAMP(2) is stuck in the inactive conformation, it binds to DNA

as strongly as wild-type CAP-cAMP(2) with its binding driven by a large conformational entropy originating in enhanced protein motions induced by DNA binding. These results provide strong evidence that changes in protein motions may activate allosteric proteins that appear to be structurally inactive.[25]

Thrombin is the central protease of the blood coagulation cascade. Tight regulation of its activity is essential to ensure quick blood clotting while preventing uncontrolled thrombosis. The binding of numerous ligands to thrombin at exosite I and the coordination of Na^+ have been associated with changes in thrombin conformation and activity, known as thrombin allostery. For over 30 years thrombin allostery has been described using a two state model where it can adopt an anticoagulant (slow) conformation and, after Na^+ binding, a structurally distinct procoagulant (fast) state.[54] In a recent study, the residues responsible for the transverse relaxation-optimized spectroscopy (TROSY) NMR cross peaks for seven distinct ligation states of thrombin were assigned. Mapping the assignments back to crystal structures have made it possible to distinguish between local and long-range conformational effects.[55] These results indicated that the active site, exocite I and the Na^+ binding sites all remain in a disordered, dynamic state. A more updated model of thrombin allostery, relying on the plasticity of the enzyme, has been proposed where the low activity of the 'slow' form is due to the rapid sampling of multiple states. It is likely that most thrombin substrates will engage exosite I first, where binding is directed by electrostatics[56], and therefore do not require a rigid conformation. Subsequent hydrophobic interactions occur via an induced-fit

mechanism that stabilizes exosite I. The occupancy of exosite I improves the affinity of thrombin for Na^+ by helping to form the coordination site. Na^+ is in rapid equilibrium, so as soon as exosite I is engaged it will bind stably to fully form the active site.[57]

Recently developed NMR relaxation dispersion experiments have enabled the detection and characterization of weakly populated states.[47,49] Interconversion between the ground and excited states occurs on the μs–ms timescale, allowing information about the kinetics and thermodynamics of the chemical exchange process as well as the chemical shifts of the excited state to be determined by NMR. In an interesting application of this method, it was shown that binding of the mixed lineage leukemia (MLL) transcription factor to the KIX domain of CREB binding protein promotes the formation of a weakly populated, about 7%, conformation in which the remote c-Myb binding site adopts the c-Myb-bound conformation.[58] Consequently, the binding of the first ligand (MLL) alters the structure of the distant second site so that the binding competent conformation seen in the structure of the ternary complex performs in the MLL-CREB binary complex.[58] NMR data also reveal an evolutionarily conserved network of hydrophobic amino acids that constitute the pathway through which the allosteric signal is dynamically propagated.

Calmodulin (CaM), a key player in calcium mediated cell signaling, has been used as a model system to investigate the role of changes in fast (subnanosecond) internal dynamics and its associated conformational entropy in protein–ligand

binding.[59] CaM serves as a messenger protein and transduces calcium signals by binding calcium ions and then modifying its interactions with various target proteins. Backbone and side chain order parameters were measured by NMR for CaM in complex with a series of different peptides from physiological targets of calmodulin. It was found that the apparent change in conformational entropy was linearly related to the change in the overall binding entropy.[59] Their observations provide strong evidence that modifier binding induced changes in protein conformational entropy can contribute significantly to the energetics of protein ligand association, in contrast to the commonly held belief that they are necessarily energetically dominated by enthalpic interactions.

Extension of NMR to Study Allostery in Large Systems

The traditional triple resonance (^{13}C, ^{15}N, ^{1}H) multi-dimensional NMR experiments that are standard for making resonance assignments in proteins are not very effective for proteins with a molecular weight greater than 50 kDa due to increased linewidths associated with the slower tumbling of large molecules, and the spectral overlap from the large number of unique signals. Recent advances in isotope labeling and the development of pulse sequences that take advantage of them have extended the applicability of NMR spectroscopy to protein systems of molecular weights up to 1 MDa.[60] The most common approach involves selective $^{13}CH_3$ methyl labeling otherwise completely deuterated proteins and employing experiments that make use of a methyl-TROSY effect. Methyl groups are abundant

throughout protein structure, and especially in the hydrophobic core, making them great probes of both structure and dynamics of proteins. In addition, the complex $^{13}CH_3$ spin system can be taken advantage of by developing pulse sequences that transfer the magnetism in way that minimizes relaxation loss and gives rise to spectra with high sensitivity.[61]

Methyl-TROSY NMR enabled the characterization of the 306-kDa aspartate transcarbamoylase (ATCase) enzyme[62], a prototypic system for understanding allostery and cooperative binding processes. ATCase catalyzes the first step in the biosynthesis of pyrimidines in which the substrates carbamoylphosphate and aspartate are converted to carbamoylaspartate and inorganic phosphate. The researchers used methyl-TROSY NMR to analyze the binding of substrates, and their effect on the R–T equilibrium in the context of a two-state model. Although only the T state of the enzyme can be observed in spectra, the binding of substrates at the active site shift the equilibrium so that correlations from the R state become visible, allowing the equilibrium constant between ligand-saturated R and T forms of the enzyme to be measured. The equilibrium constant between unliganded R and T forms is also obtained indirectly from relations that emerge due to the fact that ligand binding and the R–T equilibrium are linked. Titrations established that MgATP binding directly perturbs the R–T equilibrium, consistent with the MWC model.[62] Prominent studies of the 300-kDa ClpP protease[63] and the 20S core-particle proteasome[64], also completed by Lewis Kay's lab, revealed important links

between dynamics and function by quantifying conformational exchange processes that regulate catalytic activity.

Methyl-TROSY NMR combined with paramagnetic relaxation enhancement (PRE) studies of the SecA translocase ATPase revealed dynamic allosteric cross talk between the nucleotide binding cleft and the pre-protein binding domain (PBD)[65]. In addition, the PBD was found to interconvert between an open and a closed conformation, with the conformational equilibrium potentially serving as a simple translocation mechanism.

Part 3: Phosphofructokinase and the Present Study

Phosphofructokinase-1 (PFK-1 or PFK) catalyzes the transfer of a phosphoryl group from MgATP to fructose-6-phosphate (Fru-6-P) producing MgADP and fructose-1, 6-bisphosphate. This reaction represents one of the most characterized enzymes in one of the best studied, most highly conserved metabolic pathways known. PFK catalyzes the phosphorylation reaction by inducing nucleophilic attack by the C1-hydroxyl of Fru-6-P on the γ-phosphorus of MgATP.[66] Mg^{2+} plays a critical role chelating the β- and γ-phosphoryl oxygen molecules, and in most PFK isoforms Mg^{2+} is essential for enzyme activity.[67-69] In PFK from prokaryotes, Saccharomyces cerevisiae, and rabbit muscle sources the reaction is catalyzed in a random sequential mechanism.[70,71] The reaction represents the essential and first committed step of the glycolytic pathway, as the only metabolic

fates of fructose-1,6-bisphosphate are dephosphorylation to Fru-6-P or oxidation to pyruvate. Consequently, the PFK catalyzed reaction is under very tight control and the enzyme is allosterically regulated by a variety of effectors that differ between variants of the enzyme from different sources.

The glycolytic pathway is conserved among most organisms. PFK is likewise conserved, showing homology in many diverse organisms. There are differences between prokaryotic and eukaryotic PFKs in quaternary structure, size, and regulation. However, the mechanism, sequence, and fundamental mechanisms of regulation been highly conserved throughout evolution. Comparing prokaryotic and eukaryotic PFK*, B. stearothermophilus* PFK has 44% sequence identity to the N-terminal domain of rabbit muscle PFK and 35% identity to the C-terminal domain.[72,73] This has led to the hypothesis that mammalian PFK has undergone gene duplication at some point in evolutionary history.[74] Between eukaryotic PFK isoforms, rabbit muscle and human muscle are 95% identical. Among prokaryotic PFK variants, *E. coli* and *B. stearothermophilus* have 54% identity, while *B. stearothermophilus* and *T. thermophilus* are 58% identical.[73,75] The high degree of sequence similarity and evolutionary conservation hints at the essential role PFK plays in the central metabolic pathways of organisms.

In addition to the ATP-dependent PFK discussed above, plants also have a second type of phosphofructokinase present that uses pyrophosphate (PP_i) instead of ATP as the phosphoryl donor called pyrophosphate-fructose-6-phosphate-

phosphotransferase (PFP). PFP reacts near equilibrium and can catalyzes a net flux in the direction of either glycolysis or gluconeogenesis *in vivo*.[76]

While the metabolites that are responsible for regulation vary between organisms, most PFK isoforms are under allosteric regulation of some type and to some extent. In the context of linked function thermodynamics, the structural or energetic basis for communication between active and allosteric sites for many of these PFK isoforms is an active focus of investigation. PFK from mammalian tissues was originally the most studied, and has a subunit molecular weight from 75 to 95 kDa.[77-79] It forms a tetramer that self-associates into larger oligomers.[80,81] Eukaryotic PFK is subject to complex allosteric regulation.[74,82] It is inhibited by MgATP, citrate, and [H^+], whereas it is activated by MgADP, AMP, fructose-2, 6-bisphosphate (Fru-2,6-BP), fructose-1,6-bisphosphate, cAMP and P_i. The quaternary structure of the enzyme is highly dependent on the presence of allosteric ligands, adding another level of complexity. Specifically, rabbit muscle and rat liver PFK undergo vast self-association that leads to a lowered k_m for Fru-6-P under conditions of substrate and/or activator binding or high protein concentration.[83]

Bacterial PFKs form a tetramer with a molecular weight of 34 kDa for each subunit. Prokaryotic PFK is still highly allosterically regulated; however there are fewer effector molecules than seen in eukaryotic variants. The less complex allosteric regulation of the prokaryotic enzyme makes it a good model for studying

the allosteric response in PFK. Most prokaryotic PFK isoforms are inhibited by PEP and are activated by MgADP.

Although not the focus of this work, there is a second form of prokaryotic PFK, phosphofructokinase-2 (PFK-2). PFK-2 is the minor isozyme and is not homologous to PFK-1. Unlike PFK-1, PFK-2 does not show cooperative interactions with fructose-6-P, inhibition by phosphoenol-pyruvate, or activation by ADP.[84] The kinetic mechanism of PFK-2 is a ordered sequential bi-bi reaction mechanism where F6P binds first and Fructose-1,6-bisphosphate is the last product released.[85] In the case of PFK-2 MgATP appears to act not only as a K-type inhibitor, antagonizing the binding of fructose-6-P as in PFK-1, but also as a V-type inhibitor, decreasing the value of k_{cat}.[86] Differences and similarities in the patterns of fructose-6-P binding and the mechanism of inhibition for PFK-1 and PFK-2 provide an example of evolutionary convergence.

Allostery in Prokaryotic Phosphofructokinase

MgADP activates prokaryotic PFK by increasing its affinity for Fru-6-P binding, which is a response to the low energy in the cell. Phosphoenol-pyruvate, PEP, is a downstream product of glycolysis and inhibits prokaryotic PFK by decreasing the affinity of enzyme for Fru-6-P binding. Thus, prokaryotic PFK is subject to "K-type" regulation. The other substrate is MgATP. MgATP and Fru-6-P antagonize one another's binding markedly, and MgATP brings about positive cooperativity in the Fru-6-P binding profile.[87] However, compared to eukaryotic

PFK, the allosteric interaction between MgATP and the effectors is relatively small. MgADP and PEP bind to identical allosteric sites at the allosteric interface of prokaryotic PFK. Exactly how these two different effector molecules regulate PFK from the same site with different effects is still an active area of research. More specifically, the mechanism by which the allosteric signal is transmitted between active sites and allosteric sites is a key unanswered question.

EcPFK and BsPFK are the most studied prokaryotic PFK isoforms and have many similar characteristics. For instance, they show 73% similarity and 54% identity in amino acid sequence. The crystal structures of both enzymes have been solved and the α-carbon traces are nearly superimposable.[88-90] The crystal structures of EcPFK and BsPFK also indicate almost identical active site binding residues.[90-92] Both structures represent a tetrameric enzyme consisting of four identical subunits arranged as a dimer of dimers. Each 34 kDa subunit is composed of a large domain and a small domain, and each domain contains a central β-sheet sandwiched between several α-helices. Within a tetramer, each subunit makes significant protein-protein contacts with two other subunits, and minimal contact with the remaining subunit.[89-91,93] Both the Fru-6-P binding and the allosteric effector binding sites are located at the two different dimer-dimer interfaces of the tetramer. Consequently, each subunit contributes two half Fru-6-P sites and two half allosteric sites, resulting in an average of each subunit containing one full active site and one full allosteric site. The Fru-6-P site is at the cleft between the

large domain and the small domain. The MgATP binding site, located close to the Fru-6-P binding site, is located entirely in the large domain of the subunit.

Despite the fact that BsPFK and EcPFK have a lot of similarity in general characteristics and structure, the kinetic and allosteric characteristics are quantitatively different. Without any effectors and in the presence of a saturating concentration of MgATP, EcPFK displays positive cooperativity for Fru-6-P binding with a Hill number of 3.8.[87,94] No such cooperativity is observed for Fru-6-P binding to BsPFK.[95] However, positive cooperativity between Fru-6-P binding sites is observed at only intermediate PEP concentrations, termed subsaturating heterotropic cooperativity.[35,96] The magnitude of inhibition by effector PEP is greater for BsPFK than EcPFK. The other effector, MgADP, is a strong allosteric activator of EcPFK, but has a small activation effect on BsPFK at 25 °C and below 16 °C inhibition is observed in BsPFK.[97] The allosteric properties of BsPFK are also dependent on pH, unlike those of EcPFK.[98]

The disproportionation equilibria that define allosteric regulation in BsPFK and EcPFK have been extensively examined. The amino acids involved in the binding of the substrate and the allosteric effectors have been extensively substituted and additional specific amino acids lying between the two binding sites have been substituted in an effort to reveal the pathway by which allosteric inhibition and activation are transferred through the enzyme.[35,43,87,96-98] Furthermore, the thermodynamic parameters of ligand binding and allosteric coupling free energy have been determined as a function of temperature, pH, and

hydrostatic pressure.[35,97,99] Each of these various methods is utilized to perturb the disproportionation equilibrium underlying the allosteric response and to study the effects thereon.

Despite their close structural, mechanistic and regulatory likeness, another distinction between EcPFK and BsPFK exists in the thermodynamic driving forces that form the basis for their allosteric inhibition. Van't Hoff analyses have demonstrated that the inhibition of EcPFK is driven by enthalpy and inhibition of BsPFK is governed by entropy. In both cases, the overall coupling free energy, ΔG_{ay}, is positive, as expected for inhibition, and only a few kcal/mol in magnitude.[97,100,101] This represents a phenomenon referred to as entropy-enthalpy compensation, which arises from a small difference between large, opposing entropic and enthalpic components of the free energy. In the case of EcPFK both entropy and enthalpy are positive and the ΔH_{ay} term is larger in magnitude than the ΔS_{ay} term, leading to positive ΔG_{ay}. For BsPFK both entropy and enthalpy are negative and the ΔS_{ay} is larger in absolute value than ΔH_{ay}, similarly leading to positive overall ΔG_{ay}.

Van't Hoff analyses have also revealed that an allosteric effector can undergo a temperature induced inversion of allosteric effect. Below 16 °C, Fru-6-P binding by BsPFK is inhibited by MgADP rather than activated as it is at higher temperatures.[97] Similarly, above 40 °C, MgATP binding by EcPFK is inhibited by PEP, whereas activation is observed at lower temperatures[87]. Subsequently, additional means of perturbing of the disproportionation equilibrium have similarly been shown to induce inversion of allosteric effects. For example, low pH

is predicted to cause the MgADP dependent activation of Fru-6-P binding to become inhibition and the PEP dependent inhibition of Fru-6-P binding by BsPFK to become activation.[42,97] In the cases of both pH and temperature, either the entropic or enthalpic component of the coupling free energy is more sensitive to the perturbation and at some critical value of perturbation the coupling free energy crosses zero, at which point the inversion of allosteric effect is observed.

Phosphofructokinase from *Lactobacillus delbrueckii* subspecies *bulgaricus* (LbPFK) is another PFK isoform studied in our laboratory. LbPFK was reported to be non-responsive to MgADP. Inhibition by PEP was observed at pH 6, but not at pH 8.2.[102] The amino acid sequence of LbPFK is 47% identical and 66% similar to that of EcPFK, and 56% identical and 74% similar to BsPFK. The crystal structure that has been solved essentially overlays with that of the other prokaryotic PFKs.[103] This relatively non-allosteric enzyme can be used as a blank template to study allosteric regulation. In addition, sequence alignment between LbPFK and the prokaryotic PFKs with stronger allosteric couplings may suggest some important residues for allosteric communication.

Thermus thermophilus PFK (TtPFK) binds both inhibitor, PEP, and activator, MgADP, significantly more tightly than other bacterial PFKs while exhibiting a significantly smaller extent of inhibition or activation. These characteristics reinforce the principle that binding affinity and allosteric coupling can be both independent and uncorrelated to one another. In addition, the tighter bindings and modest allosteric coupling allow for the easy obtainment of ternary complex

compared to other prokaryotic PFKs studied in the lab.[104] It was reported in the past that TtPFK undergoes dissociation along the active site interface under conditions of inhibitor binding, manifesting a similar effect on Fru-6-P binding as has been seen in the eukaryotic isoforms.[105] In our lab in it has been determined that the coupling free energies are entropy dominated, as observed previously for PFK from *Bacillus stearothermophilus* but not for PFK from *Escherichia coli*, supporting the hypothesis that entropy dominated allosteric effects may be a characteristic of enzymes derived from thermophilic organisms.[104]

The Present Study

The current study uses an energetics based allosteric linkage framework to examine the forces that make up the allosteric coupling free energy and determine the poise of the disproportionation equilibrium that describes it. Specifically, the effect of enzyme perturbation on the entropy and enthalpy components of the coupling free energy, as well as the coupling free energy itself, are observed. First, the allosteric parameters are determined as a function of urea concentration for both BsPFK and EcPFK. Particular attention is paid to the effects of sub-dissociating concentrations of urea. The structure of the enzyme was also perturbed by introducing conservative isoleucine to valine mutations, essentially making the structure more flexible by adding small "holes" via the removal of single methyl groups from four different native isoleucines. Both the urea studies and the hole

mutant data support the notion of different underlying mechanisms for inhibition of PFK in BsPFK and EcPFK.

Methyl-TROSY NMR was employed in order to obtain structural information on BsPFK in all four states of ligation relevant to the allosteric coupling. BsPFK was uniformly ^{15}N and ^{2}H labeled and specifically labeled with δ-[$^{13}CH_3$]-isoleucine using an isotopically labeled α-keto acid precursor. Methyl-TROSY experiments were conducted in all four ligation states, and the analysis has allowed specific regions of the enzyme involved in the binding of allosteric ligands and the propagation of the allosteric signal to be identified.

CHAPTER II

CHARACTERIZATION OF THE W179F/F240W MUTANT OF *BACILLUS STEAROTHERMOPHILUS* PHOSPHOFRUCTOKINASE

Introduction

Phosphofructokinase (PFK) transfers the γ-phosphate of MgATP to fructose-6-phosphate (Fru-6-P) forming fructose-1,6-bisphosphate in the first committed step of glycolysis. Due to its significance in glucose metabolism, the reaction is subject to strong metabolic regulation. The regulation of eukaryotic PFK is very complex, however insight into the allosteric regulation of eukaryotic PFK can be gained through the study of the much simpler regulation exhibited by prokaryotic PFK. As a consequence, prokaryotic PFK has been thoroughly characterized and often serves as a model allosteric enzyme.[88,90,93,101,106,107] PFK from *Bacillus stearothermophilus* (BsPFK) and *Escherichia coli* (EcPFK) are two extensively studied prokaryotic PFK homologs. Both enzymes are homotetramers in which monomers associate into a dimer of dimers creating two unique pairs of identical subunit-subunit interfaces. One pair, termed the substrate binding interfaces, contain two Fru-6-P binding sites each for a total of four identical Fru-6-P binding sites per homotetramer. Similarly, each effector binding interfaces have two effector binding sites each, creating four identical effector binding sites.

The activities of EcPFK and BsPFK are inhibited by phosphoenol-pyruvate (PEP)[98,108] and activated by MgADP[109,110] binding at the same effector binding site. PEP and MgADP both function as K-type effectors, meaning they alter the affinity of PFK for Fru-6-P as opposed to changing the enzyme's maximum velocity. In both EcPFK and BsPFK there is a prominent antagonism between MgATP and Fru-6-P binding.[69,87,111,112] In the case of EcPFK, the antagonism appears to be the result of an allosteric interaction between neighboring active sites as well as within single active sites.[87,113] The antagonism observed with BsPFK , however, has been hypothesized to be the result of either an alternative pathway mechanism in which rate limiting binding of MgATP results in a kinetically disfavored pathway at high concentrations of MgATP and low concentrations of Fru-6-P or abortive binding of MgATP in the Fru-6-P binding site.[69] In either case, the observed antagonism between Fru-6-P and MgATP binding appears to be a non-allosteric phenomenon.

BsPFK and EcPFK each have a single tryptophan per monomer. The indole group of the amino acid tryptophan can serve as a naturally occurring fluorophore in a protein. The λ_{max} of tryptophan is quite sensitive to the polarity of its local environment, ranging from ~308 nm (azurin) to ~355 nm (glucagon) and roughly correlates with the degree of solvent exposure of the indole. More precisely, the wavelength is determined principally by the electrical potential difference across the long axis of the indole ring.[114] This means that the relative direction of a charge from the tryptophan ring is crucial: positive charges create a red shift when on the benzene ring end and a blue shift when on the pyrrole ring end, with the size of the

shift being inversely proportional to the distance from the center of the tryptophan ring. The reverse is true for negative charges. Frequently, spectral shifts are also observed as a result of other phenomena that alter the local environment of the residue, such as the binding of ligands or protein-protein interactions.[115]

In theory, the single tryptophan residues of BsPFK and EcPFK can be used as fluorescence probes to study and compare the biophysical properties of the enzymes. Turnover is not a problem when measuring ligand dissociation constants or the allosteric coupling constant using a tryptophan fluorescence probe, therefore these values are best determined under equilibrium conditions in the absence of turnover. The fluorescence intensity of the native tryptophan residue in EcPFK, at position 311, is in fact responsive to both substrate and effector binding. Unfortunately, the native tryptophan in BsPFK is largely unresponsive to ligand binding.[116] The native position, 179, in BsPFK has been shown to be inaccessible to the bulk solvent and quenchers such as acrylamide.[116] This was confirmed by X-ray crystallography structures showing that the residue is buried deep within the core of the protein.[91,116]

In order to overcome the failure of tryptophan as an effective fluorescence probe in its native position, the present study constructs and characterizes a tryptophan-shifted mutant. In this mutant the native tryptophan at position 179 has been substituted to a phenylalanine and the phenylalanine at position 240 has been substituted to a tryptophan. Phenylalanine was chosen, in an attempt to make the substitutions as conservative as possible, due to its bulky structure and non-

polar, hydrophobic nature that resemble tryptophan. As pictured in Figure 2-1, X-ray crystallography structures show that the residue is likely to be at least partially exposed to the solvent. In addition, work completed previously in our lab indicates that changes in the dynamics in the region around position 240 in BsPFK may be associated with the propagation of the allosteric signal.[117]

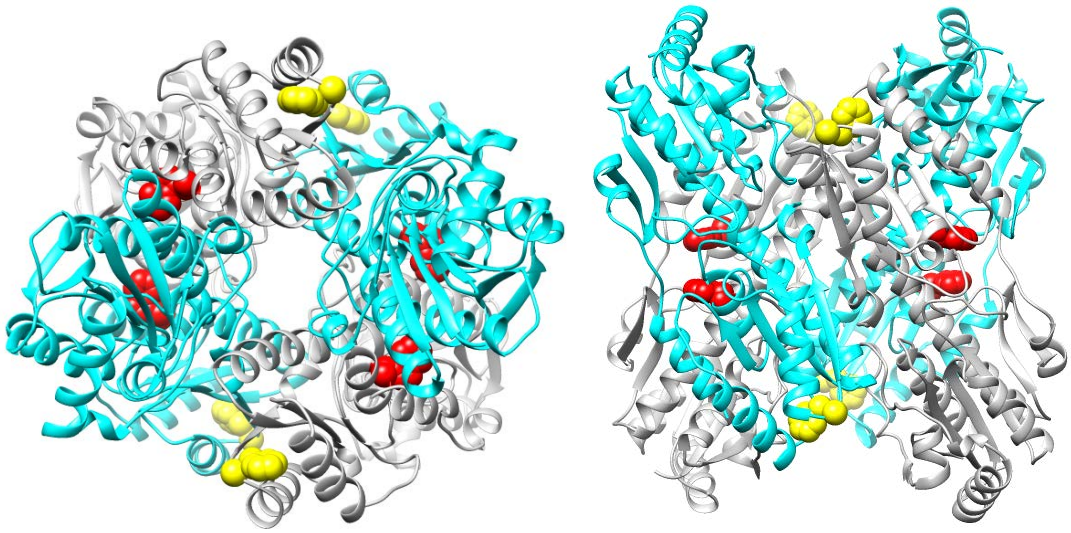

Figure 2-1: X-ray crystallography structure highlighting the location of the native tryptophan residue (red) and the phenylalanine (yellow) that was mutated to tryptophan in W179F/F240W-BsPFK.

The allosteric coupling between PEP binding and Fru-6-P binding assessed by steady-state kinetic assays is similar to the allosteric coupling seen in the wild-type (WT) enzyme thus indicating that the mutation has not significantly affected the structure or function of the enzyme. Additionally, the kinetic data show that the

apparent dissociation constant for Fru-6-P in the absence of PEP, $K_{ia}°$, for the variant is equivalent to WT-BsPFK and the apparent dissociation constant for PEP binding in the absence of Fru-6-P, K_{iy}^{o}, is only 2-fold greater than what is observed for wild-type BsPFK. Moreover, the similarity between this BsPFK variant and WT-BsPFK make the variant a good substitute for WT-BsPFK when a fluorescence probe is needed to study the ligand binding properties of the enzyme.

Importantly, the variant's tryptophan at position 240 has a fluorescence intensity that changes more in response to ligand binding than WT-BsPFK and can serve as a fluorescence probe for looking at the allosteric coupling between substrate, Fru-6-P, and effector, PEP. Due to the similarities between WT-BsPFK and the variant structurally and functionally, and the contrasting fluorescence properties, we were able to use the variant to examine the validity of the rapid equilibrium assumption in BsPFK by comparing the ligand binding and coupling parameters determined kinetically to those determined thermodynamically under equilibrium conditions.

Materials and Methods

Materials

All chemical reagents used in buffers for protein purification, enzymatic assays, and fluorescence assays were of analytical grade and were purchased from Sigma-Aldrich (St. Louis, MO), Fisher Scientific (Fair Lawn, NJ), or Research

Products International (Mt. Prospect, IL). Deionized distilled water was used throughout. Lyophilized creatine kinase, the ammonium sulfate suspension of glycerol-3-phosphate dehydrogenase, and the potassium salt of phosphoenol-pyruvate were purchased from Roche (Indianapolis, IN). The ammonium sulfate suspensions of aldolase, the ammonium sulfate suspension of triosephosphate isomerase, the disodium salt of fructose-6-phosphate, and the disodium salt of phosphocreatine were purchased from Sigma-Aldrich (St. Louis, MO). The coupling enzymes were extensively dialyzed against 50 mM EPPS pH 8.0, 100 mM KCl, 5 mM $MgCl_2$, and 0.1 mM EDTA before use. NADH and DTT were purchased from Research Products International (Mt. Prospect, IL). Mimetic Blue 1 A6XL resin used in protein purification was purchased from Promatic BioSciences (Rockville, MD). The Mono-Q HR anion exchange column used in protein purification was purchased prepacked for FPLC use from Pharmacia (currently GE Healthcare, Uppsala, Sweden). Macro-Prep High-Q anion exchange resin was purchased from Bio-Rad (Hercules, CA). Amicon Ultra centrifugal filter units (spin concentrators) were from Millipore Corporation (Billerica, MA) and poly(ethylene glycol)-3000 was from Sigma-Aldrich (St. Louis, MO). Site-directed mutagenesis was performed using the QuikChange Site-Directed Mutagenesis System from Stratagene (La Jolla, CA). Oligonucleotides were synthesized and purchased from Integrated DNA Technologies, Inc (Coralville, IA). DNA modifying enzymes and dNTPs were purchased from Stratagene (Cedar Creek, TX), New England Biolabs (Ipswich, MA), or Promega (Madison, WI).

Site-Directed Mutagenesis

The plasmid pBR322/BsPFK[118] contains the gene for BsPFK behind the native *Bacillus stearothermophilus* promoter and was received as a generous gift from Simon H. Chang (Louisiana State University). Two successive rounds, one for each mutation, of mutagenesis were performed following the protocol outlined in the QuikChange Site-Directed Mutagenesis System from Stratagene. For each mutation, two complementary oligonucleotides were designed to target the sequence surrounding the codon for each of the mutated amino acids; the template oligonucleotides are shown below:

F240W-BsPFK: 5' – CCA GGA AGC GAC CGG CTG GGA GAC GCG TGT GAC G – 3'

W179F-BsPFK: 5' – CGA CAT CGC CTT ATT TTC GGG GCT GGC CGG – 3'

Protein Purification of Wild-Type and W179F/F240W BsPFK

Wild-type BsPFK was expressed in *E. coli* RL257 cells[119], which is a strain of *E. coli* lacking both the pfkA and pfkB genes. The purification of BsPFK was performed as described previously, with a few modifications.[95] RL257 cells containing the plasmid pBR322/BsPFK were grown at 37 °C for 16 - 18 hours in LB (Lysogeny Broth) tetracycline (tryptone 10 g/L, yeast extract 5 g/L, NaCl 10 g/L, and tetracycline 15 μg/mL). Cells were harvested by centrifugation and frozen at -20 °C for a minimum of 12 hours. The cells were resuspended in 60 mL of purification buffer (10 mM Tris-HCl pH 8.0, 1 mM EDTA) and sonicated using a Fisher 550 Sonic Dismemberator at 0 °C in 15 second pulses at setting six for 8-12

minutes. The crude lysate was centrifuged at 22,500 x g for 30 minutes at 4 °C. The clarified supernatant was incubated in a 70 °C water bath for 15 minutes, cooled on ice for 15 minutes, and centrifuged again at 22,500 x g for 30 minutes at 4 °C. The supernatant was diluted to at least 500 mL and then loaded onto a 100 mL Mimetic Blue 1 A6XL column that was previously equilibrated with purification buffer. The column was washed with purification buffer until the A_{280} reached a baseline, and the enzyme was eluted with a 0 - 1.5 M NaCl gradient. Fractions containing enzyme activity were pooled and dialyzed into 20 mM Tris-HCl pH 8.5 and loaded onto a Pharmacia/GE Healthcare Mono-Q HR anion exchange column that was pre-equilibrated with the same buffer. The enzyme was eluted with a 0 - 1 M NaCl gradient, and fractions containing pure BsPFK were combined, concentrated with either a spin concentrator or poly(ethylene glycol) 3000, and then dialyzed into EPPS buffer (50 mM EPPS pH 8.0, 10 mM $MgCl_2$, 100 mM KCl, 0.1 mM EDTA). The final enzyme was determined to be pure by SDS-PAGE, and stored at 4 °C. The enzyme concentration was determined by measuring the absorbance at 280 nm (ε = 18910 $M^{-1}cm^{-1}$).[120]

Steady-State Kinetic Assays

Activity measurements for PFK were carried out using a coupled enzyme system[121,122] in a 0.6 mL reaction volume of EPPS buffer containing 50 mM EPPS, 5 mM $MgCl_2$, 100 mM KCl, 0.1 mM EDTA, 2 mM DTT, 0.2 mM NADH, 3 mM ATP, 250 µg aldolase, 50 µg of glycerol-3-phosphate dehydrogenase, and 5 µg of

triosephosphate isomerase at pH 8.0 and 25 °C unless otherwise noted. 40 μg/mL of creatine kinase and 4 mM phosphocreatine were added as an ATP regenerating system to avoid the accumulation of MgADP, which is an activator. Temperature was controlled using a NESLab RTE-111 circulating water bath. Fru-6-P and PEP were added at varied concentrations as indicated. Assays were started by the addition of 10 μL of appropriately diluted PFK and the reaction was monitored as the absorbance at 340 nm decreased over time. The rate of the reaction was measured on Beckman Series 600 spectrophotometers using a linear regression calculation to convert change in absorbance at 340 nm to PFK activity. One unit of PFK activity is described as the amount of enzyme needed to produce 1 μmol of fructose-1,6-bisphosphate per minute.

Steady-State Fluorescence Assays

Fluorescence intensity measurements were performed using an ISS KOALA fluorometer. Enzyme concentration was 0.5 μM and ligand titrations were performed in buffer containing 50 mM EPPS, 100 mM KCl, 5 mM $MgCl_2$, and 0.1 mM EDTA at pH 8.0 and 25˚C unless otherwise indicated. Samples were excited using a xenon arc lamp and an excitation monochromator to select for 295 nm. The fluorescence intensity was detected using the 2-mm 335 nm Schott cut-on filter or an emission monochromator. Neutral density filters in were placed between the excitation monochrometer and the sample to keep the number of counts in the range of 100,000 counts/sec. Titrations were carried out with a 1.5 mL initial

volume in a standard 1 cm x 1 cm cuvette. All measurements were blank subtracted, and corrected for dilution of enzyme concentration.

Data Analysis

Steady-state kinetics and steady-state fluorescence data were fit using the non-linear least-squares fitting analysis option in Kaleidagraph software version 4.5 (Synergy). For the steady-state kinetic assays the initial velocity data were plotted against concentration of Fru-6-P and fit to the Hill equation[8]:

$$v = \frac{V[A]^{n_H}}{K_a^{n_H} + [A]^{n_H}} \tag{2-1}$$

where, v is the initial velocity, $[A]$ is the concentration of the substrate Fru-6-P, V is the maximal velocity, and n_H is the Hill coefficient. K_a is the concentration of Fru-6-P at which the enzyme's activity is half maximal. Assuming rapid equilibrium for Fru-6-P, which was shown to be valid in EcPFK using a steady-state kinetic method, K_a is equivalent to the dissociation constant for Fru-6-P from the binary enzyme-substrate complex[34,101]. MgATP, the other substrate, does not achieve rapid equilibrium during catalytic turnover.[87] Data collected using steady-state fluorescence assays were plotted as the relative fluorescence intensity as a function of PEP concentration. The data were fit using eq 2-2.

$$F = \frac{(F - F^o)[Y]^{n_H}}{K_y^{n_H} + [Y]^{n_H}} + F^o \tag{2-2}$$

where, F is the relative intensity, F^o is the relative intensity in the absence of PEP, $[Y]$ is the concentration of PEP, n_H is the Hill coefficient, and K_y is the apparent dissociation constant for PEP. K_a values obtained from the initial velocity experiments, and K_y values obtained from the steady-state fluorescence experiments were plotted against the concentration of opposing ligand and fit to eq 2-3 or 2-4

$$K_a = K_{ia}^o \left(\frac{K_{iy}^o + [Y]}{K_{iy}^o + Q_{ay}[Y]} \right) \tag{2-3}$$

$$K_y = K_{iy}^o \left(\frac{K_{ia}^o + [A]}{K_{ia}^o + Q_{ay}[A]} \right) \tag{2-4}$$

where K_{ia}^o is the dissociation constant for Fru-6-P in the absence of PEP, K_{iy}^o is the dissociation constant for PEP in the absence of Fru-6-P, and Q_{ay} is the coupling coefficient[32,33,123]. Q_{ay} describes the effect of the allosteric effector on the binding of the substrate and/or the effect of the substrate on the binding of the allosteric effector, and is defined below:

$$Q_{ay} = \frac{K_{ia}^o}{K_{ia}^\infty} = \frac{K_{iy}^o}{K_{iy}^\infty} \tag{2-5}$$

where K_{ia}^∞ is the dissociation constant for Fru-6-P in the saturating presence of PEP, and K_{iy}^∞ is the dissociation constant for PEP in the saturating presence of Fru-6-P. Based on its definition, Q_{ay} represents the equilibrium constant for the following disproportionation equilibrium:

$$[\mathrm{EA}] + [\mathrm{YE}] \overset{Q_{ay}}{\longleftrightarrow} [\mathrm{YEA}] + [\mathrm{E}] \tag{2-6}$$

where E is free enzyme, YE is the PEP bound binary complex, EA is the Fru-6-P bound binary complex, and EAY is the ternary complex were both ligands are bound simultaneously. The coupling constant, Q_{ay} , is related to the coupling free energy (ΔG_{ay}) and its entropy ($T\Delta S_{ay}$) and enthalpy (ΔH_{ay}) components through the following relationship:

$$\Delta G_{ay} = \Delta H_{ay} - T\Delta S_{ay} = -RTln(Q_{ay}) \quad (2\text{-}7)$$

ΔG_{ay} represents a standard free energy, although the superscript "0" is removed from the designation to avoid confusion with the use of that superscript for other purposes in notation.[32] The coupling entropy and enthalpy components were determined by measuring the coupling constant as a function of temperature and the data were fit to eq 2-8:

$$\log(Q_{ay}) = \frac{\Delta S_{ay}}{R \times 2.303} - \frac{\Delta H_{ay}}{R \times 2.303}\left(\frac{1}{T}\right) \quad (2\text{-}8)$$

where, T is absolute temperature in Kelvin, and R is the gas constant (R=1.99 cal K^{-1} mol^{-1}).

Results

To determine whether or not the tryptophan residue in W179F/F240W-BsPFK serves as a functional fluorescence probe, emission spectra of the enzyme were collected from free enzyme and the two binary complexes. Shown in Figure 2-

2, all emission spectra were taken at 25 ˚C, pH 8.0, λ_{ex} = 295 nm, and with an enzyme concentration of 0.5 µM. The emission spectrum of W179F/F240W-BsPFK

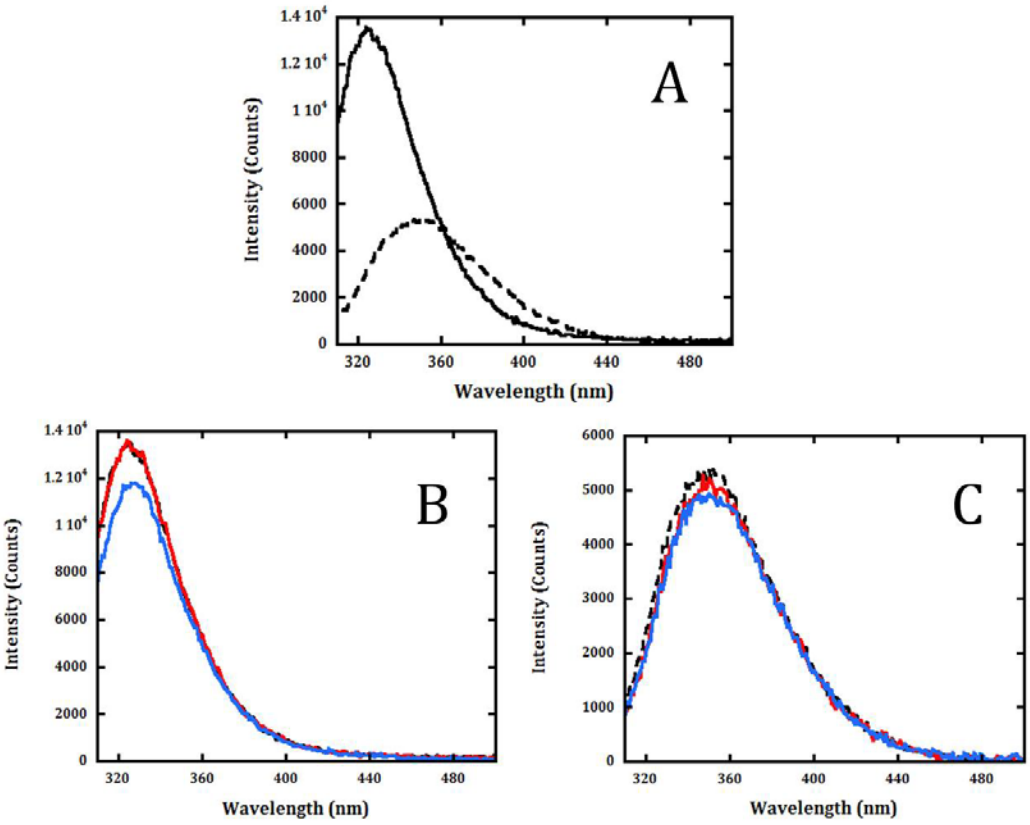

Figure 2-2: A) Emission spectra of WT-BsPFK, solid lines, and W179F/F240W-BsPFK, broken lines. B) is WT-BsPFK and C) is W179F/F240W-BsPFK in the apo-form and in the presence of 2 mM PEP, red, or 1 mM Fru-6-P, blue.

is red shifted in comparison to WT-BsPFK (from 332 nm to 350 nm). Another major difference between the two spectra is the overall intensity, which is much greater in the WT-BsPFK enzyme. Figure 2-2B and C show the emission spectra of WT and W179F/F240W-BsPFK in the absence and presence of ligands, respectively. As

anticipated, moving the tryptophan to a more solvent exposed location generated an increase in responsiveness of its intrinsic fluorescence to the binding of ligands. A decrease in the fluorescence intensity of 16 – 20% is associated with PEP binding and a decrease of 5 - 6 % is associated with Fru-6-P binding. WT-BsPFK displays no change in fluorescence intensity in response to the binding of Fru-6-P and only a 10% decrease in response to PEP. The changes in fluorescence intensity were further examined by titrating the mutant with ligand. Again, a similar response to ligand binding is observed (Figure 2-3).

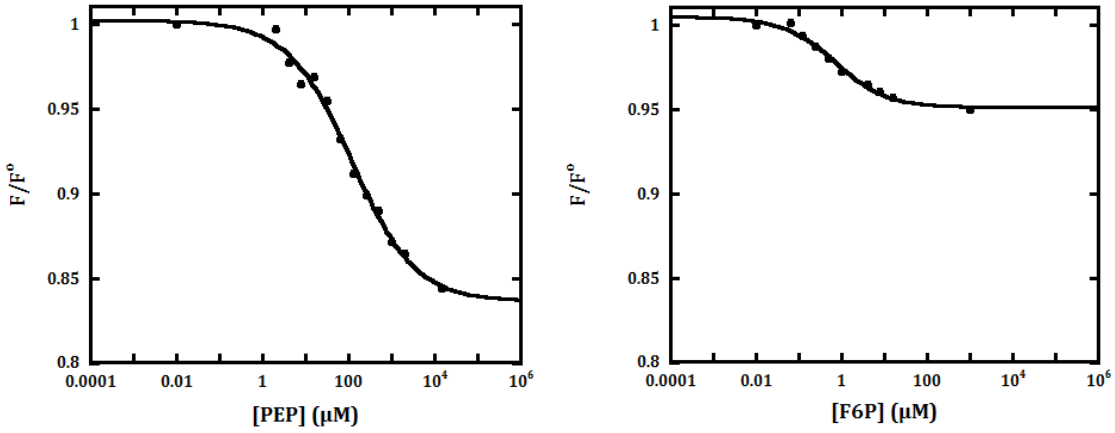

Figure 2-3: A) Relative fluorescence intensity as a function of [PEP] and B) [Fru-6-P] for W179F/F240W-BsPFK.

To determine whether or not the structure of the enzyme had been significantly altered in response to the mutation, the functional characteristics of W179F/F240W -BsPFK were determined by steady-state kinetic assays and compared to WT-BsPFK. First, the specific activity of W179F/F240W-BsPFK (169 ±

4 U/mg) was determined to be comparable to WT-BsPFK (178 ± 5 U/mg). Eq 2-1 was used to determine the K_a values for Fru-6-P at varying concentrations of PEP. Eq 2-3 was then used to determine the binding constants, K_{ia}^{o} and K_{iy}^{o}, and coupling constant, Q_{ay}, for both mutant and WT enzymes. MgATP concentration was held constant at a saturating concentration of 3 mM and the results are presented in Figure 2-4. Fru-6-P binding in the mutant enzyme is equivalent to that displayed by

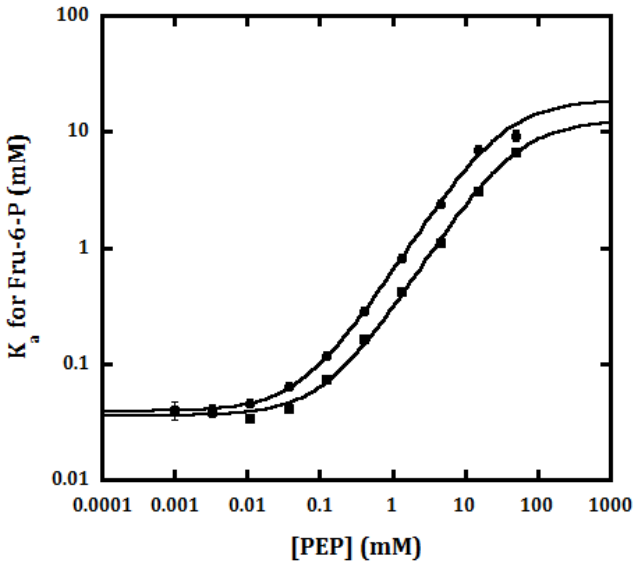

Figure 2-4: K_a vs. [PEP] for WT and W179F/F240W-BsPFK by steady-state kinetic assays. Circles are wild-type BsPFK in the presence of 3 mM MgATP. Squares are the mutant BsPFK in the presence of 3 mM MgATP.

WT-BsPFK. PEP binding is about 2-fold weaker in the mutant enzyme, as indicated by the shift in the curve to the right. PEP's ability to inhibit the binding of Fru-6-P is

not affected, as indicated by the similar values for the allosteric coupling constant, Q_{ay}.

Kinetics data indicate that W179F/F240W-BsPFK is a good substitute for WT-BsPFK, and it has the added functionality of containing a sensitive fluorescence probe. Due to the requirement of MgATP as the second substrate in the PFK reaction, the binding of Fru-6-P in the absence of MgATP cannot be directly determined via steady-state kinetic assays without extrapolation. This variant allowed the determination of the dissociation constants associated with the allosteric response in the absence of MgATP and under equilibrium conditions. Thermodynamic linkage dictates reciprocity between the binding of Fru-6-P and PEP. In other words, the effect of PEP on Fru-6-P binding is equivalent to the effect of Fru-6-P on PEP binding. Therefore, dissociation constants can be obtained for either ligand. In this case, W179F/F240W-BsPFK, the percent change in fluorescence intensity in response to PEP binding is greater than that seen with Fru-6-P, making it easier to determine K_y than K_a. The dissociation constant for PEP, K_y, was determined as shown above in Figure 2-3A as a function of Fru-6-P concentration and fit to eq 2-4 (Figure 2-5). The numerical values obtained from the fit are compared to steady-state kinetic data in Table 2-1. Q_{ay} and K_{iy}^{o} are not

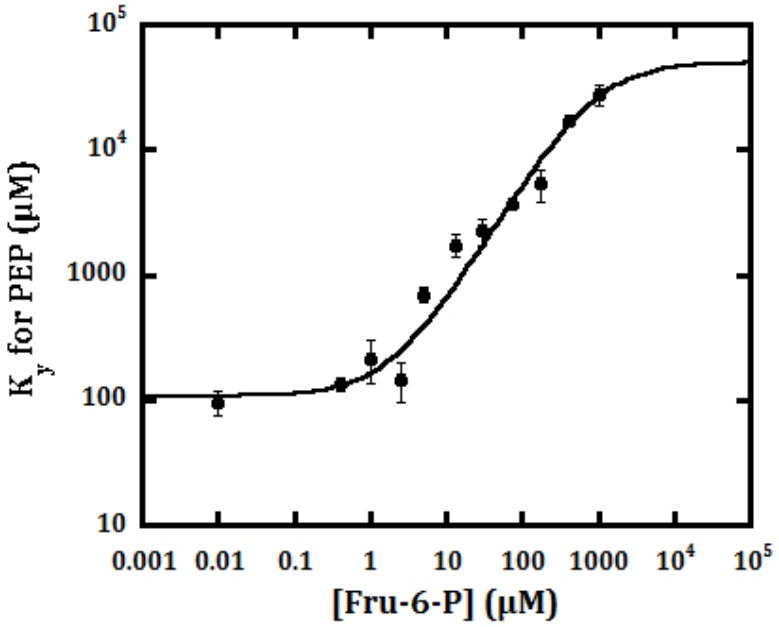

Figure 2-5: K_y vs. [Fru-6-P] for W179F/F240W-BsPFK by steady-state fluorescence assays in the absence of MgATP.

Table 2-1: Thermodynamic parameters for WT and the W179F/F240W mutant of BsPFK determined in the presence (K) and absence (F) of MgATP.

	K_{ia}^{o} (μM)	K_{iy}^{o} (μM)	Q_{ay}
WT (K)	39 ± 2	63 ± 2	0.0021 ± 0.0002
W179F/F240W (K)	36 ± 1	128 ± 6	0.0029 ± 0.0001
W179F/F240W (F)	1.9 ± 0.3	110 ± 10	0.0022 ± 0.0007

affected by MgATP. K_{ia}^{o}, however, is more than an order of magnitude smaller in the absence of MgATP. This is consistent with previous studies that illustrate the ability of MgATP to act as an antagonist to Fru-6-P binding in BsPFK.[106] K_a for Fru-6-P was

determined using steady-state kinetics at varying concentrations of MgATP (Figure 2-6) with W179F/F240W-BsPFK. As the concentration of MgATP was decreased from 3 mM to 2 μM, the value of K_a for Fru-6-P decreased from 36.0 to 6.6 μM. The curve was extrapolated to get a K_a^o value of 6.5 ± 0.1 μM.

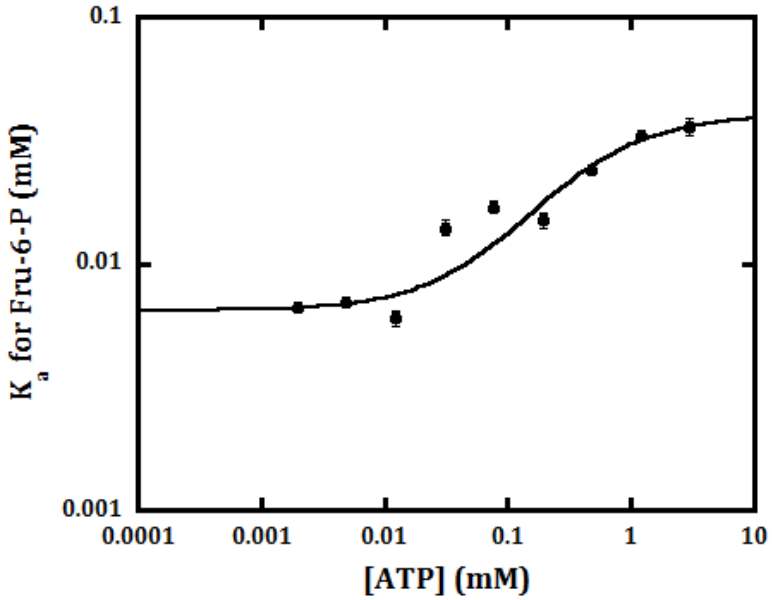

Figure 2-6: K_a for Fru-6-P as a function of [ATP] concentration at 25 °C and pH 8.0 measured with steady-state kinetics.

To further verify that the mutations have not substantially modified the allosteric behavior of W179F/F240W-BsPFK, the coupling constant was then determined as a function of temperature for both wild-type and the mutant (Figure 2-7). Van't Hoff analysis for the mutant was performed both in the presence of

MgATP by steady-state kinetic assays, and in the absence of MgATP and turnover by steady-state fluorescence assays. Using eq 2-7 van't Hoff analysis allowed for the

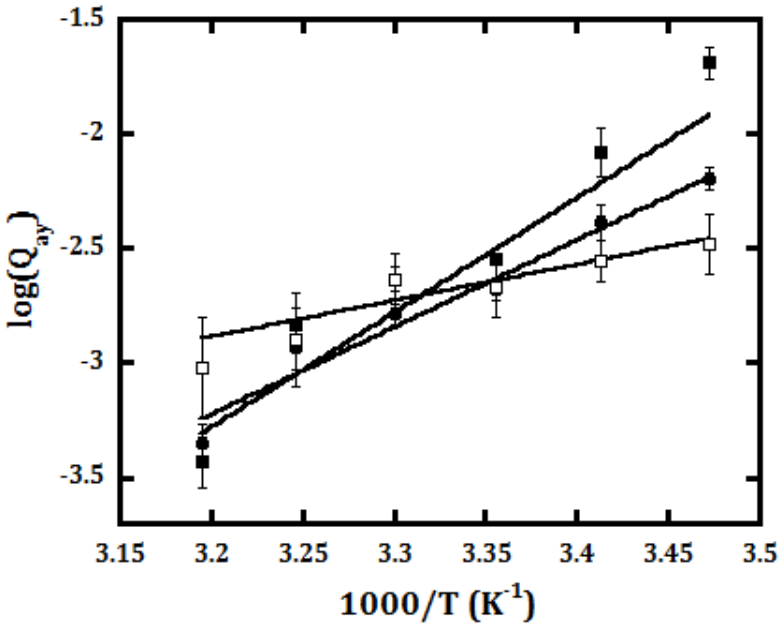

Figure 2-7: Van't Hoff analysis of wild-type and W179F/F240W-BsPFK. Circles are WT-BsPFK in the presence of MgATP. Filled squares are the mutant BsPFK in the presence of MgATP. Open squares are the mutant BsPFK in the absence of MgATP.

determination of the entropy and enthalpy components of the coupling free energy, which are shown below in Table 2-2. The values for $\Delta H_{ay,}$ and $T\Delta S_{ay}$ are only

Table 2-2: Thermodynamic parameters associated with the allosteric interaction between Fru-6-P and PEP for wild-type and mutant W179F/F240W-BsPFK at 25 °C in the presence (K) and absence (F) of MgATP.

	ΔH_{ay} (kcal/mol)	$T\Delta S_{ay}$ (kcal/mol)	ΔG_{ay} (kcal/mol)
WT (K)	-17.4 ± 1.3	-21.0 ± 1.3	3.65 ± 0.03
W179F/F240W (K)	-22.9 ± 1.6	-26.2 ± 1.6	3.46 ± 0.04
W179F/F240W (F)	-7.2 ± 3.1	-10.8 ± 3.1	3.6 ± 0.2

slightly different between mutant and WT-BsPFK in the presence of MgATP. Although the absolute values for ΔH_{ay}, and $T\Delta S_{ay}$ are substantially different for the mutant BsPFK in the presence and absence of MgATP, in both cases the entropy and enthalpy components are compensating (i.e. have the same sign). In addition, the sign of ΔG_{ay} is determined by the larger absolute value of the entropy component in all cases, which is in agreement with previous data.[42]

An additional observation was made in regards to the fluorescence intensity of the W179F/F240W-BsPFK mutant. With increasing enzyme concentration, the % change in response to PEP binding is decreased as shown in Figure 2-8. Upon

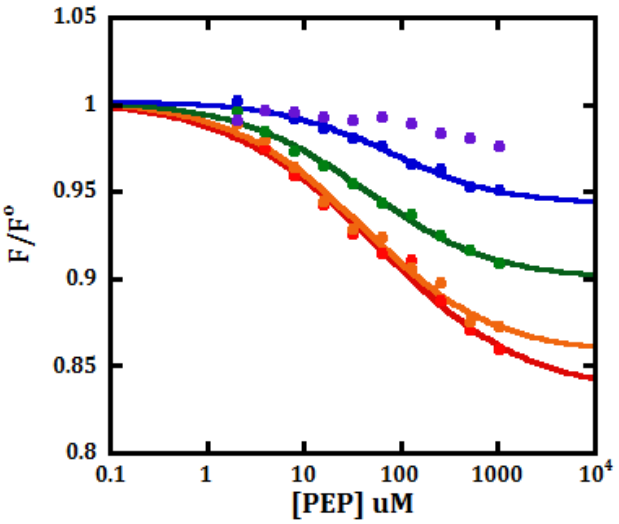

Figure 2-8: Relative fluorescence intensity as a function of [PEP] at a range of enzyme concentrations from 0.25 µM (red) to 6 µM (purple).

further investigation, it was determined that PEP binding to the variant led to a loss in enzymatic activity corresponding with the decrease in intensity. This loss in activity could be restored by incubation in Fru-6-P, indicating that PEP binding is likely causing dissociation into dimers at low enzyme concentrations.

Discussion

The primary purpose of this study was to construct a variant of BsPFK that would both have a fluorescence intensity that is responsive to ligand binding and maintain all of the ligand binding and allosteric properties of the unresponsive WT-BsPFK. The added ability to study BsPFK using a purely thermodynamic approach,

using the engineered fluorescence probe, is beneficial because there is no need to invoke the rapid-equilibrium assumption in order to justify a thermodynamic interpretation of the data. As demonstrated by the data above, W179F/F240W-BsPFK meets both of these requirements.

It is critical to be able to relate fluorescence characterization of the mutant directly to wildtype. Overall, the kinetic assessment of WT-BsPFK and W179F/F240W-BsPFK shows that the mutation did not significantly alter the activity or allosteric functionality of the enzyme. However, as the above data indicate, there are a few small differences between the two enzymes. Namely, the binding of PEP is 2-fold weaker in the mutant compared to WT-BsPFK, and the allosteric effect of PEP on Fru-6-P binding is very slightly diminished in the mutant (decrease in ΔG_{ay} of 0.19 kcal/mol). Van't Hoff analysis shows that the allosteric coupling between PEP and Fru-6-P is entropy driven at 25 °C for the variant. This means that it is the larger absolute value of the negative entropy component, opposed to the enthalpy component, which determines the positive allosteric coupling free energy that defines PEP as an inhibitor. W179F/F240W-BsPFK's entropy-driven coupling is in direct contrast to what has been reported for EcPFK[43,101], but is agreement with what has been previously reported for WT-BsPFK[42]. Overall, the kinetic comparison indicates that data obtained using the mutant BsPFK can be extrapolated to wild-type BsPFK and that the mutant is a good candidate for further studies probing a deeper understanding of the biophysical properties involved in BsPFK allosterism.

Using F179W/W240F-BsPFK, the extent of allosteric coupling between fru-6-P and PEP was determined to be the same regardless of whether determined by steady-state kinetic or steady-state fluorescence techniques. The fluorescence assays are performed in the absence of the second substrate, MgATP, demonstrating that MgATP does not have an effect on the allosteric coupling between Fru-6-P and PEP. The apparent dissociation constant for PEP, K_{iy}^{o}, is unchanged by the presence of MgATP. On the other hand, there is a 19-fold increase in K_{ia}^{o} in the presence of MgATP. This result was expected, as it has been shown previously that MgATP antagonizes Fru-6-P binding at the active sites.[69] In addition, these results are in agreement to those determined previously with another BsPFK tryptophan-shifted mutant[112], and with EcPFK[101]. The steady-state kinetic data presented in Figure 2-6 demonstrate the decrease in K_a as a function of MgATP concentration, and were extrapolated to obtain a value for K_a^o in the absence of MgATP of 6.5 ± 0.1 μM. The validity of the rapid equilibrium assumption depends on the agreement of this value to the K_{ia}^{o} value obtained by the fit of the data in Figure 2-4 to eq 2-2, which is 1.9 μM. Even though these values are in very close agreement, they are not within error of each other. One explanation for this discrepancy could be possible failure of the rapid equilibrium assumption at low ATP concentrations due to tight binding. It was also demonstrated that PEP likely causes a dissociation of the tetramer at low enzyme concentrations in W179F/F240W-BsPFK. It is probable that this effect only occurs in the absence and at very low concentrations of Fru-6-P, as Fru-6-P is able to stabilize the active site

interface. This effect could lead to an illusion of tighter binding at these low concentrations, providing an additional potential explanation for the discrepancy in K_{ia}^{o}.

CHAPTER III

THE EFFECT OF UREA ON THE ALLOSTERIC PARAMETERS OF PHOSPHOFRUCTOKINASE FROM *BACILLUS STEAROTHERMOPHILS* AND *ESCHERICHIA COLI*

Introduction

There is some controversy over the mechanism by which urea denatures proteins, however it is generally described as either indirect, direct or a combination of the two.[124] Indirect denaturation refers to a mechanism where urea denatures proteins by disrupting the water structure, which in turn weakens the hydrophobic interaction and makes the protein's hydrophobic residues less compact and more readily solvated. Through a direct mechanism urea unfolds through direct interactions with proteins, either through stronger electrostatic interactions with the backbone and/or polar residues or through favored van der Waals attractions with protein residues. Most recent studies are in support of a more direct mechanism, although a few indicate that the indirect mechanism probably also plays a role in urea induced protein denaturation.

Even less well understood than the mechanism of urea denaturation is how the structural and energetic properties of proteins change in response to urea. X-ray crystallography structures have shown that protein crystals soaked in low concentrations of urea, and other denaturants, display a reduced average isotropic

MSD (mean square deviations).[125,126] This suggests a reduction in the flexibility of the protein in response to the addition of subdenaturing concentrations. Previous studies indicate that polyfunctional interaction between proteins groups and denaturants are responsible for such stabilization.[127,128] The interaction of the denaturant molecule with different groups of protein through noncovalent bonding can established nonspecific network of intramolecular interaction. Such denaturant mediated crosslinking of different parts of the protein leads to a decrease of intramolecular dynamics. Although data exists supporting a protein stabilization role for low concentrations of urea, there is a lack of direct biochemical evidence for increased rigidity in the presence of low concentrations of denaturants.

Prokaryotic phosphofructokinase (PFK) catalyzes the phosphorylation of fructose-6-phosphate (Fru-6-P) by MgATP to form fructose 1,6-bisphosphate and MgADP in the first committed step of glycolysis. This crucial glycolytic reaction is allosterically inhibited by the downstream pathway intermediate, phosphoenol-pyruvate (PEP), and activated by product MgADP in a classic example of K-type allosteric regulation. Even though these two small molecules have an opposite effect on the enzyme's affinity for substrate, Fru-6-P, they bind at the same allosteric site.[101,109] In the case of allosteric inhibition of PFK, there is an increase in the K_a for Fru-6-P while PEP is bound at the allosteric site. This change is accompanied by a diminution in the magnitude of the absolute values for the free energy of substrate binding. Accordingly, an allosteric coupling free energy can be defined which relates the difference between the substrate binding energy when

effector is saturating to the binding energy in the absence of effector, or the equivalent reciprocal effect.[9-11]

$$Q_{ay} = \frac{K_{ia}^{o}}{K_{ia}^{\infty}} = \frac{K_{iy}^{o}}{K_{iy}^{\infty}} = \frac{[PEP{:}\,PFK{:}\,\text{Fru–6–P}][PFK]}{[PFK{:}\,\text{Fru–6–P}][PEP{:}\,PFK]} \quad (3\text{-}1)$$

K_{ia}^{o} represents the thermodynamic dissociation constant for substrate in the absence of allosteric effector, K_{ia}^{∞} is the dissociation constant with allosteric effector saturating the enzyme and Q_{ay} is the ratio of these two parameters. From the above equations, it is evident that Q_{ay} also represents the equilibrium constant for the shown disproportionation equilibrium. K_{ia}^{o} represents the thermodynamic dissociation constant for substrate in the absence of allosteric effector, K_{ia}^{∞} is the dissociation constant with allosteric effector saturating the enzyme and Q_{ay} is the ratio of these two parameters. From the above equations, it is evident that Q_{ay} also represents the equilibrium constant for the shown disproportionation equilibrium.

$$PFK{:}\,\text{Fru–6–P} + PEP{:}\,PFK \overset{Q_{ay}}{\longleftrightarrow} PEP{:}\,PFK{:}\,\text{Fru–6–P} + PFK \quad (3\text{-}2)$$

Q_{ay} is related to the coupling free energy though the following relationship

$$\Delta G_{ay} = -RTln(Q_{ay}) \quad (3\text{-}3)$$

ΔG_{ay} represents a standard free energy, although the superscript "0" is dropped from the designation to avoid confusion with the use of that superscript for other purposes in notation.[32] Since ΔG_{ay}describes quantitatively both the nature and the magnitude of the allosteric effect, understanding the basis for that effect requires

one to understand why the disproportionation equilibrium is poised to achieve the value that is does.[33]

The allosteric coupling free energy between ligands Fru-6-P and PEP for PFK from both *Bacillus stearothermophilus* (BsPFK) and *Escherichia coli* (EcPFK) results from compensating enthalpy and entropy components.[97,101] However, there is a very important difference between the two enzymes when it comes to the balance of these thermodynamic forces. In BsPFK, the positive coupling free energy that defines PEP as an inhibitor is opposite in sign of the negative enthalpy term and is therefore determined by the larger absolute value of the negative entropy term.[42] This is indicated by the positive slope in the van't Hoff plot in Figure 3-1.

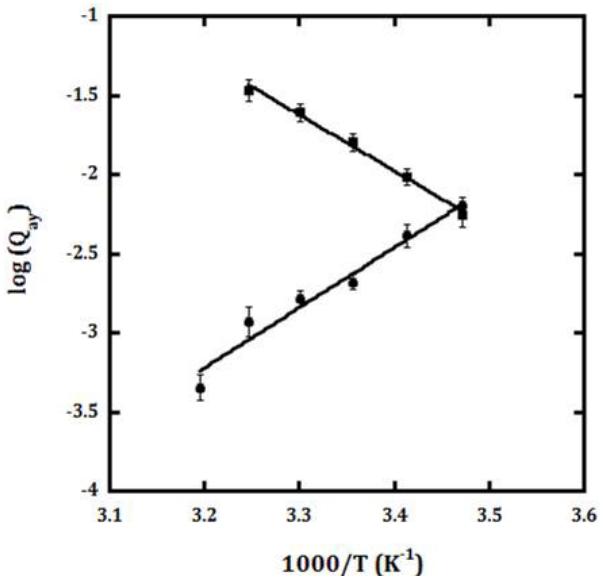

Figure 3-1: Van't Hoff plots of BsPFK (circles) and EcPFK (squares).

However, in EcPFK the positive coupling free energy that defines inhibition by PEP is established by the positive enthalpy component[101] and leads to a negative slope with the same analysis. This striking contrast between BsPFK and EcPFK suggests that fundamentally different mechanisms may be responsible for transmitting the allosteric signal between binding sites.

The inactivation, dissociation, and unfolding of EcPFK by urea has been thoroughly examined both in the absence of ligands and in the presence of substrate, Fru-6-P.[129-131] The following mechanism has been proposed to describe effect of urea on EcPFK[129]:

$$N \leftrightarrow 2D \leftrightarrow 4M \leftrightarrow 4U$$

Where N, the only active species, is the native tetramer, D is the dimer that forms the effector site interface, M is a partially folded monomer and U is a largely unfolded monomer. According to the above mechanism, the quaternary structure of PFK is disrupted before the tertiary structure. Previous data from our lab clearly demonstrates that stabilizing the quaternary structure via covalent disulfide bonds along the allosteric dimer–dimer interface, which also strengthens the active site subunit interface, has essentially no impact on the maximally inhibited or activated state of EcPFK with respect to allosteric perturbations by PEP and MgADP.[131] Less work has been done to characterize the effects of urea on BsPFK. However, studies did show that in the absence of ligands, the transition from tetramer to monomer occurs in an apparently concerted dissociation.[132] This result is attributed to comparable relative affinities between the allosteric site interface of the dimer and

active site interface of the tetramer. In addition, it is apparent when comparing urea-dependent deactivation curves of BsPFK and EcPFK that activity declines at lower concentrations of urea for EcPFK than BsPFK.[129,132]

The disproportionation equilibrium, eq 3-2, that defines the allosteric response has been studied by perturbation in various manners including mutation of the amino acid residues involved in catalysis, binding or allosteric communication, adjustment of the pH, variation of temperature, and pressurization.[97-99,113] The dissociation and unfolding effects of urea on BsPFK and EcPFK have been previously studied, however the low concentration effects of urea, those that precede dissociation, have been previously ignored. In this chapter, the effect of low concentrations of urea on both the ligand-binding equilibria and the disproportionation equilibrium are determined and compared between BsPFK and EcPFK.

Materials and Methods

Materials

All chemical reagents used in buffers for protein purification, enzymatic assays, and fluorescence assays were of analytical grade and were purchased from Sigma-Aldrich (St. Louis, MO), Fisher Scientific (Fair Lawn, NJ), or Research Products International (Mt. Prospect, IL). Deionized distilled water was used throughout. Creatine kinase, glycerol-3-phosphate dehydrogenase, and the

potassium salt of phospho(enol)pyruvate were purchased from Roche (Indianapolis, IN). The ammonium sulfate suspensions of aldolase, the ammonium sulfate suspension of triosephosphate isomerase, the disodium salt of fructose-6-phosphate, and the disodium salt of phosphocreatine were purchased from Sigma-Aldrich (St. Louis, MO). The coupling enzymes were extensively dialyzed against 50 mM EPPES, 100 mM KCl, 5 mM $MgCl_2$, and 0.1 mM EDTA at pH 8.0 before use. NADH and DTT were purchased from Research Products International (Mt. Prospect, IL). Mimetic Blue 1 A6XL resin used in protein purification was purchased from Promatic BioSciences (Rockville, Maryland). The Mono-Q HR anion exchange column used in protein purification was purchased prepacked for FPLC use from Pharmacia (Uppsala, Sweden). Amicon Ultra centrifugal filter units (spin concentrators) were from Millipore Corporation (Billerica, Massachusetts) and poly(ethylene glycol)-3000 was from Sigma-Aldrich (St. Louis, MO). Site-directed mutagenesis was performed using the Quikchange Site-Directed Mutagenesis System from Stratagene (La Jolla, CA). Oligonucleotides were synthesized and purchased from Integrated DNA Technologies, Inc (Coralville, IA). DNA modifying enzymes and dNTPs were purchased from Stratagene (Cedar Creek, TX), New England Biolabs (Ipswich, MA), or Promega (Madison, WI).

Protein Purification of BsPFK

The plasmid pBR322/BsPFK [118] contains the gene for BsPFK behind the native *Bacillus stearothermophilus* promoter and was received as a generous gift

from Simon H. Chang (Louisiana State University). Wild-type BsPFK was expressed in *E. coli* RL257 cells[119], which is a strain of *E.coli* lacking both the pfkA and pfkB genes. The purification of BsPFK was performed as described previously, with a few modifications.[95] RL257 cells containing the plasmid pBR322/BsPFK were grown at 37 °C for 16 - 18 hours in LB (Lysogeny Broth) tetracycline (tryptone 10 g/L, yeast extract 5 g/L, NaCl 10 g/L, and tetracycline 15 μg/mL). Cells were harvested by centrifugation and frozen at -20 °C for a minimum of 12 hours. The cells were resuspended in 60 mL of purification buffer (10 mM Tris-HCl pH 8.0, 1 mM EDTA) and sonicated using a Fisher 550 Sonic Dismemberator at 0 °C in 15 second pulses at setting 6 for 8 - 12 minutes. The crude lysate was centrifuged at 22,500 × g for 30 minutes at 4 °C. The clarified supernatant was incubated in a 70 °C water bath for 15 minutes, cooled on ice for 15 minutes, and centrifuged again at 22,500 × g for 30 minutes at 4 °C. The supernatant was diluted to at least 500 mL and then loaded onto a 100 mL Mimetic Blue 1 A6XL column that was previously equilibrated with purification buffer. The column was washed with purification buffer until the A_{280} reached a baseline, and the enzyme was eluted with a 0 - 1.5 M NaCl gradient. Fractions containing enzyme activity were pooled and dialyzed into 20 mM Tris-HCl pH 8.5 and loaded onto a Pharmacia Mono-Q HR anion exchange column that was pre-equilibrated with the same buffer. The enzyme was eluted with a 0 - 1 M NaCl gradient, and fractions containing pure BsPFK were combined, concentrated with either a spin concentrator or poly(ethylene glycol)-3000, and then dialyzed into EPPS buffer (50 mM EPPS pH 8.0, 10 mM MgCl2, 100 mM KCl, 0.1 mM EDTA).

The final enzyme was determined to be pure by SDS-PAGE, and stored at 4 °C. Enzyme concentration was determined by measuring absorbance at 280 nm (ε = 18910 $M^{-1}cm^{-1}$).[120]

Protein Purification of EcPFK

The plasmid p-ALTER1/EcPFK contains the gene EcPFK and expression occurs via the tac promoter. The purification of EcPFK followed the protocol of Johnson et al. with a few modifications[87], and is the same as above with the following exceptions. RL257 cells containing the p-ALTER1/EcPFK plasmid were grown to OD_{600} = 0.6 and then induced with 2 mM IPTG in LB media containing 100 μg/mL ampicillin at 37 °C. After induction the cells were grown to an OD_{600} of 1.2 and harvested by centrifugation. Instead of a heat step, the supernatant after sonication and clarification was incubated in the presence of DNase at 37 °C for 15 minutes and then centrifuged for thirty minutes to get rid of the remaining cell debris. The supernatant containing EcPFK was then further purified as above with a Mimetic Blue 1 A6XL column followed by an anion exchange step. Protein determined pure by SDS-PAGE was then concentrated and dialyzed into EPPS buffer (50 mM EPPS pH 8.0, 10 mM $MgCl_2$, 10 mM NH_4Cl, 0.1 mM EDTA). Protein concentration was calculated by measuring absorbance at 278 nm (ε = 0.6 $mg^{-1}cm^2$).[133]

Steady-State Kinetic Assays

Activity measurements for PFK were carried out using a coupled enzyme system[121,122] in a 0.6 mL reaction volume of EPPS buffer containing 50 mM EPPS, 5 mM MgCl2, 100 mM KCl, 0.1 mM EDTA, 2 mM DTT, 0.2 mM NADH, 3 mM ATP, 250 µg aldolase, 50 µg of glycerol-3-phosphate dehydrogenase, and 5 µg of triosephosphate isomerase at pH 8.0 and 25 °C unless otherwise noted. 40 µg/mL of creatine kinase and 4 mM of phosphocreatine were added as an ATP regenerating system to avoid the accumulation of MgADP, which is an activator. Temperature was controlled using a NESLab RTE-111 circulating water bath. Fru-6-P and PEP were added at varied concentrations as indicated. Assays were started by the addition of 10 µL of appropriately diluted PFK and the reaction was monitored as the absorbance at 340 nm decreased over time. The rate of the reaction was measured on Beckman Series 600 spectrophotometers using a linear regression calculation to convert change in absorbance at 340 nm to PFK activity. One unit of PFK activity is described as the amount of enzyme needed to produce 1 µmol of fructose-1,6-bisphosphate per minute. Protein was diluted to a concentration of 5.9 µM and was incubated at 25°C for 24 hours at the specified concentration of urea before the assays were performed.

Data Analysis

Data were fit using the non-linear least-squares fitting analysis option in Kaleidagraph software version 4.5 (Synergy). For the steady-state kinetic assays

the initial velocity data were plotted against concentration of Fru-6-P and fit to the Hill equation[8]:

$$v = \frac{V[A]^{n_H}}{K_a^{n_H} + [A]^{n_H}} \tag{3-4}$$

where, v is the initial velocity, $[A]$ is the concentration of the substrate Fru-6-P, V is the maximal velocity, and n_H is the Hill coefficient. K_a is defined as the concentration of Fru-6-P at which the enzymes activity is half maximal. Assuming rapid equilibrium, K_a is equivalent to the dissociation constant for Fru-6-P from the binary enzyme-substrate complex. K_a values obtained from the initial velocity experiments were plotted against the concentration of opposing ligand and fit to eq 3-5.

$$K_a = K_{ia}^o \left(\frac{K_{iy}^o + [Y]}{K_{iy}^o + Q_{ay}[Y]} \right) \tag{3-5}$$

where K_{ia}^o is the dissociation constant for Fru-6-P in the absence of PEP, K_{iy}^o is the dissociation constant for PEP in the absence of Fru-6-P, and Q_{ay} is the coupling coefficient[32,33,123]. Q_{ay} describes the effect of the allosteric effector on the binding of the substrate and/or the effect of the substrate on the binding of the allosteric effector. Based on its definition, Q_{ay} represents the equilibrium constant for the disproportionation equilibrium (eq 3-2). The coupling constant, Q_{ay} , is related to the coupling free energy (ΔG_{ay}) and its entropy ($T\Delta S_{ay}$) and enthalpy (ΔH_{ay}) components through the following relationship, which is an elaboration of eq 3-3:

$$\Delta G_{ay} = \Delta H_{ay} - T\Delta S_{ay} = -RTln\big(Q_{ay}\big) \tag{3-6}$$

The coupling entropy and enthalpy components were determined by measuring the coupling constant as a function of temperature and the data were fit to eq 3-7:

$$\ln(Q_{ay}) = \frac{\Delta S_{ay}}{2.3\times R} - \frac{\Delta H_{ay}}{2.3\times R}\left(\frac{1}{T}\right) \quad (3\text{-}7)$$

where, T is absolute temperature in Kelvin, and R is the gas constant (R=1.99 cal K^{-1} mol^{-1}).

Results

First, the effect of urea on the specific activity of both BsPFK and EcPFK was established. Enzyme samples were stored at a concentration of 59 μM and 4 °C after purification. Prior to preforming any steady-state kinetic assays, the enzyme stocks were diluted 10-fold and incubated at 25 °C at the indicated concentration of urea for 24 hours. It was determined that after 24 hours no further changes in the enzyme activity were occurring, and we concluded that the system was at equilibrium. The enzyme remained in the presence of urea until right before preforming the assay, when it was diluted into buffer to a concentration appropriate for running the assay. The enzyme activity did not change over the course of the assays, which were always run within 5 minutes of dilution. The reactivation of EcPFK has been thoroughly characterized and clearly shows that no enzymatic activity is regained during the course of the assays.[129] At urea concentrations ranging from 0 to 5 M, it is apparent from Figure 3-2A, urea is

causing a dramatic loss of activity at high concentrations. Loss of activity indicates that the enzyme is no longer in the tetrameric form, which is the simplest active form of the enzyme. This effect, however, occurs at lower concentrations of urea for EcPFK than BsPFK. In the case of BsPFK, we begin to see a 50% reduction in the enzyme's specific activity at 4.5 M urea. EcPFK reaches this point at 2.2 M urea. At lower concentrations, 0 - 0.5 M urea, another difference is observed between the two enzymes. BsPFK steadily gains specific activity from 0 to 0.2 M urea and then maintains the higher level of activity at the low concentration range as shown in Figure 3-2B. This effect on PFK activity is not observed in EcPFK.

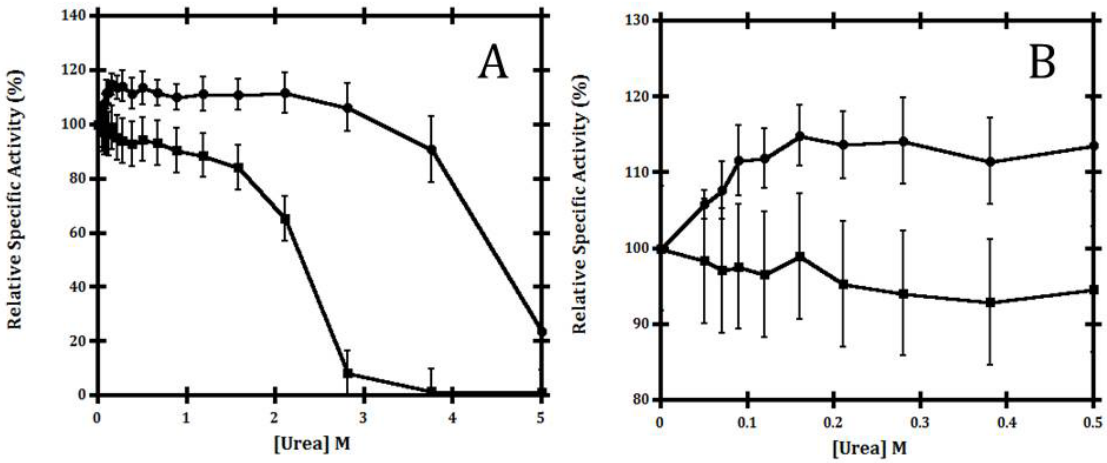

Figure 3-2: Relative specific activity of EcPFK (squares) and BsPFK (circles) as a function of urea concentrations ranging from A) 0 - 5 M and B) 0 - 0.5 M.

To establish the magnitude of PEP inhibition in BsPFK and EcPFK at various concentrations of urea, the apparent dissociation constants for Fru-6-P were determined as a function of PEP concentration at 0, 0.5 and 2 M urea. Urea concentrations of 0, 0.5, and 2 M all represent low concentrations of urea that precede dissociation of the tetramer in BsPFK. In EcPFK the specific activity in 2 M urea is at 70 % of the value obtained at 0 M urea, however all of the activity measured is produced by enzyme portion remaining in the tetrameric form. The dissociation constants for Fru-6-P were obtained from individual titration curves and fit to eq 3-4 at various PEP concentrations. The data for the apparent dissociation constants as a function of PEP concentration, fit to eq 3-5 to obtain the allosteric coupling parameter (Q_{ay}), are shown in Figure 3-3A and B for BsPFK and EcPFK, respectively. In addition, the dissociation constants for Fru-6-P in the

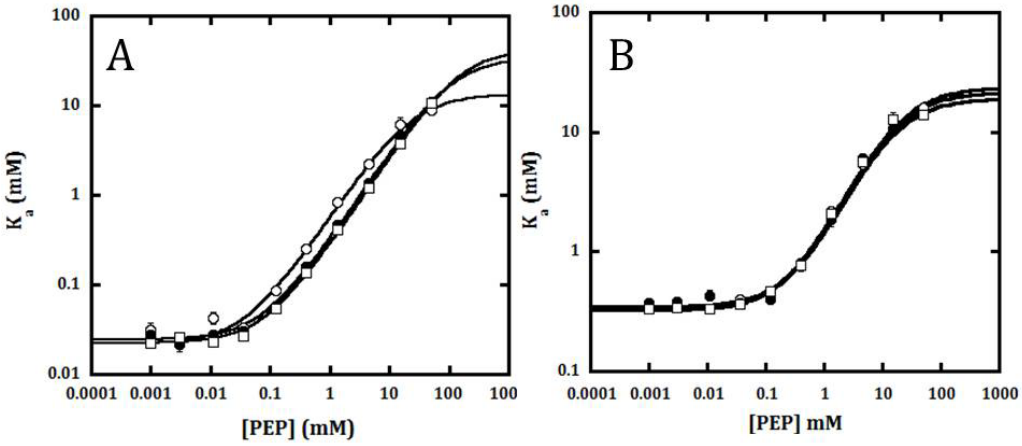

Figure 3-3: The log of the apparent K_a for Fru-6-P as a function of the log of [PEP] for A) BsPFK and B) EcPFK. Data in absence of urea are shown with open circles, data in the presence of 0.5 M urea with closed circles and 2 M urea with open squares.

absence of PEP (K_{ia}^{o}) and for PEP in the absence of Fru-6-P (K_{iy}^{o}) are obtained from these fits. K_{ia}^{o} was not changed by the addition of urea in either BsPFK or EcPFK. There was a 2-fold increase in K_{iy}^{o} at 0.5 and 2 M urea compared to 0 M urea in the case of BsPFK, but no change was seen for EcPFK. The magnitude of inhibition in BsPFK was enhanced 2.3-fold in 0.5 M urea, and 3.2 fold in 2 M urea, compared to native conditions. Conversely, no effect was seen on the allosteric coupling in EcPFK at 0.5 or 2 M urea compared to 0 M. The data for the allosteric coupling parameters were used to calculate the standard allosteric coupling free energies, ΔG_{ay}. The resulting values of K_{ia}^{o}, K_{iy}^{o}, Q_{ay}, and ΔG_{ay} are presented in Table 3-1 for both BsPFK and EcPFK along with the same values obtained at 0.5 and 2 M urea.

Table 3-1: Ligand dissociation constants and coupling constants for *B. stearothermophilus* and *E. coli* PFK at various concentrations of urea and 25 °C.

	[Urea] (M)	K_{ia}^{o} (mM)	K_{iy}^{o} (mM)	Q_{ay}	ΔG_{ay} (kcal/mol)
BsPFK	0	0.022 ± 0.001	0.038 ± 0.001	0.0016 ± 0.0001	3.8 ± 0.1
-	0.5	0.024 ± 0.001	0.077 ± 0.002	0.0007 ± 0.0001	4.3 ± 0.1
-	2	0.022 ± 0.001	0.081 ± 0.003	0.0005 ± 0.0001	4.5 ± 0.2
EcPFK	0	0.346 ± 0.009	0.28 ± 0.02	0.015 ± 0.001	2.5 ± 0.1
-	0.5	0.338 ± 0.013	0.27 ± 0.03	0.018 ± 0.001	2.4 ± 0.1
-	2	0.323 ± 0.007	0.24 ± 0.01	0.015 ± 0.001	2.5 ± 0.1

To further characterize the effect of urea on the allosteric coupling in BsPFK, the allosteric coupling was measured at additional concentrations of urea and the data is shown in Figure 3-4. The numerical values corresponding to the coupling

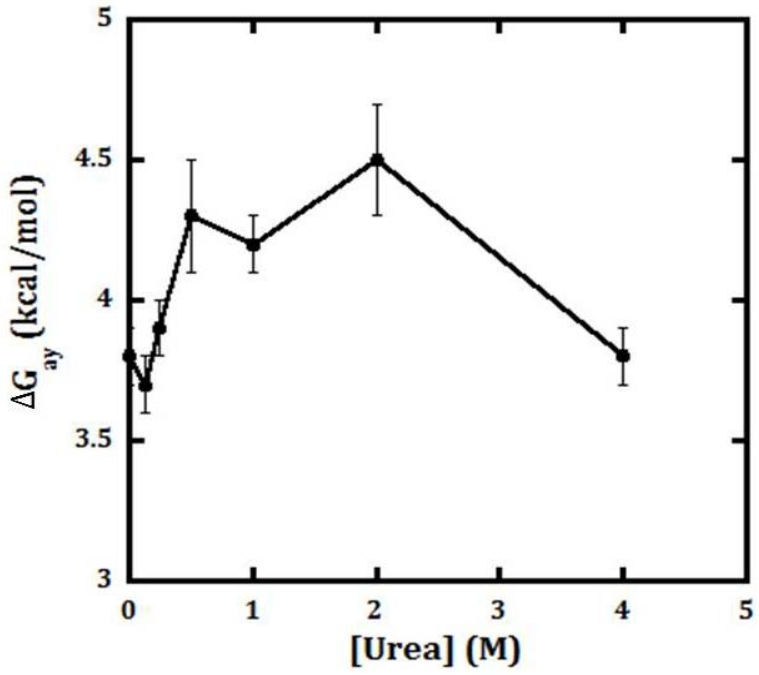

Figure 3-4: The allosteric coupling free energy, ΔG_{ay}, for BsPFK at a range of urea concentrations from 0 - 4 M.

free energy at the range of urea concentrations from 0 - 4 M are shown in Table 3-2. The allosteric coupling between Fru-6-P and PEP is enhanced as a function of urea concentration from 0 to 0.5 M urea, and the effect is maintained until urea concentrations reach about 2 M. At 4 M urea the extent of coupling is reduced back to levels seen in the absence of urea.

Table 3-2: Numerical values for the allosteric coupling free energy at a range of urea concentrations from 0 - 4 M and 25 °C.

[Urea] (M)	ΔG_{ay} (kcal/mol)
0	3.8±0.1
0.125	3.7±0.1
0.25	3.9±0.1
0.5	4.3±0.2
1	4.2±0.1
2	4.5±0.2
4	3.8±0.1

In order to further explore the thermodynamic basis for the augmentation of allosteric coupling seen at low urea concentrations van't Hoff analysis was employed. Enthalpy (ΔH_{ay}) and entropy (ΔS_{ay}) components of the coupling free energy (ΔG_{ay}) were obtained by determining the Q_{ay}, or allosteric coupling constant, at a range of temperatures. This analysis of the coupling for BsPFK in the absence of urea and at low concentrations of urea allows for a thorough description of the thermodynamic forces that determine the coupling free energy in each case by parsing out the entropy and enthalpy components. The allosteric coupling free energy remains entropy driven under all conditions, as indicated by the positive slopes in Figure 3-5. In addition, all of the data are well described by straight lines,

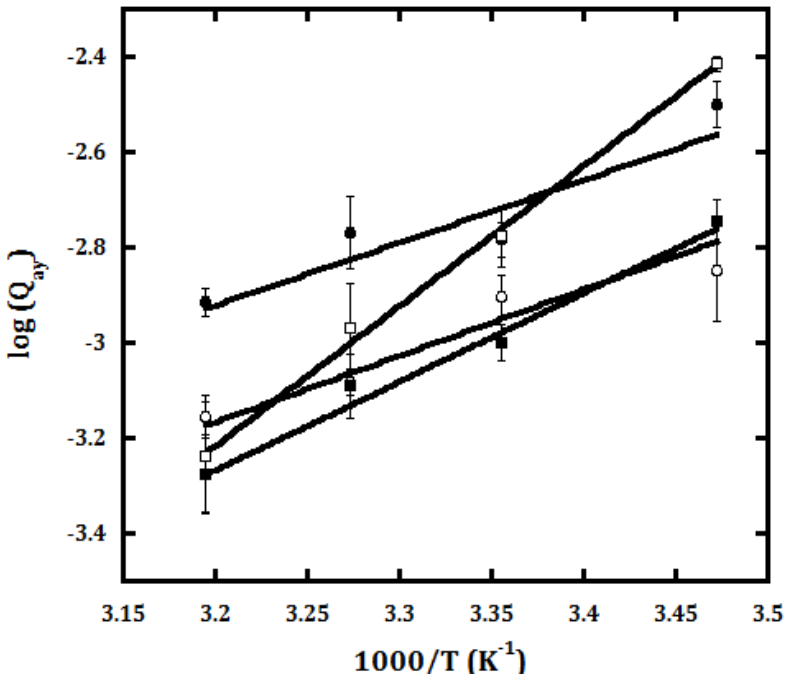

Figure 3-5: Variation in the log of Q_{ay} verses reciprocal temperature of BsPFK at various concentrations of urea. Closed circles represent the absence of urea, open circles are at 0.25 M urea, closed squares are at 1 M urea and open squares are at 4 M urea.

signifying that there is not a temperature dependent change in heat capacity, ΔC_p, over this range of temperatures at any of the tested concentrations of urea. The plot reveals that at 0.250 M both the entropy and enthalpy components of the coupling free energy become more negative compared to 0 M urea. There is a larger change in the $T\Delta S_{ay}$ component, leading to an overall decrease in entropy-enthalpy compensation and increased allosteric coupling. This trend continues when the concentration of urea is further increased to 1 M. From 0 to 4 M urea we see an even further decrease in both the entropy (7.5 ± 1.5 kcal/mol) and enthalpy (7.4 ±

1.6 kcal/mol) terms. However, at this concentration of urea ΔG_{ay} has returned to the value obtained in the absence of urea and compensation remains the same. The values corresponding to ΔH_{ay}, $T\Delta S_{ay}$, and ΔG_{ay} are listed below in Table 3-3 for 0, 0.250, 1 and 4 M urea.

Table 3-3: Thermodynamic parameters quantifying the inhibition of BsPFK by PEP at various concentrations of urea and 25 °C.

[Urea] (M)	ΔH_{ay} (kcal/mol)	$T\Delta S_{ay}$ (kcal/mol)	ΔG_{ay} (kcal/mol)	Rel. SA (%)
0	-6.0 ± 0.9	-9.7 ± 0.8	3.8 ± 0.1	100
0.25	-6.4 ± 1.5	-10.4 ± 1.4	3.9 ± 0.1	114
1	-8.5 ± 1.3	-12.6 ± 1.3	4.2 ± 0.1	112
4	-13.4 ± 1.3	-17.2 ± 1.3	3.8 ± 0.1	90

Discussion

We began to see the dissociation effects of urea, shown as a decrease in the specific activity, at lower concentrations in EcPFK than in BsPFK. In fact, it takes 4.5 M urea, more than twice the concentration of urea that was required to have the same effect on EcPFK, to reduce the specific activity of BsPFK by 50%. These stability differences likely stem from the fact that BsPFK is a thermophilic enzyme, whereas EcPFK is a more flexible mesophilic enzyme. Previous work has shown using a combination of steady-state kinetic assays, which monitor dissociation at the active site interface, and intrinsic fluorescence assays, which monitor the

allosteric site interface, that in EcPFK the decrease in activity with urea corresponds to the dissociation of the tetramer at the active site interface into dimers.[129] This is in contrast to what is believed to occur in BsPFK, which appears to undergo the transition from tetramer to monomer in a concerted dissociation with changes in activity and intrinsic fluorescence occurring simultaneously.[132]

The remainder of this study focused on the previous uncharacterized effects of low concentrations of urea on BsPFK and EcPFK. An increase in specific activity at low urea concentrations was seen uniquely in BsPFK. The effect of urea on the allosteric coupling between Fru-6-P and PEP was also determined. The extent of inhibition by PEP is given by the standard free energy, ΔG_{ay}, for the disproportionation equilibrium (eq 3-1). All four of the species that contribute to the poise of this equilibrium are potentially influenced by urea. The value for ΔG_{ay} is derived from the difference between the perturbations of the free energy of formation when both ligands simultaneously versus the sum of the perturbations experienced by the binding of each ligand individually. Changes to the enzyme, as the result of urea, must enhance or relieve conflict in the ternary complex in order to alter the value for ΔG_{ay}, thereby altering the degree of inhibition.

In the case of EcPFK, at urea concentrations up to 2 M, there is no effect on the allosteric coupling. This is not true for BsPFK, which has increased allosteric coupling over the same range of low urea concentrations for which it has an increased specific activity. The different effects seen on PEP inhibition in the presence of urea between BsPFK and EcPFK are intriguing. There is one additional

observation made from the data presented in Figure 3-3. For BsPFK in low urea conditions the binding of inhibitor PEP, or K_{iy}^{o}, is 2-fold weaker. However, from 0 to 1 M urea, the allosteric coupling free energy between Fru-6-P and PEP increased by 0.4 ± 0.1 kcal/mol, signifying that PEP is a significantly more effective inhibitor. The fact that low concentrations of urea produced an increase in coupling while making the PEP binding weaker suggests that the binding of the inhibitor and the actual inhibition are independent of one another as we have observed previously.[100,134,135]

There is evidence for fundamentally different mechanisms of coupling between binding sites in these two PFK isoforms, as indicated by contrasting thermodynamic driving forces. A possible explanation for the different effects at low urea concentrations is that urea is a producing a stabilizing effect on the tertiary structure of the enzyme, altering the conformational dynamics, when concentrations are low. The allosteric coupling in BsPFK is entropically driven; on the other hand, coupling in EcPFK is enthalpy driven. Conceivably, altering the conformational dynamics would not necessarily have the same effect on both enzymes.

Van't Hoff analysis on the allosteric coupling in BsPFK reveals that both the entropy and enthalpy components of the coupling free energy increase in absolute value, becoming more negative. At low concentrations of urea, less than 1M, the entropy term decreases to a larger extent than the enthalpy term. This alters the degree of entropy enthalpy compensation leading to the observed increase in allosteric coupling. The dramatic decrease observed in the entropy component of

the coupling indicates that reduced thermal fluctuations are present in the propagation of the allosteric signal at low concentrations of urea than are under native conditions, supporting the notion that urea stabilizes protein structures at low concentrations of urea. It is evident from the data that the enzyme compensates for the dramatic decrease in coupling entropy with a decrease in the coupling enthalpy. Stabilizing the enzyme with low concentrations of urea changes the entropy and enthalpy terms to such a great degree that the balance between them is also vulnerable to change. These changes alter the poise of the disproportionation equilibrium and consequently the effectiveness of PEP as an inhibitor.

CHAPTER IV

THE EFFECT OF ADDING SMALL CAVITIES TO THE STRUCTURE OF PHOSPHOFRUCTOKINASE FROM *BACILLUS STEAROTHERMOPHILUS* AND *ESCHERICHIA COLI* ON THE ALLOSTERIC COUPLING FREE ENERGY VIA SINGLE ISOLEUCINE TO VALINE MUTATIONS

Introduction

The enzymes that catalyze the commitment steps of metabolic pathways are subject to intense regulation via allosteric mechanisms. The molecular basis of allosteric regulation is still not well understood in most cases. However, due to the key role these enzymes play, the ability to manipulate allosteric control mechanisms holds promise for drug design.[136-141] For this reason, an enhanced view of the molecular mechanisms behind the regulation of allosteric enzymes is a prerequisite for rational drug design.

Prokaryotic phosphofructokinase (PFK) has been extensively studied and characterized, resulting in an abundance of kinetic, structural, and thermodynamic knowledge.[43,87,88,90,93,98,101,106-110,120] Consequently, prokaryotic PFK in general, and PFK from *Bacillus stearothermophilus* (BsPFK) and *Escherichia coli* (EcPFK) specifically, serve as model allosteric enzymes to explore the molecular mechanisms of allosteric regulation as well as the thermodynamic basis of the allosteric coupling. Prokaryotic PFK catalyzes the phosphorylation of fructose-6-

phosphate (Fru-6-P) by MgATP to form fructose-1,6-bisphosphate and MgADP in the first committed step of glycolysis. This crucial glycolytic reaction is allosterically inhibited by the downstream pathway intermediate, phosphoenol-pyruvate (PEP), and activated by MgADP, which competes for the same effector binding sites as PEP. These K-type allosteric effects are revealed by a change in the enzyme affinity for substrate, Fru-6-P, upon binding of the allosteric effector. The nature and magnitude of this effect are quantified by the allosteric coupling free energy between Fru-6-P and the effector ligand.[33]

The allosteric coupling free energy (ΔG_{ay}), that describes the allosteric inhibition of PFK by PEP, is the standard free energy for the following disproportionation equilibrium[33]

$$\text{PFK:Fru-6-P} + \text{PEP:PFK} \leftrightarrow \text{PFK} + \text{PEP:PFK:Fru-6-P} \qquad (4\text{-}1)$$

where PFK:Fru-6-P represents PFK with Fru-6-P bound, PEP:PFK represents PFK with PEP bound and PEP:PFK:Fru-6-P represents the ternary complex with both ligands bound at the same time. Since ΔG_{ay} describes quantitatively both the nature and the magnitude of the allosteric inhibition, understanding the basis for that effect requires one to understand why the disproportionation equilibrium achieves the value that it does.[33] There is a very important difference between the prokaryotic PFK isoforms BsPFK and EcPFK when it comes to the balance of thermodynamic forces that make up the allosteric coupling free energy as evident from the contrasting behavior shown in Figure 4-1. The allosteric coupling free

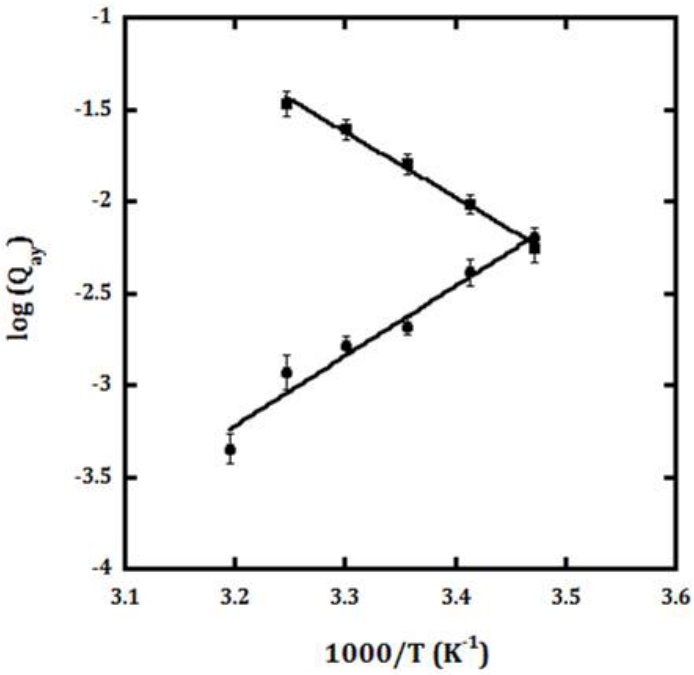

Figure 4-1: Van't Hoff plots of BsPFK (circles) and EcPFK (squares).

energy between ligands Fru-6-P and PEP for both BsPFK and EcPFK results from compensating enthalpy and entropy components under normal conditions at 25 °C.[97,101] In EcPFK, the positive coupling free energy that defines inhibition by PEP is established by the larger positive enthalpy component.[101] This is indicated by the negative slope in the van't Hoff plot in Figure 4-1. However, in BsPFK the positive coupling free energy that defines PEP as an inhibitor is opposite in sign of the negative enthalpy term and is therefore determined by the larger absolute value of the negative entropy term[42] and leads to a positive slope with the same analysis. This striking contrast between BsPFK and EcPFK suggests that fundamentally

different mechanisms may be responsible for transmitting the allosteric signal between the Fru-6-P and PEP binding sites.

Despite evidence for unique PEP inhibition mechanisms, the prokaryotic PFK homologs BsPFK and EcPFK share 73% similarity and 54% identity in amino acid sequence. The X-ray crystallographic structures of these two enzymes with various ligand combinations bound have α-carbon traces that are nearly superimposable.[88-90] This is demonstrated by an overlay of BsPFK and EcPFK monomers in Figure 4-2. The crystal structures of EcPFK and BsPFK also indicate

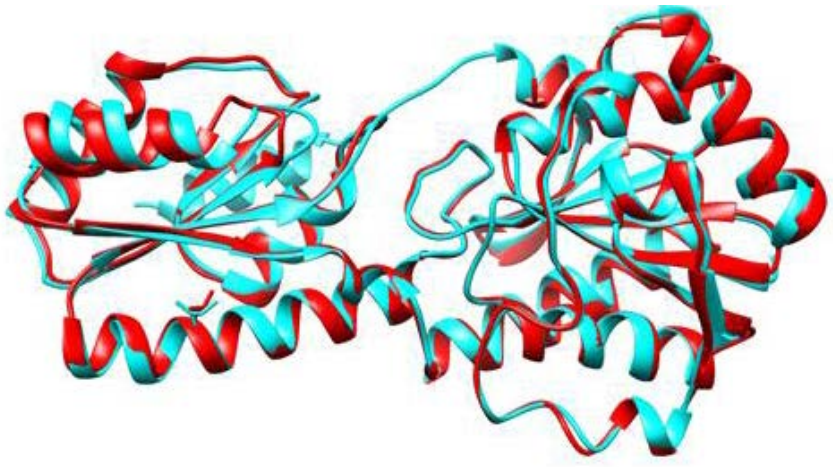

Figure 4-2: Overlay of the apo-BsPFK structure (cyan) and the apo-EcPFK structure (red).

almost identical active site binding residues.[90-92] Both enzymes are a tetrameric structure consisting of four identical subunits arranged as a dimer of dimers with the substrate and effector binding sites located at alternating interfaces.

B. stearothermophilus is a moderate thermophile that grows natively at 55 °C, and BsPFK is correspondingly temperature-stable. The stability of the enzyme reflects the evolutionary requirement for enzyme stability under high environmentally imposed temperatures. Many studies have attempted to uncover the source of increased thermal stability in thermophilic enzymes, but it appears that there is not a single molecular or thermodynamic explanation.[142] Instead, increased thermostability appears to rely on a variety of stabilizing effects. In a recent review, Razvi and Scholtz compiled the available data and generated stability curves for 26 sets of homologous proteins from thermophiles and mesophiles to determine the thermodynamic mode of stabilization used in each case.[142] Stability curves demonstrate how the conformational stability varies with temperature and it was concluded that the most common way that thermophilic proteins in the study achieve higher stability is by increasing their intrinsic stability at all temperatures.

The comparison of three-dimensional structures of homologous pairs of proteins from mesophiles and thermophiles has shown that the increase in stability can be achieved in various ways. The most general stabilizing feature is an increased number, and optimization, of electrostatic interactions.[143] Other common features include the stabilization of α-helices, an increase in the number of proline and C-β-branched residues and a decrease in the number of uncharged polar amino acids. Other features that tend to have a more minor influence include an increased number of hydrogens bonds, higher packing densities, improved hydrophobic

interactions, optimized surface areas, decreased volumes, fewer cavities, and a shortening of the polypeptide chain.[143] Many of these characteristics also lead to increased rigidity. In the case of BsPFK, Kim *et al.* showed that the native tryptophan position is quite rigid.[116] Additional fluorescence studies using tryptophan-shifted mutants revealed that a majority of the BsPFK structure is rigid.[112,120,144]

In the present study, four different isoleucine to valine mutations were made to the BsPFK enzyme in an attempt to make the BsPFK structure more flexible, and perhaps, modify the extent of inhibition by PEP. Each modification resulted in the loss of a single methylene group from the native structure, leaving a small cavity at the affected location. In a structural and genetic analysis of protein stability, Matthews compiled systematic mutational analyses of hydrophobic residues in proteins including 9 different Ile → Val mutations.[145] The change in denaturation free energy between WT and mutants ranged from 0.5 to 1.8 kcal/mol, with an average $\Delta\Delta G$ of 1.3 ± 0.4 kcal/mol. In another study, the thermodynamic parameters for the denaturation of five Ile → Val lysozyme mutants determined by scanning calorimetry showed decreased stability compared to wild-type lysozyme in all cases.[146] Larger and diverse changes in denaturation enthalpy were observed in comparison to the denaturation free energy, which were largely compensated for by changes in the denaturation entropy. X-ray crystallography studies of these lysozyme variants revealed identical overall structures and only small structural rearrangements were observed locally around

some mutation sites. More recently, Roche *et al.* used 10 cavity containing mutants of staphylococcal nuclease to establish that pressure unfolds proteins primarily as a result of cavities that are present in the folded state and absent in the unfolded one.[147]

Based on previous studies analyzing the effect of cavities in protein structures, we hypothesized that the addition of such a small cavity to the BsPFK enzyme should not substantially alter the overall structure of the enzyme. On the other hand, the cavity would likely have a modest effect on the stability of all four forms appearing in eq 4-1. This, in return, would possibly alter the allosteric coupling free energy that defines the magnitude of inhibition by shifting the poise of the equilibrium between the four relevant species. As a comparison, we also introduced a similar mutation into EcPFK, which has a more flexible structure. The different thermodynamic composition of allosteric coupling in EcPFK adds extra intrigue. In EcPFK there is a leucine instead of a valine at this position. Therefore, in the case of I154V, we are also removing a methylene group. This shortens the overall length of the R-group and still creates a small cavity in structure of the enzyme, analogous to the isoleucine to valine mutations made in BsPFK.

Materials and Methods

Materials

All chemical reagents used in buffers for protein purification, enzymatic assays, and fluorescence assays were of analytical grade and were purchased from Sigma-Aldrich (St. Louis, MO), Fisher Scientific (Fair Lawn, NJ), or Research Products International (Mt. Prospect, IL). Deionized distilled water was used throughout. Lyophilized creatine kinase, the ammonium sulfate suspension of glycerol-3-phosphate dehydrogenase, and the potassium salt of phosphoenol-pyruvate were purchased from Roche (Indianapolis, IN). The ammonium sulfate suspensions of aldolase, the ammonium sulfate suspension of triosephosphate isomerase, the disodium salt of fructose-6-phosphate, and the disodium salt of phosphocreatine were purchased from Sigma-Aldrich (St. Louis, MO). The coupling enzymes were extensively dialyzed against 50 mM EPPS pH 8.0, 100 mM KCl, 5 mM $MgCl_2$, and 0.1 mM EDTA before use. NADH and DTT were purchased from Research Products International (Mt. Prospect, IL). Mimetic Blue 1 A6XL resin used in protein purification was purchased from Promatic BioSciences (Rockville, MD). The Mono-Q HR anion exchange column used in protein purification was purchased prepacked for FPLC use from Pharmacia (currently GE Healthcare, Uppsala, Sweden). Macro-Prep High-Q anion exchange resin was purchased from Bio-Rad (Hercules, CA). Amicon Ultra centrifugal filter units (spin concentrators) were from Millipore Corporation (Billerica, MA) and poly(ethylene glycol)-3000 was from

Sigma-Aldrich (St. Louis, MO). Site-directed mutagenesis was performed using the QuikChange Site-Directed Mutagenesis System from Stratagene (La Jolla, CA). Oligonucleotides were synthesized and purchased from Integrated DNA Technologies, Inc (Coralville, IA). DNA modifying enzymes and dNTPs were purchased from Stratagene (Cedar Creek, TX), New England Biolabs (Ipswich, MA), or Promega (Madison, WI).

Site-Directed Mutagenesis

The plasmids p-ALTER1/BsPFK and p-ALTER1/EcPFK contain the gene for BsPFK and EcPFK, respectively. Mutagenesis was performed on these plasmids following the protocol outlined in the QuikChange Site-Directed Mutagenesis System from Stratagene. Two complementary oligonucleotides were designed to target the sequence surrounding the codon for each of the mutated amino acids; the template oligonucleotides are shown below:

I150V-BsPFK: 5'– ATA CGG TCA TTG ATG CCG TCG ACA AAA TCC GCG AC –3'

I53V-BsPFK: 5'– GCC ATC GAC AAA GTG CGC GAC ACG G –3'

I234V-BsPFK: 5'– GAC TTC GGC CGG CAA GTG CAG GAA G –3'

L154V-EcPFK: 5'– TGT AGA AGC GAT CGA CCG TGT GCG TGA CAC –3'

Protein Purification of Wild-Type, I150V, I153V, and I234V-BsPFK

The plasmid p-ALTER1/BsPFK contains either the gene for BsPFK or the mutated genes. Expression from this plasmid occurs via the tac promoter. Wild-

type BsPFK was expressed in *E. coli* RL257 cells[119], which is a strain lacking both the pfkA and pfkB genes. The purification of BsPFK was performed as described previously[95], with a few modifications. RL257 cells containing the plasmid p-ALTER1/BsPFK were grown at 37 °C for 16 - 18 hours in Lysogeny Broth with tetracycline (tryptone 10 g/L, yeast extract 5 g/L, NaCl 10 g/L, and tetracycline 15 μg/mL). Induction of expression with 2 mM IPTG was carried out at the beginning of the growth. Cells were harvested by centrifugation and frozen at -20 °C for a minimum of 12 hours. The cell pellet was resuspended in 60 mL of purification buffer (10 mM Tris-HCl pH 8.0, 1 mM EDTA) and sonicated using a Fisher 550 Sonic Dismemberator at 0 °C in 15-second pulses at setting six for 8 - 12 minutes. The crude lysate was centrifuged at 22,500 × g for 30 minutes at 4 °C. The clarified supernatant was incubated in a 70 °C water bath for 15 minutes, cooled on ice for 15 minutes, and centrifuged again at 22,500 × g for 30 minutes at 4 °C. The supernatant was diluted to at least 500 mL and then loaded onto a 100 mL Mimetic Blue 1 A6XL column that was previously equilibrated with purification buffer. The column was washed with purification buffer until the A_{280} reached a baseline, and the enzyme eluted with a 0 - 1.5 M NaCl gradient. Fractions containing enzyme activity were pooled and dialyzed into 20 mM Tris-HCl pH 8.5 and loaded to a Pharmacia/GE healthcare Mono-Q HR anion exchange column that was pre-equilibrated with the same buffer. The enzyme was eluted with a 0 - 1 M NaCl gradient, and fractions containing pure BsPFK were combined, concentrated with either a spin concentrator or poly(ethylene glycol)-3000, and then dialyzed into

EPPS buffer (50 mM EPPS pH 8.0, 10 mM $MgCl_2$, 100 mM KCl, and 0.1 mM EDTA). The final enzyme was determined to be pure by SDS-PAGE, and stored at 4 °C. Protein concentration was determined by measuring absorbance at 280 nm (ε = 18910 $M^{-1}cm^{-1}$).[120]

Protein Purification of Wild-Type and L154V-EcPFK

The purification of both wild-type and L154V-EcPFK proteins followed the protocol of Johnson et al.[87] with a few modifications, and is the same as above with the following exceptions. RL257 cells containing the p-ALTER1/EcPFK or p-ALTER1/L154V-EcPFK plasmid were grown to OD_{600} = 0.6 and then induced with 2 mM IPTG in Lysogeny Broth containing 100 μg/mL ampicillin at 37 °C. After induction the cells were grown until OD_{600} = 1.2 and harvested by centrifugation. Instead of a heat step, the supernatant after sonication and clarification was incubated with DNase at 37 °C for 15 minutes and then centrifuged for thirty minutes to remove the remaining cellular debris. The supernatant, containing EcPFK, was then further purified as above with a Mimetic Blue 1 A6XL column followed by an anion exchange step. Protein determined pure by SDS-PAGE was then concentrated and dialyzed into EPPS buffer (50 mM EPPS pH 8.0, 10 mM $MgCl_2$, 10 mM NH_4Cl, and 0.1 mM EDTA). Protein concentration was calculated by measuring absorbance at 278 nm (ε = 0.6 $mg^{-1}cm^2$).[133]

Steady-State Kinetic Assays

Activity measurements for PFK were carried out using a coupled enzyme system[121,122] in a 0.6 mL reaction volume of EPPS buffer containing 50 mM EPPS pH 8.0, 5 mM $MgCl_2$, 100 mM KCl, 0.1 mM EDTA, 2 mM DTT, 0.2 mM NADH, 3 mM ATP, 250 μg aldolase, 50 μg of glycerol-3-phosphate dehydrogenase, and 5 μg of triosephosphate isomerase at 25 °C unless otherwise noted. Creatine kinase (40 μg/mL) and phosphocreatine (4 mM) were added as an ATP regenerating system to avoid the accumulation of MgADP, which is an activator. Temperature was controlled using a NESLab RTE-111 circulating water bath. Fru-6-P and PEP were added at varied concentrations as indicated. Assays were started by the addition of 10 μL of appropriately diluted PFK and the reaction was monitored as the absorbance at 340 nm decreased over time. The rate of the reaction was measured on Beckman Series 600 spectrophotometers using a linear regression calculation to convert change in absorbance at 340 nm to PFK activity. One unit of PFK activity is described as the amount of enzyme needed to produce 1 μmol of fructose-1,6-bisphosphate per minute.

Data Analysis

Data were fit using the non-linear least-squares fitting analysis option in Kaleidagraph software version 4.5 (Synergy). For the steady-state kinetic assays the initial velocity data were plotted against concentration of Fru-6-P and fit to the Hill equation[8]:

$$v = \frac{V[A]^{n_H}}{K_a^{n_H} + [A]^{n_H}} \tag{4-2}$$

where, v is the initial velocity, $[A]$ is the concentration of the substrate Fru-6-P, V is the maximal velocity, and n_H is the Hill coefficient. K_a is defined as the concentration of Fru-6-P at which the enzymes activity is half-maximal. Assuming rapid equilibrium for Fru-6-P, which was shown to be valid in EcPFK using a steady-state kinetic method, K_a is equivalent to the dissociation constant for Fru-6-P from the binary enzyme-substrate complex.[34,101] Values of K_a obtained from the initial velocity experiments were plotted against the concentration of opposing ligand and fit according to

$$K_a = K_{ia}^o \left(\frac{K_{iy}^o + [Y]}{K_{iy}^o + Q_{ay}[Y]} \right) \tag{4-3}$$

where K_{ia}^o is the dissociation constant for Fru-6-P in the absence of PEP, K_{iy}^o is the dissociation constant for PEP in the absence of Fru-6-P, and Q_{ay} is the coupling coefficient.[32,33,123] Q_{ay} describes the effect of the allosteric effector on the binding of the substrate, and is defined as

$$Q_{ay} = \frac{K_{ia}^o}{K_{ia}^\infty} = \frac{K_{iy}^o}{K_{iy}^\infty} \tag{4-4}$$

where K_{ia}^∞ is the dissociation constant for Fru-6-P in the saturating presence of PEP, and K_{iy}^∞ is the dissociation constant for PEP in the saturating presence of Fru-6-P. By definition, Q_{ay} represents the equilibrium constant for the disproportionation equilibrium (eq 4-1). The coupling constant, Q_{ay}, is related to the coupling free

energy (ΔG_{ay}) and the entropy ($T\Delta S_{ay}$) and enthalpy (ΔH_{ay}) components through the relationship

$$\Delta G_{ay} = \Delta H_{ay} - T\Delta S_{ay} = -RTln(Q_{ay}) \quad (4\text{-}5)$$

ΔG_{ay} represents a standard free energy, although the superscript "0" is removed from the designation to avoid confusion with the use of that superscript for other purposes in notation.[32] The coupling entropy and enthalpy components were determined by measuring the coupling constant as a function of temperature and then fitting the data to

$$\log(Q_{ay}) = \frac{\Delta S_{ay}}{R \times 2.303} - \frac{\Delta H_{ay}}{R \times 2.303}\left(\frac{1}{T}\right) \quad (4\text{-}6)$$

where T is absolute temperature in Kelvin and R is the gas constant (R = 1.99 cal K^{-1} mol^{-1}).

Results

Three BsPFK variants, each containing a single amino acid substitution of isoleucine to valine, were constructed that essentially removed a single –CH2 group, thus creating a small cavity at the affected location in the enzyme (Figure 4-3). To establish the magnitude of PEP inhibition in the wild-type and cavity containing variants of BsPFK, the apparent dissociation constants for Fru-6-P were determined as a function of PEP concentration using kinetics. The dissociation constants for Fru-6-P were obtained from individual titration curves fit to eq 4-1

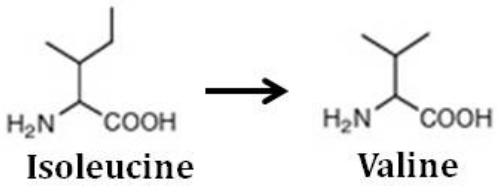

Figure 4-3: Isoleucine to a valine, "hole", mutation.

for a range of PEP concentrations. The data for these apparent dissociation constants as a function of PEP concentration were then fit to eq 4-3 as shown in Figure 4-4. The dissociation constants for Fru-6-P in the absence of PEP (K_{ia}^{o}) and for PEP in the absence of Fru-6-P (K_{iy}^{o}) and the allosteric coupling parameter were obtained from these fits. The data for the allosteric coupling parameters were used

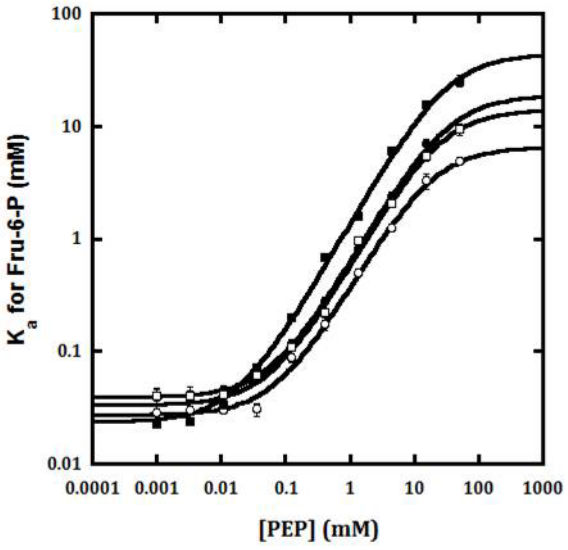

Figure 4-4: The log of the apparent K_a for Fru-6-P as a function of the log of [PEP] for wild-type (filled circles), I150V (open circles), I153V (filled squares), and I234V (open squares) variants of BsPFK.

to calculate the standard allosteric coupling free energies, ΔG_{ay}. The resulting values of K_{ia}^{o}, K_{iy}^{o}, Q_{ay}, and ΔG_{ay} are presented in Table 4-1 for wild-type BsPFK along with the three variants. One of the BsPFK mutants, I153V, was discovered to have substantially increased (0.8 ± 0.1 kcal/mol) allosteric coupling free energy in comparison to WT-BsPFK, as is seen by the increased distance between the lower plateau, K_{ia}^{o}, and the upper plateau, K_{ia}^{∞} in Figure 4-4. According to the ligand dissociation constants, the I153V variant of BsPFK has a higher affinity for both the substrate Fru-6-P and inhibitor PEP, with the effect on Fru-6-P almost 2-fold and the effect on PEP binding 3.8-fold in comparison to wild-type. The other two BsPFK variants did not exhibit the same increase in allosteric coupling, in fact I150V-BsPFK had a 0.4 ± 0.1 kcal/mol diminished allosteric coupling free energy while I234V-BsPFK displayed allosteric coupling free energy very comparable to WT-BsPFK (0.1 ± 0.1 kcal/mol). Like I153V, the other mutants had slightly lower K_{ia}^{o} values than wild-type. Unlike I153V, the other two mutants had a K_{iy}^{o} very similar to wild-type.

Table 4-1: Ligand dissociation constants and coupling constants for wild-type and variant forms of *B. stearothermophilus* and *E. coli* PFK at 25 °C.

	K_{ia}^{o} (mM)	K_{iy}^{o} (mM)	Q_{ay}	ΔG_{ay} (kcal/mol)
WT-BsPFK	0.039 ± 0.002	0.0630 ± 0.004	0.0021 ± 0.0002	3.66 ± 0.06
I150V-BsPFK	0.027 ± 0.001	0.074 ± 0.005	0.0042 ± 0.0003	3.25 ± 0.04
I153V-BsPFK	0.0236 ± 0.0005	0.0168 ± 0.0005	0.00054 ± 0.00007	4.46 ± 0.08
I234V-BsPFK	0.033 ± 0.002	0.057 ± 0.004	0.0024 ± 0.0002	3.58 ± 0.05
WT-EcPFK	0.346 ± 0.009	0.28 ± 0.02	0.015 ± 0.001	2.50 ± 0.05
L154V-EcPFK	0.237 ± 0.007	0.34 ± 0.02	0.0083 ± 0.0008	2.84 ± 0.06

In order to further explore the thermodynamic basis for both the augmentation and diminution in allosteric coupling we employed van't Hoff analysis. Enthalpy (ΔH_{ay}) and entropy (ΔS_{ay}) components of the coupling free energy (ΔG_{ay}) were obtained by determining the Q_{ay}, or allosteric coupling constant, as a function of temperature ranging from 10 - 40 °C. This analysis of the coupling for WT-BsPFK and the three BsPFK variants allows for a determination of the entropy and enthalpy contributions to the coupling free energy. The allosteric coupling free energy remains entropy driven for all of the variants, as indicated by the positive slopes of all lines in Figure 4-5. In addition, all of the data are well

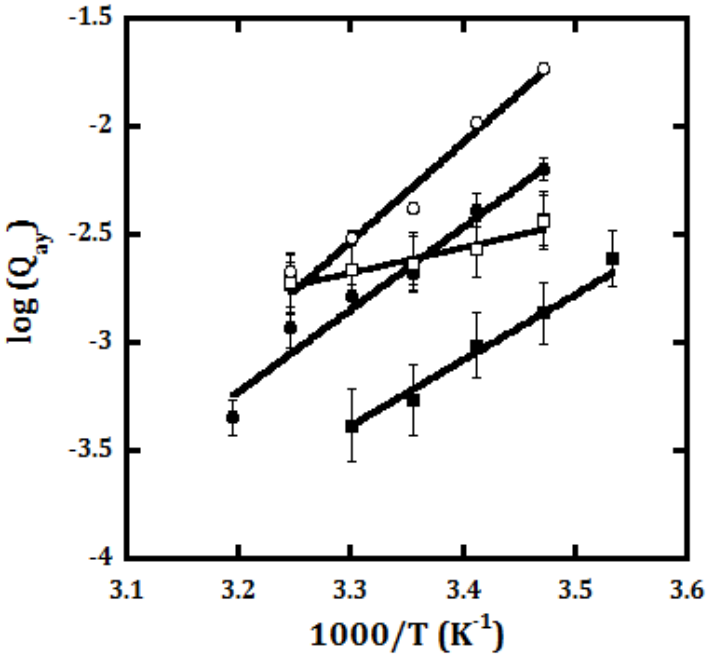

Figure 4-5: The variation in the log of Q_{ay} verses reciprocal temperature of wild-type (filled circles), I150V (open circles), I153V (filled squares), and I234V (open squares) variants of BsPFK.

described by a straight line within the temp range examined, signifying that there is not a detectable change in heat capacity, ΔC_p, over this range of temperatures. The values of ΔH_{ay}, $T\Delta S_{ay}$ and ΔG_{ay} are listed in Table 4-2. In response to the I153V mutation the enthalpy term becomes less negative by 3.5 kcal/mol, while the entropy term becomes less negative by 2.8 kcal/mol at 25 °C. The diminished allosteric coupling in I150V-BsPFK is accompanied by a decrease in both the enthalpy (3.4 kcal/mol) and the entropy (2.0 kcal/mol) components, leading to an overall increase in compensation at 25 °C. Despite opposing effects on the allosteric

Table 4-2. Parameters quantifying the inhibition of PFK from WT and variant forms of *B. stearothermophilus* and *E. coli* PFK by PEP at 25 °C.

	ΔH_{ay} (kcal/mol)	$T\Delta S_{ay}$ (kcal/mol)	ΔG_{ay} (kcal/mol)
WT-BsPFK	-17.4 ± 1.3	-21.0 ± 1.3	3.66 ± 0.06
I150V-BsPFK	-20.8 ± 0.7	-23.9 ± 0.7	3.25 ± 0.04
I153V-BsPFK	-13.9 ± 1.3	-18.2 ± 1.3	4.46 ± 0.08
I234V-BsPFK	-5.3 ± 0.9	-8.9 ± 0.9	3.58 ± 0.05
WT-EcPFK	16.2 ± 1.7	13.7 ± 1.7	2.50 ± 0.05
L154V-EcPFK	16.2 ± 1.3	13.4 ± 1.4	2.84 ± 0.06

coupling for both I150V-BsPFK and I153V-BsPFK, the ΔH_{ay} component of the allosteric coupling free energy is changed by a greater magnitude than the ΔS_{ay} component in both cases. The level of compensation between ΔH_{ay} and $T\Delta S_{ay}$ at 25 °C remains the same between I234V-BsPFK and WT-BsPFK, however each component is affected by 12.1 kcal/mol. Consequently, the inhibition of I234V-BsPFK varies from WT to a greater degree at temperatures higher and lower than 25 °C.

Since different thermodynamic components drive the allosteric coupling in BsPFK and EcPFK, despite being very similar enzymes otherwise, the next step was to evaluate the effect of a mutation in EcPFK analogous to the mutation that provided augmented allosteric coupling in BsPFK. In addition, the EcPFK enzyme is

considered more flexible than its BsPFK counterpart and can serve in that way as a useful comparison. The variant used to explore this was L154V-EcPFK, which introduces a similar, but possibly more substantial, change than the isoleucine to valine mutation. The allosteric coupling free energy is barely augmented by 0.3 ± 0.1 kcal/mol in the L154V-EcPFK variant compared to WT-EcPFK (Figure 4-6); this difference is substantially less than that in the corresponding I153V-BsPFK mutant.

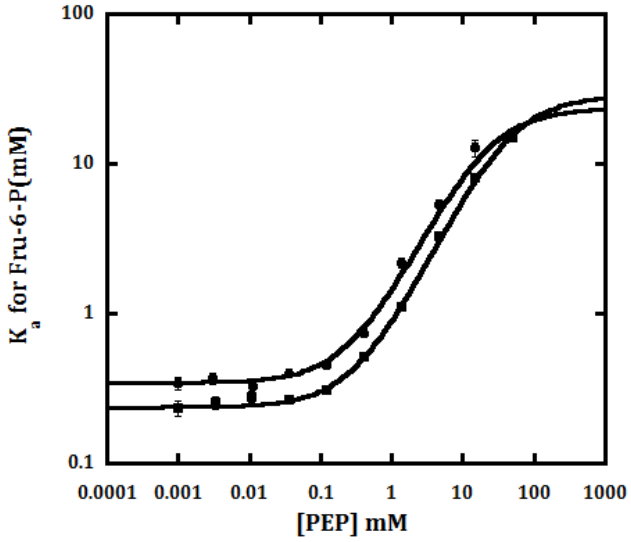

Figure 4-6: The log of the apparent K_a for Fru-6-P as a function of the log of [PEP] for wild-type (circles), and L154V (squares) variants of EcPFK.

The resulting values of K_{ia}^{o}, K_{iy}^{o}, Q_{ay}, and ΔG_{ay} are presented in Table 4-1 for both L154V-EcPFK and wild-type EcPFK. A modest decrease in K_{ia}^{o} in response to the mutation in EcPFK was observed. Unlike I153V-BsPFK, which has almost 4-fold

tighter PEP binding compared to wild-type, the L154V mutation in EcPFK resulted in slightly weaker PEP binding.

The same type of thermodynamic analysis completed with the BsPFK mutants above was repeated for WT-EcPFK and L154V-EcPFK. Plots of the log of Q_{ay} as a function of reciprocal temperature for both the mutant and WT-EcPFK enzymes show that there is little if any change in slope in response to the mutation, revealing no change in the enthalpy component of the coupling free energy (Figure 4-7). In addition, there is also not a significant change in the entropy term. The numerical values corresponding to ΔH_{ay}, $T\Delta S_{ay}$, and ΔG_{ay} are listed in Table 4-2.

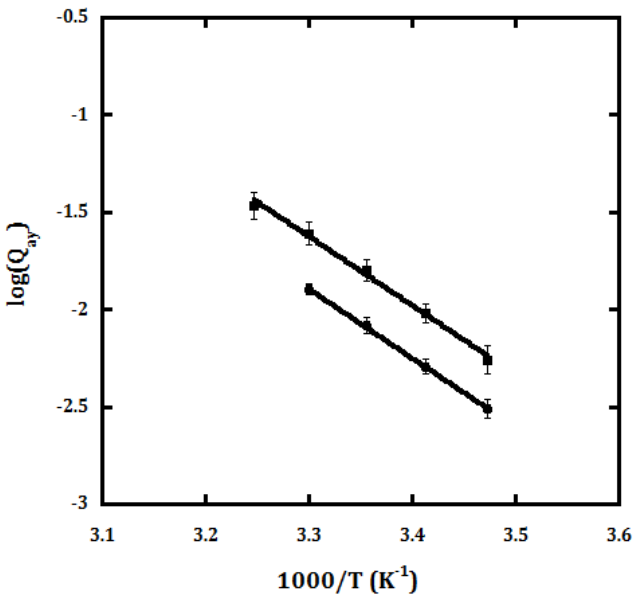

Figure 4-7: The variation in the log of Q_{ay} verses reciprocal temperature of wild-type (circles), and L154V (squares) variants of EcPFK.

Discussion

The BsPFK variants used in this study each contain a conservative single amino acid substitution of isoleucine to valine. From the X-ray crystallography structures of BsPFK, one can identify an extensive hydrogen-bonding network that stretches through the region between the allosteric site and the closest active site. The allosteric coupling between these two sites, termed the 22 Å interaction, was previously shown to make the strongest contribution to the overall heterotropic coupling free energy in both EcPFK[110] and BsPFK[98]. The residues mutated to construct the cavity containing variants in BsPFK all lie between or are in proximity to the region between these sites as shown in Figure 4-8.

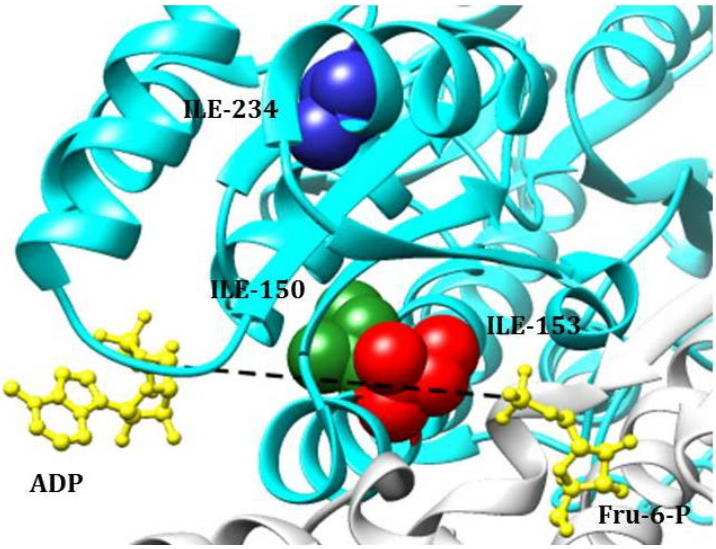

Figure 4-8: X-ray crystallography structure showing the location of the I150V (green), I153V (red), and I234V (blue) mutations in space fill. ADP and Fru-6-P are shown in the allosteric and active site, respectively (yellow).

We postulated that the removal of a methylene group, resulting in the addition of a small cavity, would not largely alter the overall structure of the enzyme. We were curious, however, if it would allow for a change in the flexibility and stability of the BsPFK enzyme and possibly the extent of PEP inhibition. EcPFK, which is not as rigid as BsPFK and has a smaller value for ΔG_{ay}, serves as an interesting comparison. The magnitude of allosteric inhibition is given by the standard free energy, ΔG_{ay}, for the disproportionation equilibrium and each of the four species in eq 4-1 that contribute to the poise of this equilibrium are potentially altered in response to the mutation. The value for ΔG_{ay} is derived from the difference between the perturbations of the free energy of formation when both ligands bind simultaneously versus the sum of the perturbations experienced by the binding of each ligand individually. In other words, the changes caused by the mutation must enhance or relieve conflict in the ternary complex in order to alter the value for ΔG_{ay}, thereby modifying the degree of inhibition.

Two of the three mutations have a substantial effect on the allosteric coupling free energy at 25 °C. The variant I153V-BsPFK has the strongest effect represented by an almost 4-fold augmentation of inhibition and a 0.8 kcal/mol increase in the allosteric coupling free energy. Residue Ile-153 is located within an α-helix that passes directly between an active and allosteric binding site pair that are 22 Å away from each. Residue Ile-150 is also located within this helix, but is positioned slightly further away from the region between the binding sites. Alternatively, the mutation at this location led to a weakening of the allosteric

coupling. The mutant with no effect on the inhibition of PFK by PEP at 25 °C, I234V, is located within another α-helix 12 Å away from the helix containing the other mutations. The effect on allosteric coupling as a result of the small cavity containing mutations ranges from no effect at all to substantially altering the allosteric coupling both positively and negatively. This implies that the allosteric coupling free energy is very sensitive to small changes in the enzyme's structure.

A recent study utilizing PFK from the extreme thermophile *Thermus thermophilus* (TtPFK) also probed the effect of residues in this region on PEP inhibition.[135] In this study, a set of three residues were identified between the pair of Fru-6-P and PEP binding sites located 22 Å apart that when mutated to the residue found natively in BsPFK enhanced allosteric inhibition by 3 kcal/mol. One of these key residues is at position 158, and is located within the same helix as Ile-153 and Ile-150. Interestingly, each individual mutation in TtPFK increased coupling essentially additively, and by a greater extent than one would expect if a linked chain of interactions was required to propagate the allosteric signal. It was hypothesized that the entropic nature of the inhibition may explain why a localized network of interactions does not seem to provide an explanation for allosteric coupling. The entropic nature of inhibition in BsPFK may also explain why we see substantial changes in the allosteric coupling with very minor perturbations.

We were surprised that the degree of allosteric coupling was altered in response to such conservative mutations. We predicted that the changes in the allosteric coupling free energy introduced by the removal of a methylene group

would be more likely due to effects on the conformational entropy as opposed to effects on the enthalpy component of the coupling free energy. Changes in the coupling entropy, $T\Delta S_{ay}$, term are in fact seen for all three of the BsPFK cavity containing mutants. Equal, or even more substantial changes in ΔH_{ay} are also seen, however. The less negative values observed in the entropy component of the coupling seen for I153V and I234V may suggest that in these cases there are increased thermal fluctuations present in the propagation of the allosteric signal. Surprisingly, the entropy component of the coupling becomes more negative in the case of I150V, suggesting less flexibility in the transfer of the signal between binding sites.

In contrast to the entropically driven allosteric coupling in BsPFK, the allosteric coupling between Fru-6-P and PEP binding sites in EcPFK is enthalpy driven, indicating the possibility that distinct mechanisms may be responsible for transmitting the allosteric signal between Fru-6-P and PEP binding sites in the two isozymes. Probing this important difference between these otherwise very similar enzymes has the potential to provide new information about the mechanisms of allosteric regulation in prokaryotic PFK in general. In addition, because the EcPFK enzyme is more flexible than the BsPFK enzyme it serves as a point of comparison for the effect of the mutations. The L154V-EcPFK mutant, which corresponds to I153V-BsPFK, also has augmented allosteric coupling, but only to a very small extent.

In conclusion, multiple mutations were made to probe the effect of adding a small cavity to the structure of the entropy dominated allosteric coupling of BsPFK. Of these mutations, two altered the allosteric coupling free energy of BsPFK substantially at 25 °C, and all three had an effect on both the entropy and enthalpy components of the coupling free energy. When the mutation with the largest effect in BsPFK was made in EcPFK very little effect was seen on the allosteric coupling. These results indicate that even very small perturbations to the BsPFK enzyme can have very substantial effects on both the entropy and enthalpy components of the coupling free energy. This is interesting because the moderate thermophile BsPFK is considered a fairly rigid enzyme[116,144,148,149], and we expect that the mutations make regions of the enzyme more flexible. Previous studies in the lab utilizing BsPFK demonstrated that temperature and pH also exert their influence on allosteric inhibition by changing the relative contributions made by the ΔH_{ay} and $T\Delta S_{ay}$ terms of the coupling free energy.[42] Regardless, because the entropy and enthalpy terms do change so much, there is ample opportunity for the balance between them to also change. These changes alter the poise of the disproportionation equilibrium and affect the extent of inhibition in BsPFK, but not in the more flexible EcPFK. Perhaps the ability to so easily modify the extent of allosteric inhibition in BsPFK has served an evolutionary advantage, allowing the enzyme to quickly adapt to varying environments. It also seems that the ability to alter the efficiency of inhibition of a major metabolic pathway with relative ease would be advantageous for drug design.

CHAPTER V

PROPAGATION OF THE ALLOSTERIC SIGNAL IN PHOSPHOFRUCTOKINASE FROM *BACILLUS STEAROTHERMOPHILUS* EXAMINED BY METHYL-TROSY NMR

Introduction

In order to isolate regions and residues of the phosphofructokinase structure from *Bacillus stearothermophilus* (BsPFK) that are involved in the propagation of the allosteric signal, we employed linkage analysis and methyl-TROSY NMR. Chemical shift changes, of the relevant resonance frequencies, were analyzed in response to ligand binding and formation of the ternary complex. These resonance frequencies vary in response to changes in the local magnetic environment of the nuclei and therefore small changes in structure and dynamics of a particular nucleus is readily detectable by monitoring the change in chemical shift.[150] This sensitivity of the nuclei to its local magnetic environment has led to the frequent use of 2D heteroneuclear experiments to generate "fingerprints" by which protein conformational changes and ligand binding can be studied.[151] Unfortunately, the utility of these traditional experiments is limited to proteins with a molecular weight of less than 50 Kda. BsPFK is a fairly large enzyme with a subunit molecular weight of 34 Kda. In its active form, the subunits form a homotetramer composed of a dimer of dimers, where opposing interfaces form the active and allosteric binding sites, with a total molecular weight of 136 Kda.

The development of NMR experiments that enable the preservation of NMR signals that would otherwise rapidly decay for large protein systems[152,153], including transverse relaxation-optimized spectroscopy (TROSY) coupled with the development of new selective isotope labeling strategies,[154,155] has allowed for the study of increasingly larger proteins by NMR spectroscopy. A general approach that extends application to high molecular weight proteins, such as BsPFK, involves the use of ^{13}C and protonated methyl group probes on alanine, methionine, isoleucine, leucine and/or valine residues in an otherwise highly deuterated environment.[155-157] Selection of this labeling scheme is motivated firstly by the fact that methyl groups are prevalent throughout the enzyme, including hydrophobic cores and at molecular interfaces, thereby serving as well distributed internal reporters of dynamics and structure.[158] Secondly, exceptional spectral sensitivity results from the three equivalent protons in each methyl group, coupled with the rapid rotation of the methyl about its threefold symmetry axis and its localization to flexible ends of side chains. Furthermore, the inherent spin physics of a methyl group enables the preservation of NMR signals, even in large biomolecular systems, via a methyl-TROSY effect that manifests in ^{13}C–^{1}H heteronuclear multiple quantum correlation (HMQC) spectra.[152] TROSY selects only the sharpest doublet component of the signal. This causes half of the signal to be lost; however, it also accounts for a large gain in signal to noise ratio which is needed when studying large proteins via NMR.

This investigation utilizes methyl-TROSY NMR to examine the four enzyme species involved in PEP inhibition of BsPFK, the enzyme that catalyzes the

phosphorylation of fructose-6-phosphate (Fru-6-P) by MgATP to produce fructose-1,6-bisphosphate. In this highly allosterically regulated first committed step of glycolysis, BsPFK is allosterically inhibited by the K-type effector phosphoenol-pyruvate (PEP). Paramount to the success of any NMR study is appropriately labeling your protein of interest. The labeling strategy used for BsPFK incorporated isoleucines which were selectively ^{13}C labeled and protonated at the δ-methyl group in an otherwise ^{12}C and deuterated enzyme. The labeling was accomplished by adding isotopically labeled α-ketobutyrate, a metabolic precursor to isoleucine biosynthesis, to the cell culture prior to induction. Figure 5-1 shows the overall reaction by which 2-keto-3-d_2-4-^{13}C-butyratebutyrate, [^{12}C, ^{2}H] D-glucose, and $^{15}NH_4Cl$ are incorporated into the isoleucine residues of BsPFK. By measuring the

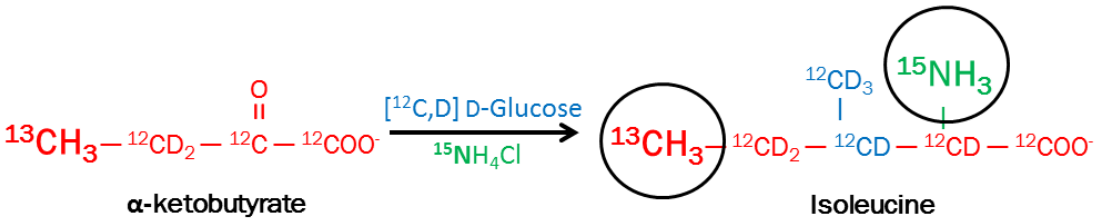

Figure 5-1: Structure of the labeled α-ketobutyrate precursor, and how each labeled component of the minimal media is incorporated into the isoleucine residues of [U-^{15}N,^{2}H];Ileδ1-[$^{13}CH_3$] BsPFK.

perturbations in NMR chemical shifts upon substrate and inhibitor binding methyl groups can serve as local reporters on the allosteric coupling. These results are especially relevant when combined with previous studies in the lab which have

identified regions of the enzyme predicted to contribute to the coupling entropy parameter.[117]

When describing the nature and magnitude of the allosteric effect between the two ligands Fru-6-P and PEP, all possible ligation states of the enzyme must be considered. BsPFK (E) is free enzyme. BsPFK:F6P (EA) and PEP:BsPFK (YE) are the two binary complexes and PEP:BsPFK:F6P (YEA) is the ternary complex. The effect the inhibitor PEP has on the subsequent binding of substrate Fru-6-P to the enzyme, and the equivalent reciprocal effect of Fru-6-P on the binding of PEP, can be quantified by the coupling constant, Q_{ay}. This coupling constant is defined by a ratio of thermodynamic dissociation constants for Fru-6-P and PEP using the following equation:

$$Q_{ay} = \frac{K_{ia}^{o}}{K_{ia}^{\infty}} = \frac{K_{iy}^{o}}{K_{iy}^{\infty}} \tag{5-1}$$

where, $K_{ia}^{o}$and K_{ia}^{∞} are the dissociation constants for Fru-6-P (A) in the absence and saturating presence of PEP (Y), respectively. Analogously, K_{iy}^{o} and K_{iy}^{∞} are the dissociation constants for PEP in the absence and saturating presence of Fru-6-P, respectively. By substituting the definitions for the dissociation constants into this equation, it can be shown that the coupling constant serves as an equilibrium constant between the four species in the following disproportionation reaction:

$$[EA] + [YE] \overset{Q_{ay}}{\longleftrightarrow} [E] + [YEA] \tag{5-2}$$

where, the left side of the equilibrium contains the two binary complexes and the right side encompasses free enzyme and the ternary complex. For this reaction, the

standard allosteric coupling free energy (ΔG_{ay}) can be defined in terms of either the equilibrium constant or its enthalpy and entropy components as follows:

$$\Delta G_{ay} = -RTln(Q_{ay}) = \Delta H_{ay} - T\Delta S_{ay} \quad (5\text{-}3)$$

where, R is the gas constant and T is the absolute temperature in Kelvin. By past convention, the superscript "0" is omitted to avoid confusion with the meaning of the superscripts appearing in eq 5-1 and the scheme in Figure 1-2.[32] In an effort to ascertain the molecular basis for the inhibition by PEP, for which $\Delta G_{ay} > 0$ by definition, one must consider the four enzyme species depicted in eq 5-2 and how their differences might ultimately generate the thermodynamic values of ΔH_{ay} and ΔS_{ay} as shown in eq 5-3.

The present study attempts to identify regions of enzyme that likely contribute to the coupling free energy. More specifically, Methyl-TROSY HMQC experiments were conducted with [U-^{2}H,^{15}N]-BsPFK specifically labeled with Ileδ1-[^{13}C,$^{1}H_3$] in order to gain more structural information about BsPFK in all four states of ligation relevant to the allosteric coupling. As a result of these experiments, specific residues of the enzyme where structural conflicts arise upon the binding of both ligands simultaneously are identified. Mapping these "interesting" residues back to the crystal structure has allowed specific regions of the enzyme involved in the propagation of the allosteric signal to be identified.

Materials and Methods

Materials

All chemical reagents used in buffers for protein purification, enzymatic assays, and NMR experiments were of analytical grade and were purchased from Sigma-Aldrich (St. Louis, MO), Fisher Scientific (Fair Lawn, NJ), or Research Products International (Mt. Prospect, IL) unless otherwise noted. Deionized distilled water was used throughout. Lyophilized creatine kinase, the ammonium sulfate suspension of glycerol-3-phosphate dehydrogenase, and the potassium salt of phosphoenol-pyruvate were purchased from Roche (Indianapolis, IN). The ammonium sulfate suspensions of aldolase, the ammonium sulfate suspension of triosephosphate isomerase, the disodium salt of fructose-6-phosphate, and the disodium salt of phosphocreatine were purchased from Sigma-Aldrich (St. Louis, MO). The coupling enzymes were extensively dialyzed against 50 mM EPPES pH 8.0, 100 mM KCl, 5 mM $MgCl_2$, and 0.1 mM EDTA before use. NADH and DTT were purchased from Research Products International (Mt. Prospect, IL). Mimetic Blue 1 A6XL resin used in protein purification was purchased from Promatic BioSciences (Rockville, MD). The Mono-Q HR anion exchange column used in protein purification was purchased prepacked for FPLC use from Pharmacia (currently GE Healthcare, Uppsala, Sweden). Amicon Ultra centrifugal filter units (spin concentrators) were from Millipore Corporation (Billerica, MA) and poly(ethylene glycol)-3000 was from Sigma-Aldrich (St. Louis, MO). Minimal media was made

using potassium phosphate, monobasic, and sodium phosphate, dibasic, from EMD Chemicals (Gibbsown, NJ). Additional components of the minimal media include D-glucose from Macron Chemicals (Center Valley, PA), magnesium sulfate and ferrous sulfate from Fisher Scientific (Fair Lawn, NJ), thiamine hydrochloride and calcium chloride dihydrate from Sigma-Aldrich (St. Louis, MO), and ammonium chloride from Acros Organics (NJ). Deuterated MES-d_{13} was from Sigma-Aldrich (St. Louis, MO). Ammonium chloride (^{15}N, 99%), L-isoleucine (^{15}N, 98%), L-isoleucine($^{13}C_6$,99%;^{15}N, 99%), α-ketobutyric acid, sodium salt (CH_3-^{13}C, 99%), D-glucose (1,2,3,4,5,6,6-D_7,97-98%), D-glucose (U-$^{13}C_6$,99%; 1,2,3,4,5,6,6-D_7,97-98%) and deuterium oxide (D, 99.9%) are from Cambridge Isotope Laboratories, INC (Andover, MA). Shigemi NMR tubes were purchased from Shigemi, Inc. (Allison Park, PA) and were used for all NMR experiments.

Protein Expression and Purification of Isotopically Labeled Wild-type BsPFK

The plasmid pBR322/BsPFK[118] contains the gene for BsPFK behind the native *Bacillus stearothermophilus* promoter. This plasmid was modified to place the BsPFK gene behind an inducible lac promoter in pALTER-1, it should be noted that an inducible plasmid was necessary to express the proteins in minimal media. BsPFK was expressed in *E. coli* RL257A cells, which are a T1 bacteriophage resistant derivation of RL257 cells[119], which intern are lacking both the *pfkA* and *pfkB* genes. RL259A cells were made by P1 transduction[159] using RL257 cells as the recipient strain and RY12459 cells as a donor strain. RY12459 cells were obtained

from Ry Young (Texas A&M University, College Station, TX) and are a derivative of MC4100[160] that contain a *tonA* gene disruption within a kanamysin cassette.

Protein expression of the [U-^{15}N,^{2}H];Ileδ1-[$^{13}CH_3$]-BsPFK was performed as described previously by Tugarinov, V. et. al., with a few minor modifications.[155] Following heat shock transformation, cells were picked from a single bacterial colony that was grown on solid Lysogeny Broth (LB)/tet/H_2O media (Tryptone 10 g/L, yeast extract 5 g/L, and Sodium Chloride 10 g/L, tetracycline 15 µg/mL). These cells were transferred to a 5 mL culture of LB/tet/H_2O media and allowed to grow in a shaking incubator at 37 °C until the cell density reached an OD_{600} of 0.7 - 0.8 (4 - 6 hours). The 5 mL culture was spun down with a speed of 1,200 × g at room temperature and the pellet was gently resuspended in 1 mL of M9/H_2O media (0.048 M Na_2HPO_4, 0.022 M KH_2PO_4, 9 mM NaCl, 19 mM NH_4Cl, 0.2 % glucose, 2 mM $MgSO_4$, 100 µM $CaCl_2$, 10 µg/mL thiamine, 10 µg/ml $FeSO_4$, 15 µg/mL tetracycline) which contained unlabeled glucose and NH_4Cl. Aliquots of the resuspension were added to 20 mL of the unlabeled M9/H_2O media until the starting OD_{600} was between 0.05 and 0.1. The culture was grown until the OD_{600} reached 0.6, which took between 8 - 10 hours. The culture was then centrifuged and resuspended in 100 mL of labeled M9/D_2O media (containing [^{2}H,^{13}C]-glucose and $^{15}NH_4Cl$) so that the beginning OD_{600} was 0.1. These cells were grown until the OD_{600} was between 0.4 - 0.5 (8 - 10 hours), then the cells were diluted to 200 mL by the addition of 100 mL labeled M9/D_2O media and were again grown until the OD_{600} reached 0.4 - 0.5 (4 - 6 hours). At this time the culture was diluted with labeled M9/D_2O media to a

volume that equaled 1 L once the α-ketobutyrate was added and allowed to grow until the OD_{600} was 0.25 (4 - 6 hours). At this time, 70 mg/L of [3-$^{2}H_2$],^{13}C α-ketobutyrate was added to the culture. Following a previously established protocol, [3-^{1}H],^{13}C α-ketobutyrate was deuterated by incubating the ^{13}C α-ketobutyrate at pH 10.5 in D_2O for 12 - 14 hours prior to its addition.[156] The culture was allowed to grow for approximately one hour until the OD_{600} was between 0.3 - 0.4. Protein expression was induced with the addition of 1 mM IPTG and the cells were allowed to grow for 8 hours. The final OD_{600} was between 0.7 - 1.0.

For [U-^{15}N,^{2}H]; Ileδ1-[$^{13}CH_3$]-BsPFK, the same procedure was followed with the following exceptions: minimal media was prepared with $^{14}NH_4Cl$ instead of $^{15}NH_4Cl$, and Ile-[^{15}N] was added to the media instead of the α-ketobutyrate precursor. For [U-^{15}N,^{2}H,]; Ile-[^{15}N, ^{13}C]-BsPFK the same procedure was followed except Ile-[^{15}N, ^{13}C] was added to the media instead of the α-ketobutyrate precursor. For [U-^{2}H,^{15}N,^{13}C]-BsPFK minimal media was prepared with D-[^{2}H, ^{13}C] glucose and $^{15}NH_4Cl$ and no selective labeling of isoleucine methyl groups was performed.

Upon completion of growth, cells were harvested from the media by centrifugation and frozen at -20 °C for at least 12 hours before resuspension in purification buffer (10 mM Tris-HCl pH 8.0 and 1 mM EDTA) and sonication in a Fisher 550 Sonic Dismemberator at 0 °C in 15 second pulses at setting 6 for 12 minutes or until the OD_{600} is no longer decreasing. The crude lysate was centrifuged at 22,500×g for 30 minutes at 4 °C. The clarified supernatant was incubated in a

water bath at 70 °C for 15 minutes, cooled on ice for 15 minutes, and centrifuged again for 30 minutes at 4 °C. The BsPFK supernatant was diluted to 1 L and loaded onto a Mimetic Blue 1 A6XL column that was equilibrated with purification buffer. The column was washed with 1 L of purification buffer, and the enzyme was eluted with a 600mL 0 - 1.5M NaCl gradient. Enzyme containing fractions were pooled and dialyzed into 20 mM Tris-HCl pH 8.5 and loaded onto a Pharmacia Mono-Q HR anion exchange column that had been equilibrated with the same buffer. The enzymes were eluted with a 200 mL 0 - 1 M NaCl gradient and PFK containing fractions were combined, concentrated, then dialyzed into MES Buffer (10mM MES, pH 6.0). Concentrated enzyme was further dialyzed and stored in MES-d_{13}/D_2O Buffer (10 mM deuterated MES pH 6.0 and 0.02 % NaN_3) at 4 °C. The final enzyme was determined to be pure by SDS-PAGE and the concentration was ascertained using the absorbance at 280 nm (ε = 18910 $M^{-1}cm^{-1}$). The final enzyme concentrations achieved for NMR experiments were between 0.4 - 0.5 mM in monomer. Approximately 325 µL of protein was added to a Shigemi NMR tube. Fru-6-P and PEP solutions that were added to the NMR protein samples were diluted in MES/D_2O buffer and were made as concentrated as possible in order to add the smallest possible volume.

Generation of the Four Enzyme-Ligand Species

To generate the PEP-BsPFK species, 50 mM PEP was added to BsPFK. For the generation of the substrate bound complex, 10 mM F6P was added to BsPFK.

The ternary complex was mixed with 10 mM Fru-6-P and 50 mM PEP to generate PEP:BsPFK:Fru-6-P. Based on the ligand dissociation constants and the allosteric coupling constant at 37 °C and pH 6.0, less than 2 % of other species were present. The ligand dissociation constants were determined using steady-state fluorescence assays with a tryptophan-shifted mutant. These assays were performed in the absence of turnover and the second substrate, ATP, to match the conditions of the enzyme during the NMR experiments. In addition, NMR titrations confirmed that spectra represent saturated complexes where indicated.

Methyl-TROSY NMR Spectroscopy

Methyl-TROSY experiments were performed on either a Bruker 600 MHz, or 800 MHz spectrometer, both instruments equipped with a cryo-probe. Two-dimensional ^{1}H-^{13}C HMQC methyl correlation experiments were acquired on samples of [U-^{15}N,^{2}H]; Ileδ1-[$^{13}CH_3$]-BsPFK using the pulse schemes described previously.[152] The temperature was set to 37 °C for all experiments. NMR data were processed and analyzed with TopSpin and analyzed using Sparky.

Resonance Assignments

Isoleucine assignments were determined through 3D HMQC-NOESY experiments with [U-^{15}N,^{2}H]; Ileδ1-[$^{13}CH_3$]-BsPFK and complementary HNCA and HNCOCA experiments with [U-^{2}H,^{15}N,^{13}C] BsPFK. In addition a 2D ^{1}H-^{15}N TROSY

spectrum of [U-^{2}H];Ile-[^{15}N]-BsPFK and triple resonance experiments with [U-^{15}N, ^{2}H];Ile-[^{15}N, ^{13}C]-BsPFK confirmed the assignments.

Steady-State Kinetic Assays

Activity measurements for BsPFK were carried out using a coupled enzyme system[121,122] in a 0.6 mL reaction volume of either 50mM EPPS buffer (pH 8.0, 25 °C) or 10 mM MES buffer (pH 6.0, 37 °C), additionally containing 5 mM $MgCl_2$, 100 mM KCl, 0.1 mM EDTA, 2 mM DTT, 0.2 mM NADH, 3 mM ATP, 250 μg aldolase, 50 μg of glycerol-3-phosphate dehydrogenase, and 5 μg of triosephosphate isomerase. 40 μg/mL of creatine kinase and 4 mM phosphocreatine were added as an ATP regenerating system to avoid the accumulation of MgADP, which is an activator. Temperature was controlled using a NESLab RTE-111 circulating water bath. Fru-6-P and PEP were added at varied concentrations as indicated. Assays were started by the addition of 10 μL of appropriately diluted PFK and the reaction was monitored as the absorbance at 340 nm decreased over time. The rate of the reaction was measured on Beckman Series 600 spectrophotometers using a linear regression calculation to convert change in absorbance at 340 nm to PFK activity. One unit of PFK activity is described as the amount of enzyme needed to produce 1 μmol of fructose-1,6-bisphosphate per minute.

Kinetic Data Analysis

Data were fit using the non-linear least-squares fitting analysis option in Kaleidagraph software version 4.5 (Synergy). For the steady-state kinetic assays the initial velocity data were plotted against concentration of Fru-6-P and fit to the Hill equation[8]:

$$v = \frac{V[A]^{n_H}}{K_a^{n_H} + [A]^{n_H}} \tag{5-4}$$

where, v is the initial velocity, $[A]$ is the concentration of the substrate Fru-6-P, V is the maximal velocity, and n_H is the Hill coefficient. K_a is defined as the concentration of Fru-6-P at which the enzyme's activity is half-maximal. Assuming rapid equilibrium for Fru-6-P, which was shown to be valid in EcPFK using a steady-state kinetic method, K_a is equivalent to the dissociation constant for Fru-6-P from the binary enzyme-substrate complex[34,101]. Values of K_a obtained from the initial velocity experiments were plotted against the concentration of opposing ligand and fit according to

$$K_a = K_{ia}^o \left(\frac{K_{iy}^o + [Y]}{K_{iy}^o + Q_{ay}[Y]} \right) \tag{5-5}$$

where K_{ia}^o is the dissociation constant for Fru-6-P in the absence of PEP, K_{iy}^o is the dissociation constant for PEP in the absence of Fru-6-P, and Q_{ay} is the coupling coefficient.[32,33,123] Q_{ay} describes the effect of the allosteric effector on the binding of the substrate, and is defined in eq 5-1.

Results

As a result of the selective labeling, all 30 of the isoleucine residues per monomer of [U-^{15}N,^{2}H]; Ileδ1-[$^{13}CH_3$]-BsPFK contain one methyl group that is potentially visible by NMR. As shown in Figure 5-2A, the isoleucine residue probes in BsPFK are all well dispersed throughout the monomer potentially providing excellent coverage of the enzyme structure. This includes many residues between the allosteric sites and the active sites in a BsPFK monomer.

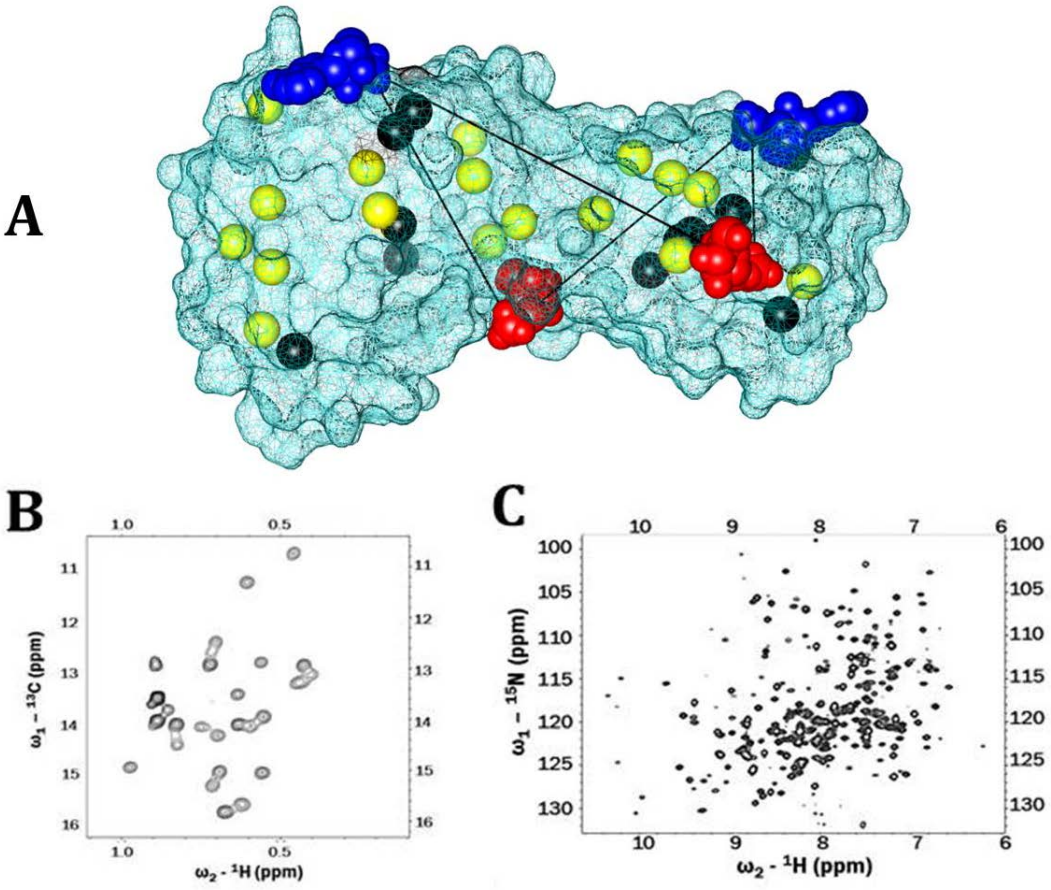

Figure 5-2: [U-^{15}N,^{2}H];Ileδ1-[^{13}CH$_3$] labeling of BsPFK provided excellent coverage of the enzyme and well resolved 2D spectra. A) X-ray crystal structure of the BsPFK monomer with all 30 isoleucine residues represented by spheres. Yellow spheres are isoleucines we were able to assign, and black spheres are isoleucines that remain unassigned. ADP is shown in the allosteric site in blue, and Fru-6-P is shown in the active site in red. B) Methy-TROSY spectrum (37 °C; pH6.0; 600MHz; 10% D$_2$0/90% H$_2$0) C) ^{1}H-^{15}N TROSY spectrum (37 °C; pH6.0; 800MHz; 10% D$_2$0/90% H$_2$0).

Specific activity, apparent ligand dissociation constants, and the allosteric coupling parameters for the isotopically labeled enzymes were comparable to their unlabeled counterparts, as shown in Figures 5-3A and B, and in Tables 5-1 and 5-2.

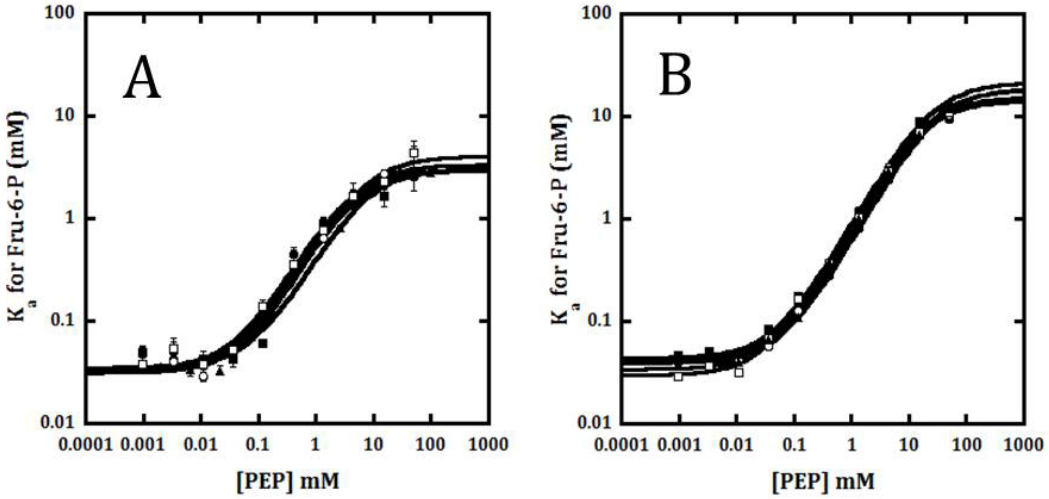

Figure 5-3: Allosteric couplings for unlabeled and isotopically labeled BsPFK variants at A) 37 ˚C and pH 6.0 and B) 25 ˚C and pH 8.0. Filled circles are unlabeled BsPFK, open circles are [U-^{15}N], [^{13}C,$^{1}H_3$]-ILE BsPFK, filled squares are [U-^{2}H,^{15}N,^{13}C] BsPFK, open squares are [U-^{2}H], [^{15}N]-ILE BsPFK, and triangles are [U-^{2}H,^{15}N], [^{13}C]-ILE BsPFK.

In addition, the activities of the labeled enzymes did not diminish over the course of the NMR experiments (data not shown). The similar values for the apparent dissociation constants and the allosteric coupling parameters indicate that the isotopic labeling did not disrupt the structure or function of the enzyme in any significant way.

Table 5-1: Allosteric coupling parameters for unlabeled and the isotopically labeled BsPFK at 25 °C and pH 8.0.

BsPFK Labeling	K_{ia}^{o} (μM)	K_{iy}^{o} (μM)	Q_{ay}	ΔG_{ay} (kcal/mol)
Unlabeled	39 ± 2	63 ± 4	0.0021 ± 0.0002	3.65 ± 0.02
[U-^{15}N,^{2}H];Ileδ1-[$^{13}CH_3$]	34 ± 2	40 ± 2	0.0022 ± 0.0002	3.63 ± 0.02
[U-^{2}H,^{15}N,^{13}C]	44 ± 3	49 ± 4	0.0021 ± 0.0003	3.65 ± 0.04
[U-^{2}H];Ile-[^{15}N]	30 ± 2	33 ± 2	0.0021 ± 0.0001	3.65 ± 0.01
[U-^{2}H,^{15}N];Ile-[^{13}C]	41 ± 1	56 ± 2	0.0022 ± 0.0002	3.63 ± 0.02

Table 5-2: Allosteric coupling parameters for unlabeled and the isotopically labeled BsPFK at 37 °C and pH 6.0.

BsPFK Labeling	K_{ia}^{o} (μM)	K_{iy}^{o} (μM)	Q_{ay}	ΔG_{ay} (kcal/mol)
Unlabeled	35 ± 2	48 ± 7	0.010 ± 0.002	2.728 ± 0.005
[U-^{15}N,^{2}H]; Ileδ1-[$^{13}CH_3$]	32 ± 1	55 ± 4	0.008 ± 0.001	2.861 ± 0.003
[U-^{2}H,^{15}N,^{13}C]	35 ± 4	42 ± 7	0.012 ± 0.002	2.620 ± 0.004
[U-^{2}H]; Ile-[^{15}N]	35 ± 4	82 ± 14	0.011 ± 0.001	2.672 ± 0.002
[U-^{2}H,^{15}N]; Ile-[^{13}C]	31 ± 1	50 ± 3	0.011 ± 0.001	2.672 ± 0.002

In chemical shift correlation maps of ^{13}C and ^{1}H all 30 isoleucines are well resolved (Figure 5-2B). These spectral maps reveal several cross peaks with chemical shifts unique to each state of ligation indicating unique structures for each

of the enzyme forms. Apo BsPFK and F6P-bound BsPFK spectra are similar to each other whereas the PEP-bound BsPFK spectrum has numerous dissimilar peaks. Distinct peaks, not seen in any other spectra, are present in the spectrum of the ternary complex. In addition, the amide backbones of all 320 amino acids are ^{15}N labeled in [U-^{15}N,^{2}H]; Ileδ1-[$^{13}CH_3$]-BsPFK and Figure 5-2C shows a ^{1}H-^{15}N TROSY spectrum with decent dispersion of resonances. However, because the entire backbone is ^{15}N labeled, there is quite a bit of crowding in the ^{1}H-^{15}N TROSY. Both 2D spectra indicate the enzyme is well folded under the conditions of the experiments, which was confirmed by the sample remaining fully active throughout the experiments.

Complementary HNCA and HN(CO)CA experiments with [U-^{2}H,^{15}N,^{13}C]-BsPFK were used to assign the resonances corresponding to the isoleucines in the ^{1}H-^{15}N TROSY spectrum. In order to transfer these assignments to the methyl-TROSY spectrum both ^{15}N-edited and ^{13}C-edited 3D-HMQC NOESY experiments were performed with [U-^{15}N,^{2}H]; Ileδ1-[$^{13}CH_3$]-BsPFK. The resulting assigned methyl-TROSY spectrum of unligated BsPFK is shown in Figure 5-4A. We were able to unambiguously assign 17 out of the 30 isoleucine residues. One residue, Ile-61

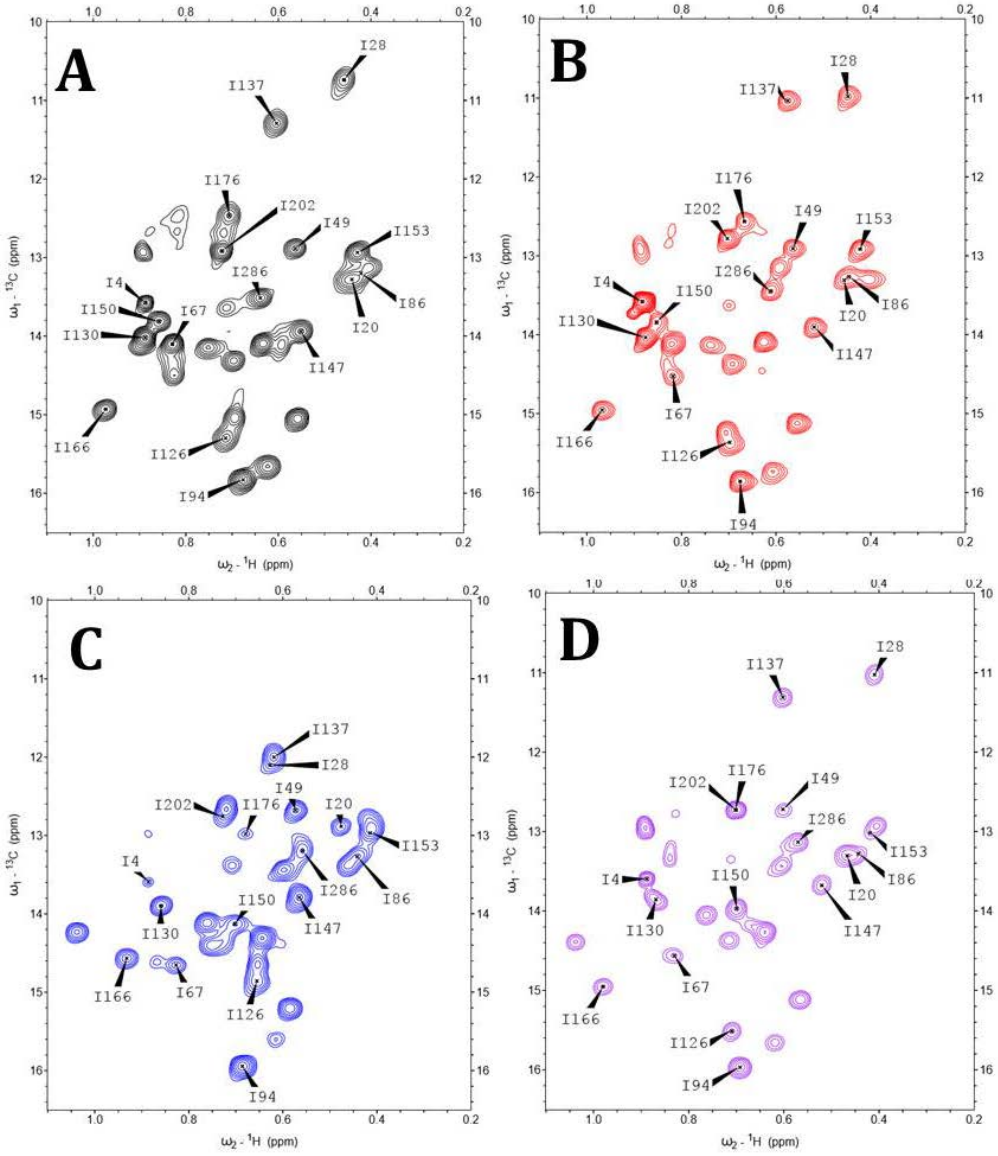

Figure 5-4: Methyl-TROSY spectra (37 °C; pH6.0; 600MHz; 10% D_20/90% H_20) of A) unligated, B) Fru-6-P bound, C) PEP bound and D) the ternary complex BsPFK with assigned isoleucine residues indicated.

was assigned in the ^{1}H-^{15}N TROSY, but was unable to be transferred to the methyl-TROSY spectrum. Of the remaining 12 unassigned isoleucines, at least eight appear

to be buried and were likely unable to undergo the H/D exchange with solvent required to be NMR visible in ^{1}H-^{15}N TROSY experiments.

Fortunately, the Fru-6-P binding process and the formation of the ternary complex by either order of ligand addition are in the fast exchange regime, allowing us to see resonances move across the magnetic field in response to an increase in ligand concentration. Resonance assignments were transferred to the ligated forms of the enzyme using these titrations as demonstrated in Figure 5-5 using Fru-6-P.

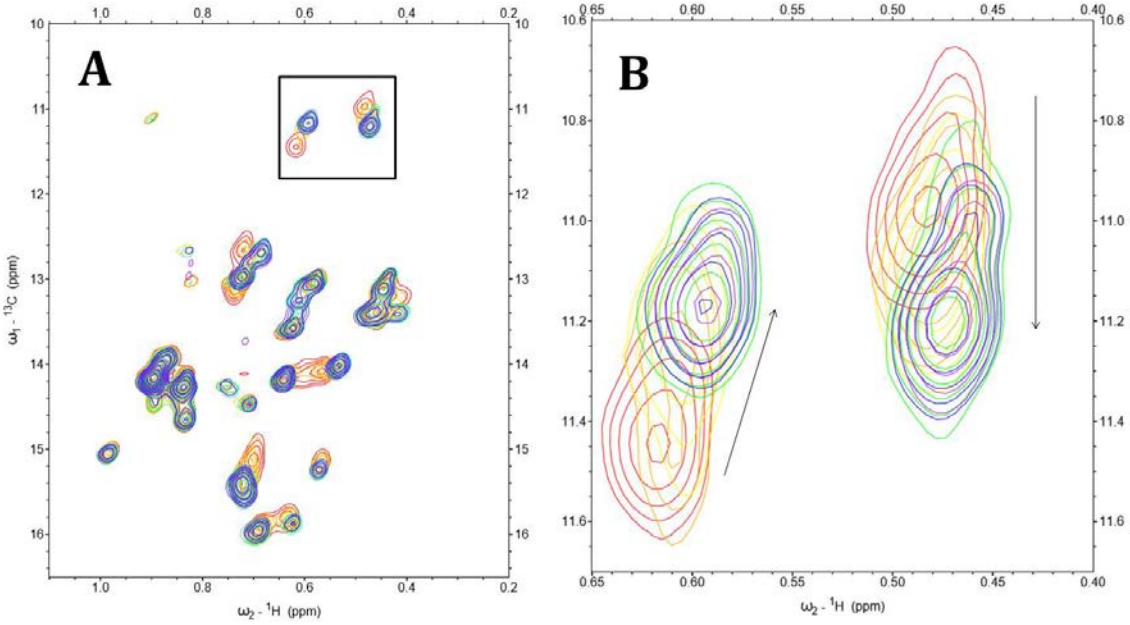

Figure 5-5: A) Overlay of methyl-TROSY spectra (37 °C; pH6.0; 800MHz; 10% D_20/90% H_20) with Fru-6-P concentrations ranging from 0 (red) to 10 mM (Purple). B) Close up of boxed region of panel A. Arrows indicate the direction of chemical shift perturbation in response to increasing ligand concentration.

To distinguish chemical shift changes involved in the allosteric inhibition of BsPFK, it was essential to first determine the chemical shift values for each ligation state of the enzyme that contributes to the disproportionation equilibrium reaction shown in eq 5-2. The coupling free energy value can further be described in terms of the free energy of formation for the products minus the free energy of formation for the reactants[33]:

$$\Delta G_{ay} = (G_{YEA} + G_E) - (G_{EA} + G_{YE}) \tag{5-6}$$

To simplify the equation in terms of free enzyme, subtracting the G_E term from both sides of the equation gives a simple rearrangement:

$$\Delta G_{ay} = \delta G_{YEA} - (\delta G_{EA} + \delta G_{YE}) \tag{5-7}$$

where, the lower case delta (δ) signifies the differences between the free energy of formation of the indicated ligated enzyme and that for free enzyme. For example, the value of δG_{YEA} is equal to $G_{YEA} - G_E$ (the difference in the free energy of formation of YEA compared to that of free enzyme) so that the perturbations in free energy arising from the binding of both A and Y simultaneously to the enzyme are described by this component. When this value is equal to the summation of the perturbations that occur when the ligands bind individually, ΔG_{ay} equals zero, and by definition there is no allosteric effect. Rather, inhibition or activation occurs when these values are not equal to each other. The same can be said for coupling enthalpy and coupling entropy:

$$\Delta H_{ay} = \delta H_{YEA} - (\delta H_{EA} + \delta H_{YE}) \tag{5-8}$$

$$\Delta S_{ay} = \delta S_{YEA} - (\delta S_{EA} + \delta S_{YE}) \quad (5\text{-}9)$$

The change in chemical shift in respect to free enzyme for each of the ligated species was examined to find local regions within the enzyme that may be part of the allosteric pathway in BsPFK. These regions of interest can be found by comparing the differences in chemical shifts when the ligands bind simultaneously to the enzyme versus the summation of chemical shifts when the ligands bind individually. As chemical shift perturbations are not thermodynamic values, care must be taken in their interpretation. However, we can qualitatively divide the 17 residues we could assign into three categories based on whether the degree of chemical shifts are substantial and whether the shifts appear to be additive in respect to the ternary complex, as demonstrated in Figures 5-6 and 5-7. Residues were said to not have substantial perturbations in response to ligand binding if the chemical shift difference between the apo form and any of the three bound forms did not exceed 20% of the largest chemical shift perturbation in either the ^{1}H and ^{13}C dimension. These cut-off values were chosen because they single out the largest perturbations observed for this particular enzyme. Table 5-3 provides the chemical shift perturbations for all of the assigned residues. Residues that did have

Table 5-3: Chemical shift δ[EA], δ[YE], δ[YEA] and δ[YEA] - (δ[EA] + δ[YE]) in the ^{1}H and ^{13}C dimensions for Ile residues. Bold numbers are those shifts qualitatively considered substantial.

Residue	^{1}H (ppm)				^{13}C (ppm)			
	δ[EA]	δ[YE]	δ[YEA]	δ[YEA] - (δ[EA] + δ[YE])	δ[EA]	δ[YE]	δ[YEA]	δ[YEA] - (δ[EA] + δ[YE])
Ile-4	-0.004	-0.001	0.001	0.006	0.005	0.018	0.020	-0.003
Ile-20	0.008	0.028	0.019	-0.017	0.025	**-0.398**	0.022	**0.395**
Ile-28	-0.010	**0.169**	**-0.049**	**-0.208**	0.243	**1.364**	**0.287**	**-1.320**
Ile-45	-	-	-	-	-	-	-	-
Ile-49	0.002	0.010	0.039	0.027	0.030	-0.210	-0.170	0.010
Ile-60	-	-	-	-	-	-	-	-
Ile-61	-	-	-	-	-	-	-	-
Ile-67	-0.008	**0.209**	**0.209**	0.008	0.015	0.136	**0.286**	0.135
Ile-86	0.014	0.010	0.011	-0.013	-0.003	0.002	0.011	0.012
Ile-94	0.000	0.010	0.016	0.006	0.028	0.116	0.139	-0.005
Ile-100	-	-	-	-	-	-	-	-
Ile-126	-0.016	**-0.059**	-0.005	**0.070**	0.065	**-0.444**	0.215	**0.594**
Ile-130	-0.012	-0.029	-0.019	0.022	0.015	-0.120	-0.164	-0.059
Ile-137	-0.030	0.014	-0.003	0.013	**-0.273**	**0.691**	0.002	**-0.416**
Ile-147	-0.034	0.012	-0.033	-0.011	-0.046	-0.160	**-0.272**	-0.066
Ile-150	-0.003	**-0.154**	**-0.157**	0.000	0.032	**0.320**	0.158	-0.194
Ile-153	-0.007	-0.015	-0.010	0.012	-0.021	0.031	0.080	0.070
Ile-166	-0.005	-0.041	0.007	0.053	0.024	**-0.366**	0.020	**0.362**
Ile-176	-0.037	-0.025	-0.002	0.060	0.077	**0.491**	0.240	**-0.328**
Ile-189	-	-	-	-	-	-	-	-
Ile-191	-	-	-	-	-	-	-	-
Ile-202	-0.019	0.006	-0.022	-0.009	-0.135	-0.161	-0.192	0.104
Ile-217	-	-	-	-	-	-	-	-
Ile-218	-	-	-	-	-	-	-	-
Ile-219	-	-	-	-	-	-	-	-
Ile-234	-	-	-	-	-	-	-	-
Ile-286	-0.024	**-0.077**	**-0.065**	0.036	-0.059	**-0.312**	**-0.376**	-0.005
Ile-296	-	-	-	-	-	-	-	-
Ile-307	-	-	-	-	-	-	-	-
Ile-320	-	-	-	-	-	-	-	-

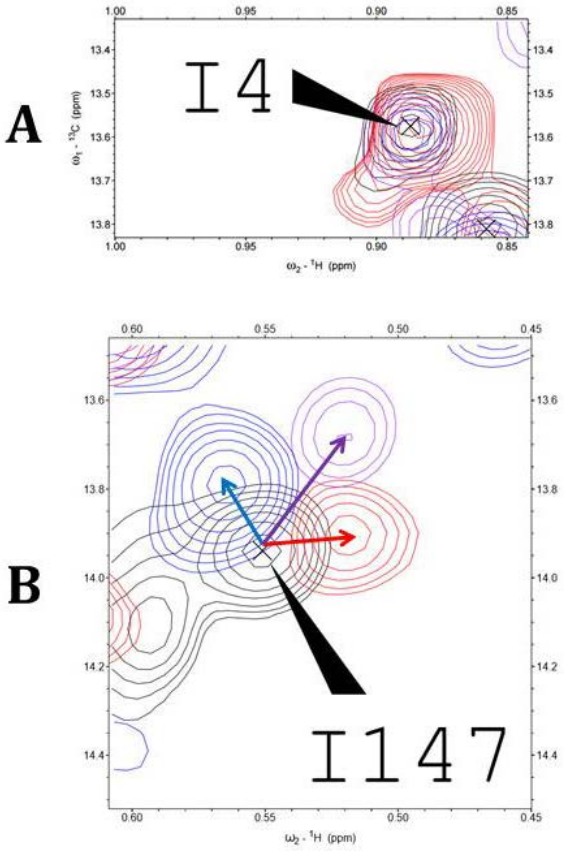

Figure 5-6: Some resonances do not shift, while others shift in either an additive or non-additive manner. A) Ile-4 is an example of a resonance that has the same chemical shift in the unligated and all three ligated forms. B) Ile-147 is an example of a resonance that shifts in an additive manner. Vectors represent the change in chemical shift upon binding of Fru-6-P (red), PEP (blue) or both simultaneously (purple). When arrows are not present the chemical shift is unchanged between the ligated and unligated form.

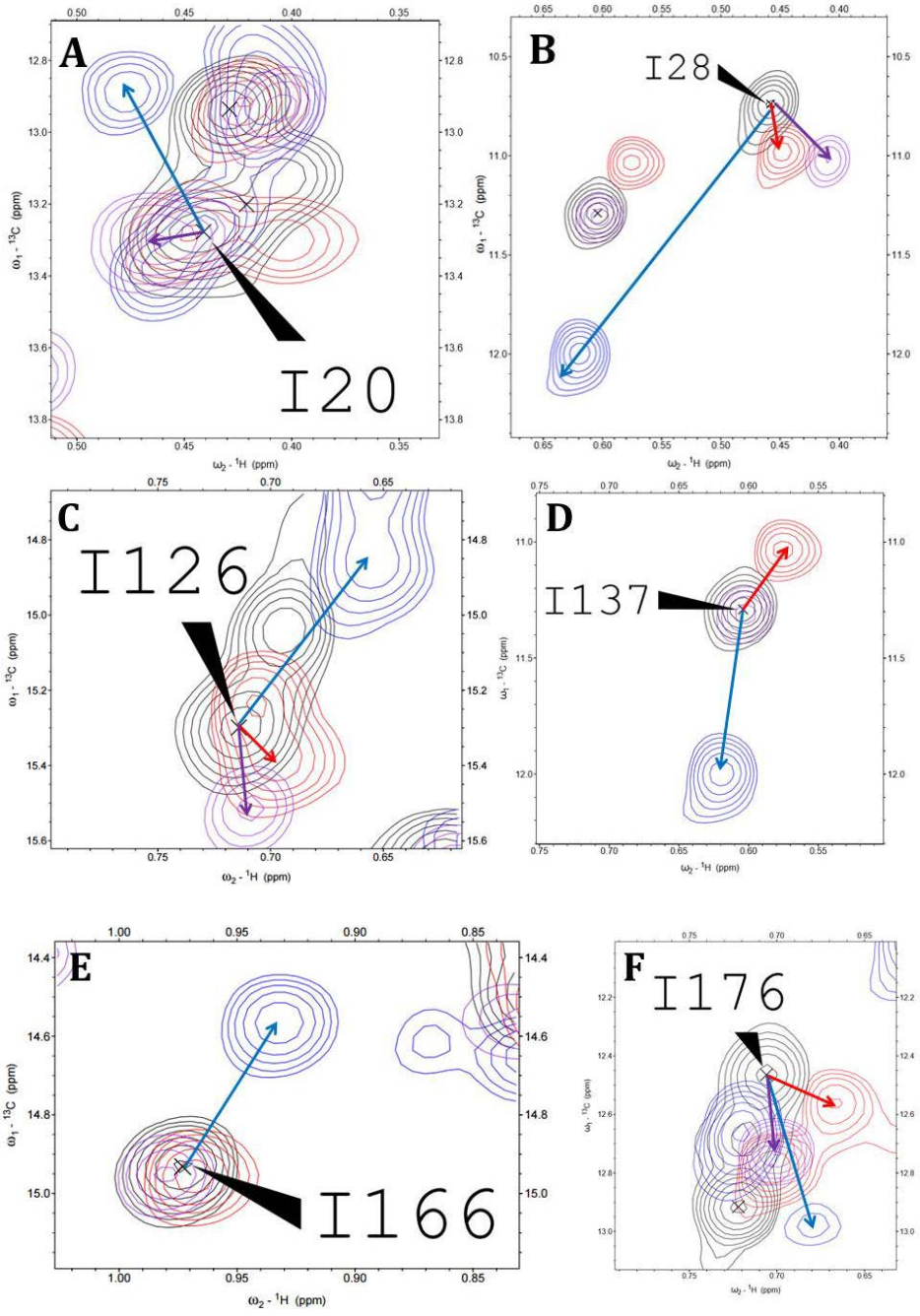

Figure 5-7: Ile-20, Ile-28, Ile-126, Ile-137, Ile-166 and Ile-176 chemical shifts are perturbed in a non-additive manner. Vectors represent the change in chemical shift upon binding of Fru-6-P (red), PEP (blue) or both simultaneously (purple). When arrows are not present the chemical shift is unchanged between the ligated and unligated form.

substantial chemical shift perturbations were further divided into two categories based on whether the chemical shift perturbations seen in the ternary complex appear to be additive or non-additive of the perturbations seen when the ligands bind individually. The same threshold was applied to δ[YEA] - (δ[EA] + δ[YE]) in order to identify the resonances which are the most substantially non-additive. We propose that the resonances with non-additive perturbations are the most likely mark a residue involved in the structural conflict that gives rise to the non-zero value of ΔG_{ay}, the allosteric coupling free energy. The perturbations in chemical shift for the residues identified as having a substantial perturbation in at least one ligation state are shown in Figure 5-8 for both the ^{1}H and ^{13}C dimensions. Figure 5-9 shows an X-ray crystallography structure of the BsPFK monomer with the residues color coded to distinguish between all three categories of chemical shift changes. Positions Ile-4, Ile-49, Ile-86, Ile-94, ILE-130, Ile-153 and Ile-202 show no

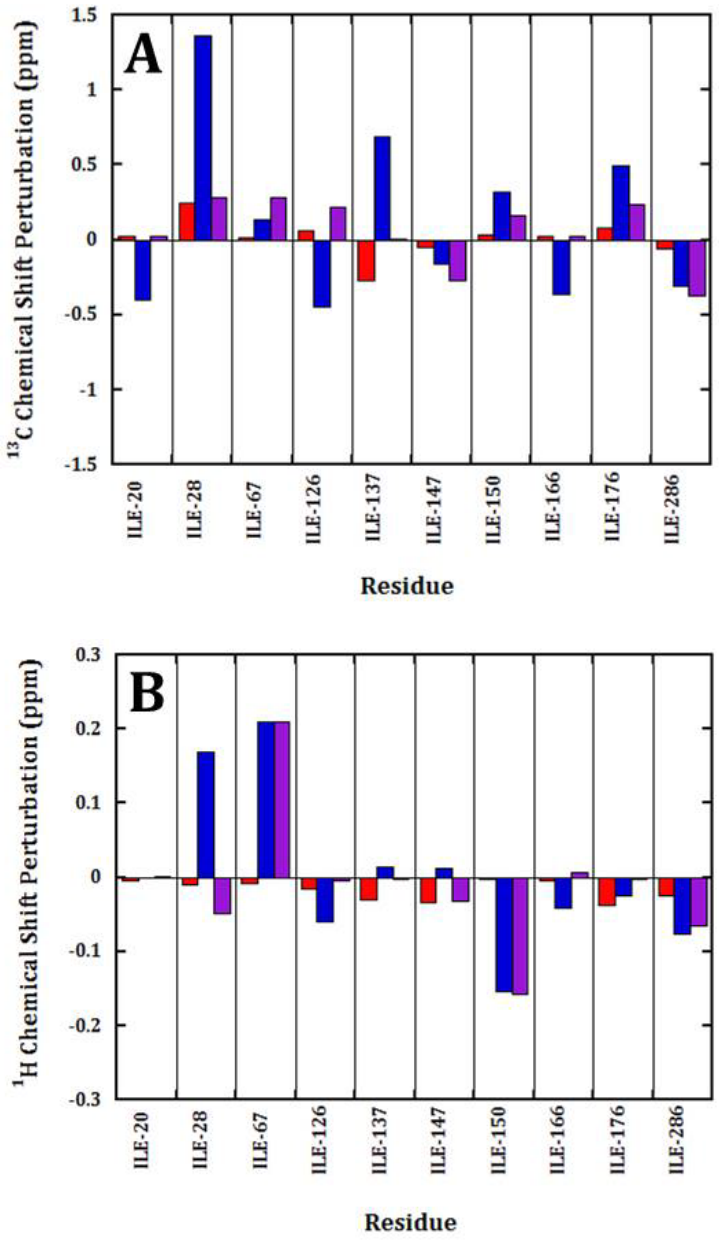

Figure 5-8: A) ^{13}C and B) ^{1}H chemical shift perturbations of Ile methyl groups of BsPFK in response to the binding of Fru-6-P (red), PEP(blue) and both simultaneously (purple) for those residues which had at least one chemical shift perturbation greater than 20% of the maximum perturbation.

substantial changes in chemical shift. Therefore, we predict that these resonances are not undergoing structural changes that contribute to the coupling free energy that defines the inhibition of BsPFK by PEP. Positions Ile-67, Ile-147, Ile-150 and Ile-286 show substantial changes in chemical shift upon ligand binding. However, the ternary complex is able to accommodate the perturbations brought on by the ligands at these locations. The lack of structural conflict at these sites indicates that

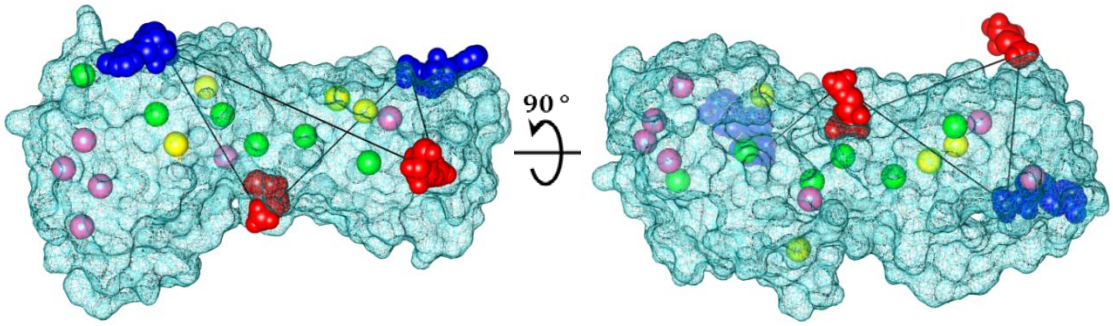

Figure 5-9: Two views of the BsPFK monomer displaying the locations of isoleucine residues with no shifts (pink), Additive shifts (yellow), and non-additive shifts (green). ADP is shown in the allosteric site in blue, and Fru-6-P is shown in the active site in red.

they are also not likely involved in the allosteric inhibition of BsPFK. Positions Ile-20, Ile-28, Ile-126, Ile-137, Ile-166 and Ile-176 possess the greatest difference in the comparison of chemical shifts between the ternary complex and the summation of the binary complexes. It is at these residues, where a conflict is reported in

response to the binding of both ligands simultaneously, that we predict the allosteric signal for inhibition is being transferred.

Discussion

Perturbations to the enzyme, reported by chemical shifts, can be qualitatively related to the energetics of allosteric coupling between Fru-6-P and PEP by elaborating on ΔG_{ay} as described previously.[33] In re-evaluating the disproportionation equilibrium equation, it is the contrast between the summation of chemical potentials on the left side of the equation and the summation of the right side that determines the value of ΔG_{ay}. This demonstrates the necessity to include structural information on all four species, with focus on changes introduced to free enzyme, in order to interpret any structural changes in the context of allosteric inhibition.

The residues identified as contributing to the coupling free energy, by perturbations in their chemical shift, are located generally in the regions near the two interfaces and directly between the substrate and effector binding sites. Four isoleucines, Ile-20, Ile-28, Ile-126 and Ile-137 lie between a pair of binding sites that are 30 Å away from each other. Interestingly, Ile-28 is the furthest away from the region between the binding sites and seems to have the strongest effect on the allosteric coupling of all of the identified residues. The other two isoleucine residues proposed to be involved in the propagation of the allosteric signal are Ile-

166 and Ile-176 and both fall between another pair of binding sites that are located 32 Å apart. This implies the lack of a single discrete structural pathway by which the allosteric signal is propagated. Ile-153, which is located between the binding sites 22 Å apart, does not seem to experience structural changes involved in the propagating of the allosteric signal. We know that coupling entropy, as opposed to coupling enthalpy, is the driving force for inhibition in BsPFK[42] suggesting that factors impact the transmission of the allosteric signal, such as changes to conformational dynamics, which may not be detected with this analysis. The conservative mutation of Ile-153 to a valine has an almost 4-fold effect on allosteric inhibition (Chapter 4), providing further evidence that this residue is involved in a way not accounted for by the NMR structural data.

Overall, PEP appears to have a more substantial effect on the structure of BsPFK than Fru-6-P, which is agreement with the crystal structures.[107] In many of the non-additive cases where PEP has a large effect on the chemical shift the Fru-6-P bound complex has a chemical shift quite similar to the apo form of the enzyme. In these cases there is a conflict within the enzyme not allowing the system to adjust for the energy released by PEP binding in same way it does when Fru-6-P is also bound. The allosteric effect, which is characterized by as a loss in binding energy, may result from these conflicts.

Previous work in our lab identified regions of the BsPFK enzyme that likely contribute to the entropy component of the coupling free energy.[117] This was accomplished by measuring the rotational correlation time of engineered

fluorescent tryptophan probes throughout the enzyme under all four ligation states. Namely, the positions identified were 164 and 240. When these residues, which are expected to contribute to the entropy component of the coupling free energy, are mapped on to the structure you see that they are isolated to a single region probed by those experiments (Figure 5-10).

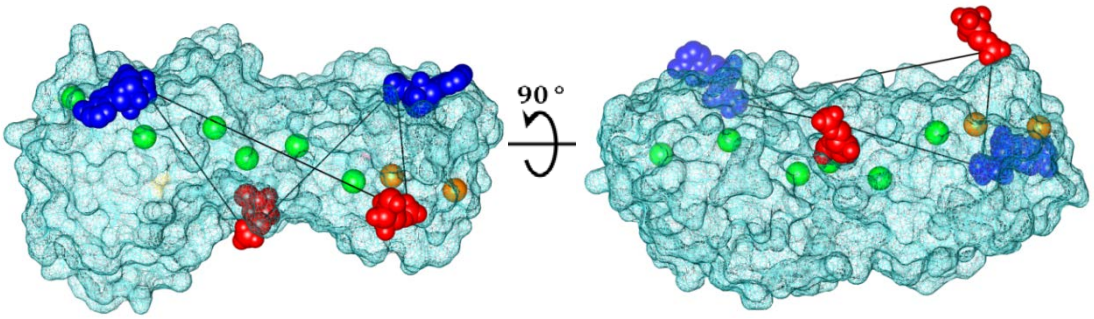

Figure 5-10: BsPFK monomer showing the locations of isoleucine residues with non-additive shifts (Green) and the residues identified previously by fluorescence spectroscopy (Orange). ADP is shown in the allosteric site in blue, and Fru-6-P is shown in the active site in red.

It is of future interest to use the methyl probes and the power of NMR spectroscopy to further explore the dynamics and more fully characterize all of the regions and interactions of the enzyme that contribute to the entropy component of the coupling free energy. Changes in the linewidth and intensities are seen between the ligation states for several of the isoleucine residues in our study, indicating that dynamics may be present on the ms-μs time scale. Relaxation dispersion experiments need to be performed to further probe these internal dynamics

involved in propagating the allosteric signal between binding sites in BsPFK. In addition, experiments probing side chain dynamics on a faster time scale may also provide additional information on how the allosteric effect is propagated in BsPFK.

CHAPTER VI

SUMMARY

Phosphofructokinase (PFK) from both *Bacillus stearothermophilus* (BsPFK) and *Escherichia coli* (EcPFK) is allosterically inhibited by downstream glycolytic pathway component phosphoenol-pyruvate (PEP). A comparison between EcPFK and BsPFK shows an overall conservation in structure and high sequence identity. The allosteric coupling free energy, ΔG_{ay}, describes the coupling in PFK between substrate, fructose-6-phosphate (Fru-6-P), and inhibitor, PEP.[32,33] Using an energetics based allosteric linkage framework , as derived in Chapter I, ΔG_{ay} is the coupling free energy for the disproportionation equilibrium below.

$$\text{PEP:PFK} + \text{PFK:Fru-6-P} \leftrightarrow \text{PFK} + \text{PEP:PFK:Fru-6-P} \qquad (6\text{-}1)$$

This equilibrium is the focus for our understanding of allosteric regulation at the molecular level. The linked function approach allows us to interpret perturbations to the enzyme in way that distinguishes changes due to the binding of the ligands individually to the changes that allow the enzyme to compensate for the simultaneous binding of two ligands. The coupling free energy can further be defined in terms of its entropy ($T\Delta S_{ay}$) and enthalpy components (ΔH_{ay}) using the following relationship:

$$\Delta G_{ay} = \Delta H_{ay} - T\Delta S_{ay} \qquad (6\text{-}2)$$

In the case of EcPFK, it is the larger positive enthalpy term that determines the positive sign for the coupling free energy that defines inhibition.[43,101] However, in

BsPFK both of the components are negative, and it is the larger absolute value of the entropy term that drives inhibition.[42] This suggests that fundamentally different mechanisms may be responsible for propagating the allosteric signal between PEP and Fru-6-P binding sites in these enzymes.

Both BsPFK and EcPFK are homotetrameric enzymes and each subunit contains a single tryptophan residue. In BsPFK, unlike EcPFK, the fluorescence intensity of the native tryptophan is not responsive to ligand binding.[116] In Chapter II, a tryptophan-shifted mutant, F179W/W240F, was constructed to look at the allosteric coupling between Fru-6-P and PEP under equilibrium conditions. The variant's kinetic and allosteric properties are similar to the wild-type enzyme as assessed by steady-state activity assays. Fortunately, the variant displays unique fluorescence properties that allow for the determination of dissociation constants for Fru-6-P and PEP in the absence of turnover. Using F179W/W240F, the extent of allosteric coupling between Fru-6-P and PEP was determined to be the same regardless of whether determined by steady-state kinetic or equilibrium fluorescence techniques demonstrating that MgATP does not affect coupling between Fru-6-P and PEP. Fru-6-P was shown to bind substantially tighter in the absence of MgATP, which is the result of non-allosteric antagonistic effects at the active sites.[69] The data presented in this chapter are in general agreement with previous studies in both BsPFK[120] and EcPFK[34,101] that validate the rapid equilibrium assumption for Fru-6-P, however some evidence is provided that this

assumption may fall apart under conditions of low ATP concentration due to very tight binding.

Since ΔG_{ay} conveys quantitatively both the nature and the magnitude of the allosteric effect, understanding the basis for inhibition in PFK involves understanding why the disproportionation equilibrium achieves its particular value. In this body of work, the enzyme was perturbed by both the denaturant urea and by "holes" engineered using site-directed mutagenesis and the effect on the poise of the equilibrium is accessed.

In Chapter III the effect of urea on the allosteric coupling in PFK from EcPFK and BsPFK is examined. Both specific activity and the allosteric coupling increase at low urea concentrations in BsPFK, but not in EcPFK. Van't Hoff analysis indicates that the increase in allosteric coupling is accompanied by a decrease in entropy-enthalpy compensation. The values for the entropy and enthalpy components of the coupling free energy indicate that at low concentrations of urea, 0.250 and 1 M, the increased coupling is the result of a larger change in the entropy component. At 4 M urea the trend of both of the entropy and enthalpy components decreasing continues, however the changes in coupling are dictated by the larger change in the enthalpy component. A possible explanation is that sub-dissociating concentrations of urea are stabilizing the tertiary structure of the enzyme, altering the conformational dynamics in BsPFK, but not so much the more flexible isoform EcPFK.

Holes are introduced into the enzyme's structure in the form of mutations that change particular isoleucines into valines in Chapter IV. We hypothesized that the addition of a small hole to the enzyme structure would not likely significantly alter the overall structure of the enzyme, but could allow for a change in the conformational entropy or flexibility of the enzyme in the effected region and possibly alter the allosteric coupling if the local region was involved in the transmission of the signal. Two of the three mutations had a significant effect on the coupling between Fru-6-P and PEP, one increasing and the other decreasing the allosteric coupling free energy. The strongest effect is an almost 4-fold augmentation of coupling in I153V-BsPFK. In this case there is decreased entropy-enthalpy compensation given a larger effect on the ΔH_{ay} component. An analogous mutation in EcPFK, L154V, has a minimal effect on the allosteric coupling in comparison.

Methyl-TROSY NMR was used to obtain structural information on all four species of BsPFK that contribute to the poise of the disproportionation equilibrium shown above in Chapter V. As a result of the selective isotopic labeling, all 30 of the isoleucine residues per monomer contain one NMR visible methyl group in a Methyl-TROSY spectrum. Complementary HNCA and HN(CO)CA experiments with [U-^{15}N,^{2}H,^{13}C]-BsPFK were used to assign the isoleucines in a ^{1}H-^{15}N TROSY spectrum. In order to transfer these assignments to the methyl-TROSY spectrum both ^{15}N-edited and ^{13}C-edited 3D -HMQC NOESY experiments were run with [U-^{15}N.^{2}H];Ileδ1-[$^{13}CH_3$]-BsPFK. To distinguish chemical shift changes necessary for

the allosteric regulation of BsPFK, it was essential to first establish the chemical shifts for each ligation state of the enzyme shown in the disproportionation equilibrium above. Fortunately, the ligand binding processes are in the fast exchange regime, allowing us to see resonances move across the field in response to the titration of ligand. Positions Ile-20, Ile-28, Ile-126, Ile-137, Ile-166 and Ile-176 possess the greatest difference in the comparison of chemical shifts between the ternary complex and the summation of the binary complexes. It is at these residues, where a conflict is experienced by the enzyme's structure in response to the binding of both ligands simultaneously, that we predict the allosteric signal for inhibition is being transferred. Interestingly, these residues are dispersed throughout the enzyme as opposed to forming a single discrete pathway.

As mentioned above, there is evidence for fundamentally different mechanisms for the coupling between binding sites in BsPFK and EcPFK, as indicated by contrasting thermodynamic driving forces. Conceivably, altering the conformational dynamics would not necessarily have the same effect on both enzymes. Both experiments at low concentrations of urea, and the hole mutant studies indicate that the coupling entropy and enthalpy that define the allosteric coupling free energy are very sensitive to even mild perturbations. This does not seem to be the case for the less rigid EcPFK, indicating that the allosteric coupling may be more "tunable" in BsPFK.

When Methyl-TROSY NMR was used to probe structural changes throughout the enzyme that relate to allosteric coupling, it was shown that in BsPFK there is

not likely a discrete pathway composed of a chain of residues involved in the propagation of the allosteric signal. Instead, residues spread throughout the enzyme are identified as contributors to the allosteric coupling. Together with the urea and hole mutant results we paint a picture of allosteric coupling in BsPFK, as opposed to EcPFK, that involves global changes in both the conformation entropy and structure throughout the enzyme. This hypothesis can be further investigated by measuring the dynamics on the relevant timescales using NMR.

REFERENCES

1. Schweizer, A.; Roschitzki-Voser, H.; Amstutz, P.; Briand, C.; Gulotti-Georgieva, M.; Prenosil, E.; Binz, H. K.; Capitani, G.; Baici, A.; Pluckthun, A.; Grutter, M. G. Inhibition of caspase-2 by a designed ankyrin repeat protein: specificity, structure, and inhibition mechanism. *Structure* **2007**, *15*, 625-636.

2. Umbarger, H. E. Evidence for a negative-feedback mechanism in the biosynthesis of isoleucine. *Science* **1956**, *123*, 848.

3. Pardee, A. B.; Yates, R. A. Pyrimidine biosynthesis in Escherichia coli. *J. Biol. Chem.* **1956**, *221*, 743-756.

4. Pardee, A. B.; Yates, R. A. Control of pyrimidine biosynthesis in Escherichia coli by a feed-back mechanism. *J. Biol. Chem.* **1956**, *221*, 757-770.

5. Changeux, J. A Ph.D. with Jacques Monod: Prehistory of allosteric proteins. In *Origins of molecular biology: a tribute to Jacques Monod*; Ullmann, A., Ed.; ASM Press: Washington, 2003; pp 229-242.

6. Monod, J.; Jacob, F. General Conclusions: Teleonomic Mechanisms in Cellular Metabolism, Growth, and Differentiation. *Cold Spring Harb. Symp. Quant. Biol.* **1961**, *26*, 389-401.

7. Koshland, D. E., Jr Enzyme flexibility and enzyme action. *J. Cell. Comp. Physiol.* **1959**, *54*, 245-258.

8. Hill, A. V. A new mathematical treatment of changes of ionic concentration in muscle and nerve under the action of electric currents, with a theory as to their mode of excitation. *J. Physiol.* **1910**, *40*, 190-224.

9. Reinhart, G. D. Linked-function origins of cooperativity in a symmetrical dimer. *Biophys. Chem.* **1988**, *30*, 159-172.

10. Weber, G. Ligand binding and internal equilibria in proteins. *Biochemistry* **1972**, *11*, 864-878.

11. Weber, G. Energetics of ligand binding to proteins. *Adv. Protein Chem.* **1975**, *29*, 1-83.

12. Perutz, M. F.; Rossmann, M. G.; Cullis, A. F.; Muirhead, H.; Will, G.; North, A. C. Structure of haemoglobin: a three-dimensional Fourier synthesis at 5.5-A. resolution, obtained by X-ray analysis. *Nature* **1960**, *185*, 416-422.

13. Kendrew, J. C.; Bodo, G.; Dintzis, H. M.; Parrish, R. G.; Wyckoff, H.; Phillips, D. C. A three-dimensional model of the myoglobin molecule obtained by x-ray analysis. *Nature* **1958**, *181*, 662-666.

14. Dickerson, R. E. X-ray studies of protein mechanisms. *Annu. Rev. Biochem.* **1972**, *41*, 815-842.

15. Fischer, E. Einfluss der configuration auf die wirkung der enzyme. *Chemische Berichte* **1894**, *27*, 3479.

16. Koshland, D. E., Jr Application of a Theory of Enzyme Specificity to Protein Synthesis. *Proc. Natl. Acad. Sci. U. S. A.* **1958**, *44*, 98-104.

17. Straub F. B, Szabolcsi G. Remarks on the dynamic aspect of enzyme structure. In *Molecular biology: problems and perspectives.*; Braunstein, A., Ed.; Nauka: Moscow, 1964; pp 182-187.

18. Monod, J.; Wyman, J.; Changeux, J. P. On the Nature of Allosteric Transitions: a Plausible Model. *J. Mol. Biol.* **1965**, *12*, 88-118.

19. Koshland, D. E., Jr; Nemethy, G.; Filmer, D. Comparison of experimental binding data and theoretical models in proteins containing subunits. *Biochemistry* **1966**, *5*, 365-385.

20. Levinthal, C. In *In How to Fold Graciously;* DeBrunner, J., E. Munck, E., Eds.; *Mossbauer Spectroscopy in Biological Systems: Proceedings of a meeting held at Allerton House, Monticello, Illinois*; Univ. of Illinois Bulletin: Urbana, IL, 1969; Vol. 67, pp 22-24.

21. Hilvert, D. Critical analysis of antibody catalysis. *Annu. Rev. Biochem.* **2000**, *69*, 751-793.

22. Goodey, N. M.; Benkovic, S. J. Allosteric regulation and catalysis emerge via a common route. *Nat. Chem. Biol.* **2008**, *4*, 474-482.

23. del Sol, A.; Tsai, C. J.; Ma, B.; Nussinov, R. The origin of allosteric functional modulation: multiple pre-existing pathways. *Structure* **2009**, *17*, 1042-1050.

24. Motlagh, H. N.; Wrabl, J. O.; Li, J.; Hilser, V. J. The ensemble nature of allostery. *Nature* **2014**, *508*, 331-339.

25. Tzeng, S. R.; Kalodimos, C. G. Dynamic activation of an allosteric regulatory protein. *Nature* **2009**, *462*, 368-372.

26. Wyman, J., Jr Heme proteins. *Adv. Protein Chem.* **1948**, *4*, 407-531.

27. Wyman, J., Jr Linked Functions and Reciprocal Effects in Hemoglobin: a Second Look. *Adv. Protein Chem.* **1964**, *19*, 223-286.

28. Wyman, J. The binding potential, a neglected linkage concept. *J. Mol. Biol.* **1965**, *11*, 631 <last_page> 644.

29. Wyman, J. Allosteric Linkage. *J. Am. Chem. Soc.* **1967**, *89*, 2202 <last_page> 2218.

30. Cleland, W. W. The kinetics of enzyme-catalyzed reactions with two or more substrates or products. I. Nomenclature and rate equations. *Biochim. Biophys. Acta* **1963**, *67*, 104-137.

31. Frieden, C. Treatment of Enzyme Kinetic Data. I. the Effect of Modifiers on the Kinetic Parameters of Single Substrate Enzymers. *J. Biol. Chem.* **1964**, *239*, 3522-3531.

32. Reinhart, G. D. The determination of thermodynamic allosteric parameters of an enzyme undergoing steady-state turnover. *Arch. Biochem. Biophys.* **1983**, *224*, 389-401.

33. Reinhart, G. D. Quantitative analysis and interpretation of allosteric behavior. *Methods Enzymol.* **2004**, *380*, 187-203.

34. Symcox, M. M.; Reinhart, G. D. A steady-state kinetic method for the verification of the rapid-equilibrium assumption in allosteric enzymes. *Anal. Biochem.* **1992**, *206*, 394-399.

35. Reinhart, G. D.; Hartleip, S. B.; Symcox, M. M. Role of coupling entropy in establishing the nature and magnitude of allosteric response. *Proc. Natl. Acad. Sci. U. S. A.* **1989**, *86*, 4032-4036.

36. Cooper, A.; Dryden, D. T. Allostery without conformational change. A plausible model. *Eur. Biophys. J.* **1984**, *11*, 103-109.

37. Popovych, N.; Sun, S.; Ebright, R. H.; Kalodimos, C. G. Dynamically driven protein allostery. *Nat. Struct. Mol. Biol.* **2006**, *13*, 831-838.

38. Petit, C. M.; Zhang, J.; Sapienza, P. J.; Fuentes, E. J.; Lee, A. L. Hidden dynamic allostery in a PDZ domain. *Proc. Natl. Acad. Sci. U. S. A.* **2009**, *106*, 18249-18254.

39. Daily, M. D.; Upadhyaya, T. J.; Gray, J. J. Contact rearrangements form coupled networks from local motions in allosteric proteins. *Proteins* **2008**, *71*, 455-466.

40. Wrabl, J. O.; Gu, J.; Liu, T.; Schrank, T. P.; Whitten, S. T.; Hilser, V. J. The role of protein conformational fluctuations in allostery, function, and evolution. *Biophys. Chem.* **2011**, *159*, 129-141.

41. Reichheld, S. E.; Yu, Z.; Davidson, A. R. The induction of folding cooperativity by ligand binding drives the allosteric response of tetracycline repressor. *Proc. Natl. Acad. Sci. U. S. A.* **2009**, *106*, 22263-22268.

42. Tlapak-Simmons, V. L.; Reinhart, G. D. Obfuscation of allosteric structure-function relationships by enthalpy-entropy compensation. *Biophys. J.* **1998**, *75*, 1010-1015.

43. Johnson, J. L.; Reinhart, G. D. Influence of substrates and MgADP on the time-resolved intrinsic fluorescence of phosphofructokinase from Escherichia coli. Correlation of tryptophan dynamics to coupling entropy. *Biochemistry* **1994**, *33*, 2644-2650.

44. Braxton, B. L.; Mullins, L. S.; Raushel, F. M.; Reinhart, G. D. Allosteric effects of carbamoyl phosphate synthetase from Escherichia coli are entropy-driven. *Biochemistry* **1996**, *35*, 11918-11924.

45. Schrank, T. P.; Bolen, D. W.; Hilser, V. J. Rational modulation of conformational fluctuations in adenylate kinase reveals a local unfolding mechanism for allostery and functional adaptation in proteins. *Proc. Natl. Acad. Sci. U. S. A.* **2009**, *106*, 16984-16989.

46. Schrank, T. P.; Elam, W. A.; Li, J.; Hilser, V. J. Strategies for the thermodynamic characterization of linked binding/local folding reactions within the native state application to the LID domain of adenylate kinase from Escherichia coli. *Methods Enzymol.* **2011**, *492*, 253-282.

47. Mittermaier, A. K.; Kay, L. E. Observing biological dynamics at atomic resolution using NMR. *Trends Biochem. Sci.* **2009**, *34*, 601-611.

48. Palmer, A. G.,3rd NMR characterization of the dynamics of biomacromolecules. *Chem. Rev.* **2004**, *104*, 3623-3640.

49. Baldwin, A. J.; Kay, L. E. NMR spectroscopy brings invisible protein states into focus. *Nat. Chem. Biol.* **2009**, *5*, 808-814.

50. Homans, S. W. Probing the binding entropy of ligand-protein interactions by NMR. *Chembiochem* **2005**, *6*, 1585-1591.

51. Shaw, D. E.; Maragakis, P.; Lindorff-Larsen, K.; Piana, S.; Dror, R. O.; Eastwood, M. P.; Bank, J. A.; Jumper, J. M.; Salmon, J. K.; Shan, Y.; Wriggers, W. Atomic-level characterization of the structural dynamics of proteins. *Science* **2010**, *330*, 341-346.

52. Massi, F.; Wang, C.; Palmer, A. G.,3rd Solution NMR and computer simulation studies of active site loop motion in triosephosphate isomerase. *Biochemistry* **2006**, *45*, 10787-10794.

53. Popovych, N.; Tzeng, S. R.; Tonelli, M.; Ebright, R. H.; Kalodimos, C. G. Structural basis for cAMP-mediated allosteric control of the catabolite activator protein. *Proc. Natl. Acad. Sci. U. S. A.* **2009**, *106*, 6927-6932.

54. Wells, C. M.; Di Cera, E. Thrombin is a Na(+)-activated enzyme. *Biochemistry* **1992**, *31*, 11721-11730.

55. Lechtenberg, B. C.; Johnson, D. J.; Freund, S. M.; Huntington, J. A. NMR resonance assignments of thrombin reveal the conformational and dynamic effects of ligation. *Proc. Natl. Acad. Sci. U. S. A.* **2010**, *107*, 14087-14092.

56. Myles, T.; Le Bonniec, B. F.; Betz, A.; Stone, S. R. Electrostatic steering and ionic tethering in the formation of thrombin-hirudin complexes: the role of the thrombin anion-binding exosite-I. *Biochemistry* **2001**, *40*, 4972-4979.

57. Ayala, Y.; Di Cera, E. Molecular recognition by thrombin. Role of the slow-->fast transition, site-specific ion binding energetics and thermodynamic mapping of structural components. *J. Mol. Biol.* **1994**, *235*, 733-746.

58. Bruschweiler, S.; Schanda, P.; Kloiber, K.; Brutscher, B.; Kontaxis, G.; Konrat, R.; Tollinger, M. Direct observation of the dynamic process underlying allosteric signal transmission. *J. Am. Chem. Soc.* **2009**, *131*, 3063-3068.

59. Frederick, K. K.; Marlow, M. S.; Valentine, K. G.; Wand, A. J. Conformational entropy in molecular recognition by proteins. *Nature* **2007**, *448*, 325-329.

60. Sprangers, R.; Kay, L. E. Quantitative dynamics and binding studies of the 20S proteasome by NMR. *Nature* **2007***, 445*, 618-622.

61. Kay, L. E. Solution NMR spectroscopy of supra-molecular systems, why bother? A methyl-TROSY view. *J. Magn. Reson.* **2011***, 210*, 159-170.

62. Velyvis, A.; Yang, Y. R.; Schachman, H. K.; Kay, L. E. A solution NMR study showing that active site ligands and nucleotides directly perturb the allosteric equilibrium in aspartate transcarbamoylase. *Proc. Natl. Acad. Sci. U. S. A.* **2007***, 104*, 8815-8820.

63. Sprangers, R.; Gribun, A.; Hwang, P. M.; Houry, W. A.; Kay, L. E. Quantitative NMR spectroscopy of supramolecular complexes: dynamic side pores in ClpP are important for product release. *Proc. Natl. Acad. Sci. U. S. A.* **2005***, 102*, 16678-16683.

64. Religa, T. L.; Sprangers, R.; Kay, L. E. Dynamic regulation of archaeal proteasome gate opening as studied by TROSY NMR. *Science* **2010***, 328*, 98-102.

65. Keramisanou, D.; Biris, N.; Gelis, I.; Sianidis, G.; Karamanou, S.; Economou, A.; Kalodimos, C. G. Disorder-order folding transitions underlie catalysis in the helicase motor of SecA. *Nat. Struct. Mol. Biol.* **2006***, 13*, 594-602.

66. Hellinga, H. W.; Evans, P. R. Mutations in the active site of Escherichia coli phosphofructokinase. *Nature* **1987***, 327*, 437-439.

67. Lardy, H. A.; Parks, R. E. Influence of ATP Concentrations on Rates of Some Phosphorylation Reactions. In *Enzymes: Units of Biological Structure and Function*; Gaebler, O. H., Ed.; Academic Press: New York, 1956; pp 584-587.

68. Fordyce, A. M.; Moore, C. H.; Pritchard, G. G. Phosphofructokinase from Streptococcus lactis. *Methods Enzymol.* **1982***, 90 Pt E*, 77-82.

69. Byrnes, M.; Zhu, X.; Younathan, E. S.; Chang, S. H. Kinetic characteristics of phosphofructokinase from Bacillus stearothermophilus: MgATP nonallosterically inhibits the enzyme. *Biochemistry* **1994***, 33*, 3424-3431.

70. Bar-Tana, J.; Cleland, W. W. Rabbit muscle phosphofructokinase. I. Anomeric specificity; initial velocity kinetics. *J. Biol. Chem.* **1974***, 249*, 1263-1270.

71. Hofmann, E.; Kopperschlager, G. Phosphofructokinase from yeast. *Methods Enzymol.* **1982***, 90 Pt E*, 49-60.

72. Parmeggiani, A.; Luft, J. H.; Love, D. S.; Krebs, E. G. Crystallization and properties of rabbit skeletal muscle phosphofructokinase. *J. Biol. Chem.* **1966**, *241*, 4625-4637.

73. Kolb, E.; Hudson, P. J.; Harris, J. I. Phosphofructokinase: complete amino-acid sequence of the enzyme from Bacillus stearothermophilus. *Eur. J. Biochem.* **1980**, *108*, 587-597.

74. Poorman, R. A.; Randolph, A.; Kemp, R. G.; Heinrikson, R. L. Evolution of phosphofructokinase--gene duplication and creation of new effector sites. *Nature* **1984**, *309*, 467-469.

75. French, B. A.; Chang, S. H. Nucleotide sequence of the phosphofructokinase gene from Bacillus stearothermophilus and comparison with the homologous Escherichia coli gene. *Gene* **1987**, *54*, 65-71.

76. Plaxton, W. C. The Organization and Regulation of Plant Glycolysis. *Annu. Rev. Plant Physiol. Plant Mol. Biol.* **1996**, *47*, 185-214.

77. Reinhart, G. D.; Lardy, H. A. Rat liver phosphofructokinase: kinetic activity under near-physiological conditions. *Biochemistry* **1980**, *19*, 1477-1484.

78. Li, Y.; Rivera, D.; Ru, W.; Gunasekera, D.; Kemp, R. G. Identification of allosteric sites in rabbit phosphofructo-1-kinase. *Biochemistry* **1999**, *38*, 16407-16412.

79. Kemp, R. G.; Gunasekera, D. Evolution of the allosteric ligand sites of mammalian phosphofructo-1-kinase. *Biochemistry* **2002**, *41*, 9426-9430.

80. Reinhart, G. D.; Lardy, H. A. Rat liver phosphofructokinase: kinetic and physiological ramifications of the aggregation behavior. *Biochemistry* **1980**, *19*, 1491-1495.

81. Reinhart, G. D.; Lardy, H. A. Rat liver phosphofructokinase: use of fluorescence polarization to study aggregation at low protein concentration. *Biochemistry* **1980**, *19*, 1484-1490.

82. Clifton, D.; Fraenkel, D. G. Mutant studies of yeast phosphofructokinase. *Biochemistry* **1982**, *21*, 1935-1942.

83. Reinhart, G. D. Influence of polyethylene glycols on the kinetics of rat liver phosphofructokinase. *J. Biol. Chem.* **1980**, *255*, 10576-10578.

84. Fraenkel, D. G.; Kotlarz, D.; Buc, H. Two fructose 6-phosphate kinase activities in Escherichia coli. *J. Biol. Chem.* **1973**, *248*, 4865-4866.

85. Campos, G.; Guixe, V.; Babul, J. Kinetic mechanism of phosphofructokinase-2 from Escherichia coli. A mutant enzyme with a different mechanism. *J. Biol. Chem.* **1984**, *259*, 6147-6152.

86. Cabrera, R.; Baez, M.; Pereira, H. M.; Caniuguir, A.; Garratt, R. C.; Babul, J. The crystal complex of phosphofructokinase-2 of Escherichia coli with fructose-6-phosphate: kinetic and structural analysis of the allosteric ATP inhibition. *J. Biol. Chem.* **2011**, *286*, 5774-5783.

87. Johnson, J. L.; Reinhart, G. D. MgATP and fructose 6-phosphate interactions with phosphofructokinase from Escherichia coli. *Biochemistry* **1992**, *31*, 11510-11518.

88. Evans, P. R.; Hudson, P. J. Structure and control of phosphofructokinase from Bacillus stearothermophilus. *Nature* **1979**, *279*, 500-504.

89. Evans, P. R.; Farrants, G. W.; Hudson, P. J. Phosphofructokinase: structure and control. *Philos. Trans. R. Soc. Lond. B. Biol. Sci.* **1981**, *293*, 53-62.

90. Shirakihara, Y.; Evans, P. R. Crystal structure of the complex of phosphofructokinase from Escherichia coli with its reaction products. *J. Mol. Biol.* **1988**, *204*, 973-994.

91. Schirmer, T.; Evans, P. R. Structural basis of the allosteric behaviour of phosphofructokinase. *Nature* **1990**, *343*, 140-145.

92. Evans, P. R.; Farrants, G. W.; Lawrence, M. C. Crystallographic structure of allosterically inhibited phosphofructokinase at 7 A resolution. *J. Mol. Biol.* **1986**, *191*, 713-720.

93. Rypniewski, W. R.; Evans, P. R. Crystal structure of unliganded phosphofructokinase from Escherichia coli. *J. Mol. Biol.* **1989**, *207*, 805-821.

94. Blangy, D. Phosphofructokinase from E. Coli: Evidence for a tetrameric structure of the enzyme. *FEBS Lett.* **1968**, *2*, 109-111.

95. Valdez, B. C.; French, B. A.; Younathan, E. S.; Chang, S. H. Site-directed mutagenesis in Bacillus stearothermophilus fructose-6-phosphate 1-kinase. Mutation at the substrate-binding site affects allosteric behavior. *J. Biol. Chem.* **1989**, *264*, 131-135.

96. Kimmel, J. L.; Reinhart, G. D. Isolation of an individual allosteric interaction in tetrameric phosphofructokinase from Bacillus stearothermophilus. *Biochemistry* **2001**, *40*, 11623-11629.

97. Braxton, B. L.; Tlapak-Simmons, V. L.; Reinhart, G. D. Temperature-induced inversion of allosteric phenomena. *J. Biol. Chem.* **1994**, *269*, 47-50.

98. Ortigosa, A. D.; Kimmel, J. L.; Reinhart, G. D. Disentangling the web of allosteric communication in a homotetramer: heterotropic inhibition of phosphofructokinase from Bacillus stearothermophilus. *Biochemistry* **2004**, *43*, 577-586.

99. Johnson, J. L.; Reinhart, G. D. Effects of high pressure on the allosteric properties of phosphofructokinase from Escherichia coli. In *High-Pressure Effects in Molecular Biophysics and Enzymology*; Markley, J. L., Northrup, D. B. and Royer, C. A., Eds.; Oxford University Press: New York, 1996; pp 242-243 - 255.

100. Pham, A. S.; Reinhart, G. D. MgATP-dependent activation by phosphoenolpyruvate of the E187A mutant of Escherichia coli phosphofructokinase. *Biochemistry* **2001**, *40*, 4150-4158.

101. Johnson, J. L.; Reinhart, G. D. Failure of a two-state model to describe the influence of phospho(enol)pyruvate on phosphofructokinase from Escherichia coli. *Biochemistry* **1997**, *36*, 12814-12822.

102. Le Bras, G.; Deville-Bonne, D.; Garel, J. R. Purification and properties of the phosphofructokinase from Lactobacillus bulgaricus. A non-allosteric analog of the enzyme from Escherichia coli. *Eur. J. Biochem.* **1991**, *198*, 683-687.

103. Paricharttanakul, N. M.; Ye, S.; Menefee, A. L.; Javid-Majd, F.; Sacchettini, J. C.; Reinhart, G. D. Kinetic and structural characterization of phosphofructokinase from Lactobacillus bulgaricus. *Biochemistry* **2005**, *44*, 15280-15286.

104. McGresham, M. S.; Lovingshimer, M.; Reinhart, G. D. Allosteric regulation in phosphofructokinase from the extreme thermophile Thermus thermophilus. *Biochemistry* **2014**, *53*, 270-278.

105. Xu, J.; Oshima, T.; Yoshida, M. Tetramer-dimer conversion of phosphofructokinase from Thermus thermophilus induced by its allosteric effectors. *J. Mol. Biol.* **1990**, *215*, 597-606.

106. Kimmel, J. L.; Reinhart, G. D. Reevaluation of the accepted allosteric mechanism of phosphofructokinase from Bacillus stearothermophilus. *Proc. Natl. Acad. Sci. U. S. A.* **2000**, *97*, 3844-3849.

107. Mosser, R.; Reddy, M. C.; Bruning, J. B.; Sacchettini, J. C.; Reinhart, G. D. Structure of the apo form of Bacillus stearothermophilus phosphofructokinase. *Biochemistry* **2012**, *51*, 769-775.

108. Tlapak-Simmons, V. L.; Reinhart, G. D. Comparison of the inhibition by phospho(enol)pyruvate and phosphoglycolate of phosphofructokinase from B. stearothermophilus. *Arch. Biochem. Biophys.* **1994**, *308*, 226-230.

109. Johnson, J. L.; Reinhart, G. D. Influence of MgADP on phosphofructokinase from Escherichia coli. Elucidation of coupling interactions with both substrates. *Biochemistry* **1994**, *33*, 2635-2643.

110. Fenton, A. W.; Paricharttanakul, N. M.; Reinhart, G. D. Disentangling the web of allosteric communication in a homotetramer: heterotropic activation in phosphofructokinase from Escherichia coli. *Biochemistry* **2004**, *43*, 14104-14110.

111. Berger, S. A.; Evans, P. R. Steady-state fluorescence of Escherichia coli phosphofructokinase reveals a regulatory role for ATP. *Biochemistry* **1991**, *30*, 8477-8480.

112. Riley-Lovingshimer, M. R.; Reinhart, G. D. Examination of MgATP binding in a tryptophan-shift mutant of phosphofructokinase from Bacillus stearothermophilus. *Arch. Biochem. Biophys.* **2005**, *436*, 178-186.

113. Fenton, A. W.; Paricharttanakul, N. M.; Reinhart, G. D. Identification of substrate contact residues important for the allosteric regulation of phosphofructokinase from Eschericia coli. *Biochemistry* **2003**, *42*, 6453-6459.

114. Vivian, J. T.; Callis, P. R. Mechanisms of tryptophan fluorescence shifts in proteins. *Biophys. J.* **2001**, *80*, 2093-2109.

115. Lakowicz, J. R. *Principles of Fluorescence Spectroscopy;* Springer: New York, New York, 2006; .

116. Kim, S. J.; Chowdhury, F. N.; Stryjewski, W.; Younathan, E. S.; Russo, P. S.; Barkley, M. D. Time-resolved fluorescence of the single tryptophan of Bacillus stearothermophilus phosphofructokinase. *Biophys. J.* **1993**, *65*, 215-226.

117. Perez, S. Illuminating the Heterotropic Communication of the Pair-wise Interactions in Phosphofructokinase from Bacillus stearothermophilus, Texas A&M University, 2012.

118. French, B. A.; Valdez, B. C.; Younathan, E. S.; Chang, S. H. High-level expression of Bacillus stearothermophilus 6-phosphofructo-1-kinase in Escherichia coli. *Gene* **1987**, *59*, 279-283.

119. Lovingshimer, M. R.; Siegele, D.; Reinhart, G. D. Construction of an inducible, pfkA and pfkB deficient strain of Escherichia coli for the expression and purification of phosphofructokinase from bacterial sources. *Protein Expr. Purif.* **2006**, *46*, 475-482.

120. Riley-Lovingshimer, M. R.; Reinhart, G. D. Equilibrium binding studies of a tryptophan-shifted mutant of phosphofructokinase from Bacillus stearothermophilus. *Biochemistry* **2001**, *40*, 3002-3008.

121. Babul, J. Phosphofructokinases from Escherichia coli. Purification and characterization of the nonallosteric isozyme. *J. Biol. Chem.* **1978**, *253*, 4350-4355.

122. Kotlarz, D.; Buc, H. Phosphofructokinases from Escherichia coli. *Methods Enzymol.* **1982**, *90 Pt E*, 60-70.

123. Reinhart, G. D. Influence of pH on the regulatory kinetics of rat liver phosphofructokinase: a thermodynamic linked-function analysis. *Biochemistry* **1985**, *24*, 7166-7172.

124. Das, A.; Mukhopadhyay, C. Urea-mediated protein denaturation: a consensus view. *J Phys Chem B* **2009**, *113*, 12816-12824.

125. Pike, A. C.; Acharya, K. R. A structural basis for the interaction of urea with lysozyme. *Protein Sci.* **1994**, *3*, 706-710.

126. Dunbar, J.; Yennawar, H. P.; Banerjee, S.; Luo, J.; Farber, G. K. The effect of denaturants on protein structure. *Protein Sci.* **1997**, *6*, 1727-1733.

127. Bhuyan, A. K. Protein stabilization by urea and guanidine hydrochloride. *Biochemistry* **2002**, *41*, 13386-13394.

128. Makhatadze, G. I.; Privalov, P. L. Protein interactions with urea and guanidinium chloride. A calorimetric study. *J. Mol. Biol.* **1992**, *226*, 491-505.

129. Bras, G. L.; Teschner, W.; Deville-Bonne, D.; Garel, J. R. Urea-induced inactivation, dissociation, and unfolding of the allosteric phosphofructokinase from Escherichia coli. *Biochemistry* **1989**, *28*, 6836-6841.

130. Teschner, W.; Deville-Bonne, D.; Garel, J. R. Fructose-6-phosphate modifies the pathway of the urea-induced dissociation of the allosteric phosphofructokinase from Escherichia coli. *FEBS* **1990**, *267*, 96-98.

131. Johnson, J. L.; Lasagna, M. D.; Reinhart, G. D. Influence of a sulfhydryl cross-link across the allosteric-site interface of E. coli phosphofructokinase. *Protein Sci.* **2001**, *10*, 2186-2194.

132. Quinlan, R. J.; Reinhart, G. D. Effects of protein-ligand associations on the subunit interactions of phosphofructokinase from B. stearothermophilus. *Biochemistry* **2006**, *45*, 11333-11341.

133. Kotlarz, D.; Buc, H. Two Escherichia coli fructose-6-phosphate kinases. Preparative purification, oligomeric structure and immunological studies. *Biochim. Biophys. Acta* **1977**, *484*, 35-48.

134. Mosser, R.; Reddy, M. C.; Bruning, J. B.; Sacchettini, J. C.; Reinhart, G. D. Redefining the role of the quaternary shift in Bacillus stearothermophilus phosphofructokinase. *Biochemistry* **2013**, *52*, 5421-5429.

135. McGresham, M. S.; Reinhart, G. D. Enhancing allosteric inhibition in Thermus thermophilus Phosphofructokinase. *Biochemistry* **2015**, *54*, 952-958.

136. Fenton, A. W. Allostery: an illustrated definition for the 'second secret of life'. *Trends Biochem. Sci.* **2008**, *33*, 420-425.

137. Groebe, D. R. Screening for positive allosteric modulators of biological targets. *Drug Discov. Today* **2006**, *11*, 632-639.

138. Treadway, J. L.; Mendys, P.; Hoover, D. J. Glycogen phosphorylase inhibitors for treatment of type 2 diabetes mellitus. *Expert Opin. Investig. Drugs* **2001**, *10*, 439-454.

139. Hardy, J. A.; Wells, J. A. Searching for new allosteric sites in enzymes. *Curr. Opin. Struct. Biol.* **2004**, *14*, 706-715.

140. Tan, X.; Osmulski, P. A.; Gaczynska, M. Allosteric regulators of the proteasome: potential drugs and a novel approach for drug design. *Curr. Med. Chem.* **2006**, *13*, 155-165.

141. Wenthur, C. J.; Gentry, P. R.; Mathews, T. P.; Lindsley, C. W. Drugs for allosteric sites on receptors. *Annu. Rev. Pharmacol. Toxicol.* **2014**, *54*, 165-184.

142. Razvi, A.; Scholtz, J. M. Lessons in stability from thermophilic proteins. *Protein Sci.* **2006**, *15*, 1569-1578.

143. Sterner, R.; Liebl, W. Thermophilic adaptation of proteins. *Crit. Rev. Biochem. Mol. Biol.* **2001**, *36*, 39-106.

144. Riley-Lovingshimer, M. R.; Ronning, D. R.; Sacchettini, J. C.; Reinhart, G. D. Reversible ligand-induced dissociation of a tryptophan-shift mutant of phosphofructokinase from Bacillus stearothermophilus. *Biochemistry* **2002**, *41*, 12967-12974.

145. Matthews, B. W. Structural and genetic analysis of protein stability. *Annu. Rev. Biochem.* **1993**, *62*, 139-160.

146. Takano, K.; Ogasahara, K.; Kaneda, H.; Yamagata, Y.; Fujii, S.; Kanaya, E.; Kikuchi, M.; Oobatake, M.; Yutani, K. Contribution of hydrophobic residues to the stability of human lysozyme: calorimetric studies and X-ray structural analysis of the five isoleucine to valine mutants. *J. Mol. Biol.* **1995**, *254*, 62-76.

147. Roche, J.; Caro, J. A.; Norberto, D. R.; Barthe, P.; Roumestand, C.; Schlessman, J. L.; Garcia, A. E.; Garcia-Moreno, B. E.; Royer, C. A. Cavities determine the pressure unfolding of proteins. *Proc. Natl. Acad. Sci. U. S. A.* **2012**, *109*, 6945-6950.

148. Zavodszky, P.; Kardos, J.; Svingor; Petsko, G. A. Adjustment of conformational flexibility is a key event in the thermal adaptation of proteins. *Proc. Natl. Acad. Sci. U. S. A.* **1998**, *95*, 7406-7411.

149. Kohen, A.; Klinman, J. P. Protein Flexibility Correlates with Degree of Hydrogen Tunneling in Thermophilic and Mesophilic Alcohol Dehydrogenases. *J. Am. Chem. Soc.* **2000**, *122*, 10738-10739.

150. Williamson, M. P. Using chemical shift perturbation to characterise ligand binding. *Prog Nucl Magn Reson Spectrosc* **2013**, *73*, 1-16.

151. Cavanagh, J.; Fairbrother, W.; Palmer, A.; Rance, M.; Skelton, N. *Protein NMR spectroscopy: principles and practice;* Academic Press: Amsterdam, 2007; , pp 885.

152. Tugarinov, V.; Hwang, P. M.; Ollerenshaw, J. E.; Kay, L. E. Cross-correlated relaxation enhanced 1H[bond]13C NMR spectroscopy of methyl groups in very high molecular weight proteins and protein complexes. *J. Am. Chem. Soc.* **2003**, *125*, 10420-10428.

153. Pervushin, K.; Riek, R.; Wider, G.; Wuthrich, K. Attenuated T2 relaxation by mutual cancellation of dipole-dipole coupling and chemical shift anisotropy indicates an avenue to NMR structures of very large biological macromolecules in solution. *Proc. Natl. Acad. Sci. U. S. A.* **1997**, *94*, 12366-12371.

154. Goto, N. K.; Kay, L. E. New developments in isotope labeling strategies for protein solution NMR spectroscopy. *Curr. Opin. Struct. Biol.* **2000**, *10*, 585-592.

155. Tugarinov, V.; Kanelis, V.; Kay, L. E. Isotope labeling strategies for the study of high-molecular-weight proteins by solution NMR spectroscopy. *Nat. Protoc.* **2006**, *1*, 749-754.

156. Goto, N. K.; Gardner, K. H.; Mueller, G. A.; Willis, R. C.; Kay, L. E. A robust and cost-effective method for the production of Val, Leu, Ile (delta 1) methyl-protonated 15N-, 13C-, 2H-labeled proteins. *J. Biomol. NMR* **1999**, *13*, 369-374.

157. Gardner, K. H.; Kay, L. E. Production and Incorporation of 15N, 13C, 2H (1H-d1 Methyl) Isoleucine into Proteins for Multidimensional NMR Studies - Journal of the American Chemical Society (ACS Publications). *J. Am. Chem. Soc.* **1997**, *119*, 7599-7600.

158. Janin, J.; Miller, S.; Chothia, C. Surface, subunit interfaces and interior of oligomeric proteins. *J. Mol. Biol.* **1988**, *204*, 155-164.

159. Thomason, L. C.; Costantino, N.; Court, D. L. E. coli Genome Manipulation by P1 Transduction. In *Current Protocols in Molecular Biology*John Wiley & Sons, Inc.: 2001; .

160. Casadaban, M. J. Transposition and fusion of the lac genes to selected promoters in Escherichia coli using bacteriophage lambda and Mu. *J. Mol. Biol.* **1976**, *104*, 541-555.

APPENDIX: NOMENCLATURE

A	Substrate
ATCase	Aspartate transcarbamoylase
ATP	Adenosine triphosphate
ADP	Adenosine diphosphate
BsPFK	Phosphofructokinase from *Bacillus stearothermophilus*
ΔC_p	Change in heat capacity
CaM	Calmodulin
cAMP	Cyclic AMP
CAP	Catabolite activator protein
CBP	CREB binding protein
ClpP	Caseinolytic protease
Da	Daltons
DNA	Deoxyribonucleic acid
dNTPs	Deoxynucleotide triphosphates
DTT	Dithiothreitol
E	Enzyme
$[E]_t$	Total enzyme concentration
EcPFK	Phosphofructokinase from *Escherichia coli*
EAM	Ensemble allosteric model
EDTA	Ethylenediamine tetraacetic acid

EPPES	N- [2-hydroxyethyl] piperazine--3-propanesulfonic acid
FPLC	Fast protein liquid chromatography
Fru-2,6-BP	Fructose-2,6-bisphosphate
Fru-6-P	Fructose-6-phosphate
ΔG_{ay}	Coupling free energy for the binding of substrate and effector
ΔH_{ay}	Coupling enthalpy for the binding of substrate and effector
HMQC	Heteronuclear multiple quantum coherence
ITC	Isothermal calorimetry
k_{cat}	Turnover number
K_a	Apparent dissociation constant for substrate A
K_{ia}°	Dissociation constant for A in the absence of effector
K_{ia}^{∞}	Dissociation constant for A in presence of saturating effector
K_{iy}°	Dissociation constant for Y in the absence of substrate
K_{iy}^{∞}	Dissociation constant for Y in presence of saturating substrate
K_m	Michaelis constant
KNF	Sequential model
LB	Lysogeny broth
LbPFK	Phosphofructokinase from *Lactobacillus delbrueckii ssp. Bulgaricus*
MES	2-(N-morpholino)ethanesulfonic acid
MLL	Mixed lineage leukemia

MSD	Mean square deviations
MWC	Concerted model
NADH	Nicotinamide adenine dinucleotide, reduced form
n_H	Hill number
NMR	Nuclear magnetic resonance
NOESY	Nuclear overhauser effect spectroscopy
P_i	Phosphate
PBD	Pre-protein binding domain
PEP	Phospo-(enol)pyruvate
PFP	Pyrophosphate-fructose-6-phosphate-phosphotransferase
PFK or PFK-1	Phosphofructokinase-1
PFK-2	Phosphofructokinase-2
PP_i	Pyrophosphate
PRE	Paramagnetic relaxation enhancement
Q_{aa}	Coupling constant for the binding of two substrates (K-type)
Q_{ay}	Coupling constant for the binding of the substrate and effector (K-type)
ΔS_{ay}	Coupling entropy for the binding of substrate and effector
SDS-PAGE	Sodium sodecyl sulfate polyacrylaAmide gel electrophoresis
SecA	Type II secretory pathway protein A
TROSY	Transverse relaxation optimized spectroscopy
TtPFK	Phosphofructokinase from *Thermus thermophilus*

v	Initial velocity
V°	maximal activity in the absence of effector
V^{∞}	maximal activity in the presence of saturating effector
W_{ay}	Coupling constant for the binding of the substrate and effector (V-type)
WT	Wild-type
Y	Effector